Karlsruher Institut für Technologie

Small molecule BAG1L inhibitors for the treatment of androgen receptor-dependent prostate cancer

Zur Erlangung des akademischen Grades einer
DOKTORIN DER NATURWISSENSCHAFTEN
(Dr. rer. nat.)

von der KIT-Fakultät für Chemie und Biowissenschaften
des Karlsruher Instituts für Technologie (KIT)
genehmigte

DISSERTATION

von

Nane Corinna Kuznik, M. Sc.
aus Landau i.d. Pfalz

1. Referent: apl. Prof. Dr. Andrew Cato
2. Referent: Prof. Dr. Jörg Kämper
Tag der mündlichen Prüfung: 23.07.2020

Eidesstattliche Erklärung Hiermit erkläre ich, dass ich diese Dissertation eigenständig angefertigt habe. Ich habe nur die angegebenen Quellen und Hilfsmittel verwendent und mich keiner unzulässigen Hilfe Dritter bedient. Wörtlich oder inhaltlich übernommenes Gedankengut als solches gekennzeichnet. Die Satzung des Karlsruher Instituts für Technologie (KIT) zur Sicherung guter wissenschaftlicher Praxis habe ich in die gültigen Fassung beachtet. Ich versichere außerdem, dass diese Arbeit in gleicher oder ähnlicher Form noch keiner Prüfungsbehörde vorgelegt wurde.

Datum: _____ Unterschrift: _____

Zusammenfassung

Prostatakrebs ist die am häufigsten diagnostizierte Krebserkrankung bei männlichen Erwachsenen in westlichen Industrienationen. Obwohl Prostatakarzinome langsam fortschreiten und in frühen Stadien kurativ behandelbar sind, stellen fortgeschrittene Prostatakarzinome die Klinik weiterhin vor eine Herausforderung. Alle in der Klinik genutzten Androgen-Deprivations-Therapien inhibieren die Aktivität der C-terminalen Liganenbindedomäne des Androgen Rezeptors. Diese Art von Therapie ist anfangs äußerst effektiv darin das Tumorvolumen zu reduzieren. Allerdings entwickeln die meisten Patienten im Verlauf ihrer Behandlung eine lethale, therapieresistente Form, die als kastrations-resistenter Prostatakrebs bezeichnet wird. Einer der Gründe dafür ist die Expression von konstitutiv-aktiven Androgen Rezeptor Varianten, die keine Ligandenbindedomäne besitzen. Neuartige Therapieformen, die die Androgen Rezeptor Aktivität auf andere Weise hemmen, sind daher von großer medizinischer Bedeutung. Eine vielversprechende Möglichkeit die Aktivität des Androgen Rezeptors zu inhibieren wäre die Unterbindung von Interaktionen zwischen Androgen Rezeptor N-Terminus und regulatorischen Proteinen. Das Co-Chaperon BAG1L ist ein solches regulatorisches Protein, dass in der Lage ist den N-Terminus des Androgen Rezeptors zu binden und so dessen Aktivität zu regulieren. BAG1L wird im Übergang zu kastrations-resistentem Prostatakrebs überexprimiert und hohe BAG1L Proteinlevel in Primärtumoren prognostizieren eine reduzierte Wirkung des Hormontherapeutikums Abirateron. In dieser Arbeit konnte ein partiell gefalteter polyAlanin-Bereich im N-terminus des Androgen Rezeptors als Bindemotiv für BAG1L identifiziert werden. Mutationen innerhalb dieser Region reduzierten die BAG1L-vermittelte Transaktivierung und die Bindung von BAG1L an den Androgen Rezeptor. Des weiteren wurde gezeigt, dass der Verlust von BAG1L zu einer reduzierten Bindung von klassischen Koaktivatoren an den Androgen Rezeptor führt. BAG1L reguliert außerdem die Expression einer Gruppe von Androgen Rezeptor Zielgenen, die eine Rolle in der Regulation der intrazellulären ROS-Level spielen. Behandlung mit dem Oxidase Inhibitor Diphenyleneiodonium chlorid inhibierte das Wachstum von BAG1L exprimierenden Prostatakrebszellen, jedoch nicht von BAG1L Knock-out Zellen. Es konnte weiterhin eine Substanz, 2-(4-fluorophenyl)-5-(trifluoromethyl)-1,3-benzothiazole, identifziert werden, die selektiv die Interaktion zwischen BAG1L und der N-Terminalen Domäne des Androgen Rezeptors inhibiert. Dieses Benzothiazol-Derivat bindet an die BAG Domäne und inhibiert das Wachstum von BAG1L exprimierenden Prostatakrebszellen. In dieser Arbeit konnte somit ein niedrigmolekularer Inhibitor identifiziert werden, der für die Behandlung von fortgeschrittenem Prostatakrebs weiterentwickelt werden könnte.

Abstract

Prostate Cancer is the most commonly diagnosed cancer in men. Although prostate carcinoma are considered slow-growing tumors and are well-manageable in early stages of the disease, advanced prostate tumors still provide a challenge for the clinics. All clinically approved androgen deprivation therapies for prostate cancer target the C-terminal ligand-binding domain of the androgen receptor. These kind of therapies are initially effective in reducing tumor volume, but fail at later stages as most patients develop a lethal, therapy-resistant state termed castration-resistant prostate cancer. One of the reasons for this is the expression of constitutively active androgen receptor variants that lack the ligand-binding domain. Therefore, novel therapy options that target AR activity through a different mechanism represent an unmet medical need. A promising possibility to reduce androgen receptor signaling would be the disruption of interaction of the androgen receptor *activation function-1* domain with regulatory proteins. The cochaperone BAG1L is such a regulatory protein which binds the N-terminus of the AR and regulates its activity. BAG1L expression increases in the progression to castration-resistant prostate cancer and high protein levels of BAG1L in primary tumors predict a poor clinical benefit for patients to abiraterone therapy. In this work a partially folded, polyalanine region at the androgen receptor N-terminal domain was identified as the binding motif for BAG1L. Mutations in this region affected BAG1L-mediated transactivation and BAG1L binding to the N-terminus of the androgen receptor. Furthermore, loss of BAG1L reduces the affinity of DHT-bound AR to some coregulator motifs of classical coregulators and affected gene expression of a subset of AR target genes involved in the regulation of oxidative stress. Treatment with the oxidase inhibitor diphenyleneiodonium chloride reduced the growth of prostate cancer cells in the presence but not in the absence of BAG1L. Furthermore, a 2-(4-fluorophenyl)-5-(trifluoromethyl)-1,3-benzothiazole (A4B17) was identified as a selective inhibitor of BAG1L androgen receptor interaction. The benzothiazole compound A4B17 was shown to bind to the BAG domain and inhibited growth of AR positive prostate cancer cells depending on their level of BAG1L expression. Therefore, this study has identified a small molecule inhibitor that could be further developed for therapy advanced BAG1L positive prostate cancers.

Table of contents

List of Figures

List of Tables

Abbreviations

% (v/v)	percent volume per volume
% (w/v)	percent weight per volume
ADP/ATP	adenosine diphosphate/adenosine triphosphate
ADT	androgen deprivation therapy
AF-1	*activation function-1*
AF-2	*activation function-2*
APS	ammonium persulfate
AR-FL	full-length androgen receptor
AR-SV	androgen receptor splice variants
AR-V7	androgen receptor splice variant 7
ARE	*androgen response elements*
BAG-1	*Bcl-2 associated athanogene*
BF-3	*binding function-3*
BSA	bovine serum albumin
CBP	*CREB-binding protein*
cDNA	complementary DNA
CRPC	castration-resistant prostate cancer
DBD	DNA-binding domain
DCF	2´,7´-dichlorofluorescein diacetate
DHT	dihydrotestosterone
DMEM	Dulbecco's Modified Eagle's Medium
DMSO	dimethyl sulfoxide
DPI	diphenyleneiodonium chloride
DTT	dithiothreitol
DUOX1	dual oxidase 1
EDTA	ethylenediaminetetraacetic acid
EtOH	ethanol
FBS	fetal bovine serum
HAT	histone acetyltransferase
HGPIN	high-grade prostatic intraepithelial neoplasia
HSQC	Heteronuclear Single Quantum Coherence
IPTG	Isopropyl β-d-1-thiogalactopyranoside
Kb	kilobases
kDa	kilodalton
LB	lysogeny broth
LBD	ligand binding domain

LGPIN	low-grade prostatic intraepithelial neoplasia
LH	luteinizing hormone
LHRH	luteinizing hormone releasing hormone
M-MLV	Moloney Murine Leukemia Virus
MAGE-11	melanoma-associated antigen 11
MAPK	mitogen-activated protein kinase
MICAL1	microtubule associated monooxygenase
MR	mineralocorticoid receptor
NADP(H)	Nicotinamide adenine dinucleotide phosphate
NLS	*nuclear localisation sequence*
NMR	uclear magnetic resonance
NNT	nicotinamide nucleotide transhydrogenase
NR	nuclear receptor
NTD	N-terminal Domain
ON	over night
PBS	phosphate buffered saline
PCa	prostate cancer
PCR	*polymerase chain reaction*
PIC	protein inhibitor cocktail
PIN	prostatic intraepithelial neoplasia
PMSF	phenylmethylsulfonyl fluoride
PR	progesterone receptor
PSA	*prostate specific antigen*
qRT-PCR	quantitative Real-Time PCR
RLU	relative light unit
ROS	reactive oxygen species
rpm	revolutions per minute
RPMI	Roswell Park Memorial Institute
SDS	sodium dodecyl sulfate
SEM	scanning electron microscope
shRNA	short hairpin RNA
SLiMs	short linear motifs
SOC	Super Optimal Broth
$\tau 5$	*transactivation unit 5*
TBP	TATA-Box binding protein
TEMED	Tetramethyl ethylen diamine
T_m	melting temperature
UAS	*upstream activation sequence*
ULD	ubiquitin-like domain

1 Introduction

1.1 Prostate Cancer

Prostate Cancer (PCa) was first described in 1853 by the London surgeon J. Adams during a histological examination. In his report Adams stated that this condition was "a very rare disease" (Adams, 1853). Intriguingly, today, PCa is one of the most commonly diagnosed cancers in men in the western industrialized nations with 58.780 new cases in 2016 (Robert-Koch-Institut, 2016). It is also one of the leading causes of cancer-related death in men with 14.417 death cases in Germany in 2016 (Robert-Koch-Institut, 2016). This apparent contradiction can be attributed to several factors:
First, in the early 1900s it was difficult to distinguish PCa from other diseases in the urinary tract. An improved medical knowledge has therefore led to an increase in the detection of PCa. Second, as the average life expectancy has improved over the past century, the number of new PCa cases has increased accordingly since the prevalence of PCa increases with age, more than for any other cancer type (Greenlee *et al.*, 2001; Siegel *et al.*, 2019). Third, early screening methods such as the detection of increased serum levels of the prostate specific antigen (PSA), a glycoprotein expressed by prostate tissue, has led to an increase in the detection of new PCa cases (Greenlee *et al.*, 2001; Siegel *et al.*, 2019). Additionally, looking at epidemiological data, it seems that a "modern, western" life-style contributes to an increase in PCa case numbers (Schottenfeld & Fraumeni Jr., 1997). Intriguingly, asian men that emigrated to Western countries are more commonly diagnosed with prostate cancer than men in their country of origin (Lee *et al.*, 2007). However, complete understanding of the risk factors contributing to the development of prostate tumors remains elusive. Age and genetics are primary risk factors. For instance PCa is very uncommon in men younger than 45, while the average age of diagnosis is 70 (Siegel *et al.*, 2019). Further, men who have first-degree family members with PCa appear to have a two-times higher risk of developing the disease compared to men without PCa in the family (Edwards & Eeles, 2004; Goh *et al.*, 2012).

PCa is a malignant tumor disease of the prostate, a walnut shaped gland in men, which produces and stores the seminal fluid (Krebsinformationsdienst des Deutschen Krebsforschungszentrums (DKFZ), 2017). Prostate tumors are usually classified as adenocarcinomas and are considered to be slow-growing tumors (Schottenfeld & Fraumeni Jr., 1997). At first, small clusters of abnormal cells restricted to normal prostate gland tissue can be identified. This condition is known as prostatic intraepithelial neoplasia (PIN) (McNeal & Bostwick, 1986). Depending on the degree of abnormality of these cell clusters, one can distinguish between high-grade PIN (HGPIN) or low-grade PIN (LGPIN). Even though there is no clear proof that PIN will eventually develop into PCa, HGPIN is often considered to be a PCa precursor (Montironi *et al.*, 2007; De Marzo *et al.*, 2003). Tumor formation takes place when the deregulated cells begin to multiply and invade the surrounding prostatic tissue (the stroma). When a tumor grows large enough it may invade the

nearby organs like the seminal vesicles or the rectum (Partin *et al.*, 1989; Gengler & Finby, 1975). Prostate carcinomas usually start to spread by lymphogenic metastasis, affecting the lymph nodes of the little pelvis, the lumbar lymph nodes and later the mediastinal lymph nodes and root of the lung. The later occurring hematogenic metastasis mainly affects the bones, rather than the lung or liver (Erbar, 2002).

1.1.1 Castration-resistant Prostate Cancer

In 1941, Charles Huggins and Clarence Hodges showed that the growth and proliferation of prostate tumors is highly dependent on androgens (Huggins & Hodges, 1941). Since then, androgen deprivation therapy (ADT) which inhibits androgen production (orchiectomy, LHRH analogs) or androgen receptor (AR) function (antiandrogens), is mainly used as a treatment for patients who have relapsed after local therapy or who were diagnosed with already disseminated tumors (Wirth *et al.*, 2009). However, despite this treatment, most patients eventually experience disease progression within a median of 18–24 months and develop a more aggressive form of PCa (Huang *et al.*, 2018). At this state the tumors develop independent of hormones, which is referred to as castration-resistant prostate cancer (CRPC) (Galletti *et al.*, 2017). Intriguingly at this stage of the disease the tumors still remain dependent on AR signalling for growth (de Bono *et al.*, 2011; Fizazi *et al.*, 2012).

The development of hormone-sensitive prostate carcinoma to CRPC is a multi-step process in which the AR still plays a key role. There are several mechanisms that can contribute to the transition to CRPC such as (i) amplification of the AR gene (Visakorpi *et al.*, 1995a), (ii) changes in the expression or mutations of the AR (Lallous *et al.*, 2016; Taplin *et al.*, 2003; Chandrasekar *et al.*, 2015), (iii) expression of AR splice variants (Dehm & Tindall, 2011; Guo *et al.*, 2009; Hu *et al.*, 2009), (iv) post-translational modifications of the AR (van der Steen *et al.*, 2013), as well as (v) changes in the expression or mutations of AR coactivators (Shiota *et al.*, 2010; Xu *et al.*, 2009) and (vi) intratumoral production of androgen (Cai *et al.*, 2011). A better understanding of the underlying molecular mechanisms of the different resistant pathways is crucial for the development of novel therapies for the treatment of CRPC.

1.2 Androgen Receptor

1.2.1 Androgren Receptor Structure

Androgens exert their growth promoting action in PCa through binding to the androgen receptor (AR) and is therefore a key protein in the development and progression of PCa and the main target in prostate cancer therapy (Brinkmann, 2011).

The AR is a nuclear receptor belonging to the family of steroid hormone receptors. The AR encoding gene is localized on the X-chromosome (q11-12), has a length of 90 kb and consists of 8 exons and 7 introns (Migeon *et al.*, 1981; Brown *et al.*, 1989; Lubahn *et al.*, 2014). The

AR-protein has a molecular mass of approximately 110 kDa and consists, like all steroid hormone receptors of four structurally and functionally distinct domains: (i) a N-terminal domain (NTD), important for transactivation (residues 1–555) (ii) a centrally-located DNA-binding domain (DBD; residues 555–623) (iii) a variable hinge region (residues 623–665) and (iv) a C-terminal ligand-binding domain (LBD) (residues 665–919) (Bennett *et al.*, 2010). The DBD shares the highest sequence homology with other steroid hormone receptors. The AR LBD is also highly conserved amongst some receptors of the family. In contrast, N-terminal domain as well as the hinge region differ greatly in size and primary sequence amongst the different receptor and can therefore be considered receptor-specific (Burris & McCabe, 2000) (Figure 1.1).

The AR NTD is encoded by exon 1 and contributes to almost half of the AR size. It is known that the AR NTD is required for full transactivation of the AR (Claessens, 2007). This activity is mediated mainly by the primary effector region *'activation function 1'* (AF-1), which can be further subdivided into the transactivation units τ1 (aminoacids 100-360) and τ5 (360-528) (Callewaert *et al.*, 2006; Chamberlain *et al.*, 1996). These regions play a crucial role in the ligand-dependent and independent transactivation of the AR. Furthermore, an ^{23}FQNLF^{27} motif is located N-terminally of the τ1 and a related ^{433}WHTLF^{437} is located in the τ5 region. Both motifs are known to play roles in the ligand-independent and interdomain interactions of the N- and C-terminal domains (N/C-interaction) of the AR (Dehm & Tindall, 2007; He *et al.*, 2000). This interaction stabilizes the AR homodimer complex and prevents ligand dissociation (Zhou *et al.*, 1995; Langley *et al.*, 1998). The NTD furthermore possesses polyglutamine (CAG) and polyglycine (GGC) repeats with varying length, which results in differences in published AR sizes. Deletion of the polyglutamine repeats results in reduced α-helical structures, whereas addition of glutamine repeats moderately increased α-helical structures. These conformational changes in the NTD impact protein-protein interactions and AR transactivation activity (Werner *et al.*, 2006; Davies *et al.*, 2008). In contrast to the AR DBD or LBD no X-ray crystallography study of the AR NTD has so far been carried out which mainly is due to its intrinsically disordered nature (Lavery & McEwan, 2008; Tan *et al.*, 2014). Intrinsically disordered regions are known to be involved in multiple protein-protein interactions and are considered to be the hubs for signaling networks inside cells. These regions most likely adapt transient structures upon binding to their interaction partner, allowing interactions with many diverse binding partners, including coactivators, the transcription machinery or transcription factors. These interactions are mostly of low affinity, however, cooperative binding of multiple partners allow for a highly specific regulation of AR activity (Wright & Dyson, 2015).

The centrally located AR DBD recognizes and binds to so called *androgen response elements* (ARE) on DNA. This binding is mediated by two *zinc finger* motifs, which consist of three α-helices and a C-terminal prolongation (Sawyers & Rauscher, 2014). The first zinc finger motif, which mediates direct binding to the DNA, contains a P box for specific sequence recognition of the ARE, which consists of two hexameric half-sites in direct repeat orientation (Umesono & Evans, 1989; Evans, 1988). The second zinc cluster contains a so called D-box (residues ^{596}-ASRND-^{600}), which mediates "head-to-head" protein-protein interactions and is therefore involved in the formation of homodimers (Glass, 1994). A nuclear localization signal which allows nuclear

import of the AR is localized at the transition of DBD to the hinge region (Kaku *et al.*, 2008; Zhou *et al.*, 1994).
The hinge region is a flexible region which is only moderately conserved among different steroid hormone receptors. The hinge region possesses acetylation sites, which regulate AR folding, subcellular localization, coactivator binding and transcriptional activity (Clinckemalie *et al.*, 2012; Haelens *et al.*, 2007).
The highly conserved C-terminal LBD is important for ligand-binding and interaction with heat shock proteins and coactivators (Tan *et al.*, 2014). Transactivation of most steroid hormone receptors is mediated by a region called *activation function 2* (AF-2), which enables the ligand-dependent transactivation activity (Moras & Gronemeyer, 1998). The prototypal LBD of steroid hormone receptors usually consists of 12 α-helices. However, helix 2 of the AR was replaced by a flexible linker, and therefore the AR LBD comprises only 11 helices (Tan *et al.*, 2015). Binding of testosterone or the more potent 5α-dihydrotestosterone (DHT) induces a conformational change in the AR LBD. Helices 3, 4 and 11 of the LBD are then reorganized and form a hydrophobic binding surface, referred to as *activation function-2*. The amphipathic helix 11 is thereby positioned on top of the binding surface to prevent dissociation of the ligand (Hur *et al.*, 2004). These conformational changes allow the binding of coactivators through their conserved motifs LxxLL or FxxLF to the AF-2. However, in contrast to other steroid hormone receptors the affinity of the AR AF-2 for coactivator binding motifs is lower in the presence of ligand (Hur *et al.*, 2004; He *et al.*, 2000; Dubbink *et al.*, 2004). Instead binding to an alternative binding motif in the AR NTD is preferred, resulting in the N/C-interaction, which exposes alternative coactivator binding sites in the AR NTD and hinge region (Claessens, 2007; Dehm & Tindall, 2007; Clinckemalie *et al.*, 2012). Additionally, a binding surface termed *binding function 3* (BF-3) had recently been identified in the LBD. This surface was found to be an allosteric modulator for AF-2 coactivator recruitment (Estébanez-Perpiñá *et al.*, 2007).

1.2.1.1 Androgen Receptor splice variants in CRPC

During castration resistance most PCa cells still depend on AR activity (Castellan *et al.*, 2018; de Bono *et al.*, 2011; Fizazi *et al.*, 2012). However, it is so far poorly understood which molecular mechanism lead to a renewed enhancement of AR action after ADT (AR reactivation). One of the mechanism suggested to contribute to continuous AR activity in the nucleus is the expression of AR splicevariants (AR-SV). Most of these AR-SV lack a ligand-binding domain and are mostly constitutively active (Dehm *et al.*, 2008; Guo *et al.*, 2009; Hu *et al.*, 2009; Sun *et al.*, 2010; Lu & Luo, 2013).
Many AR-SV have so far been identified in PCa models, xenografts or patient samples (Lu & Luo, 2013). The most commonly described and best characterized splice-variant is AR-V7. It was found that AR-V7 is overexpressed in metastases of CRPC patient (Hörnberg *et al.*, 2011; Qu *et al.*, 2015) and its expression is correlated with androgen-independent proliferation and PCa progression (Dehm *et al.*, 2008).

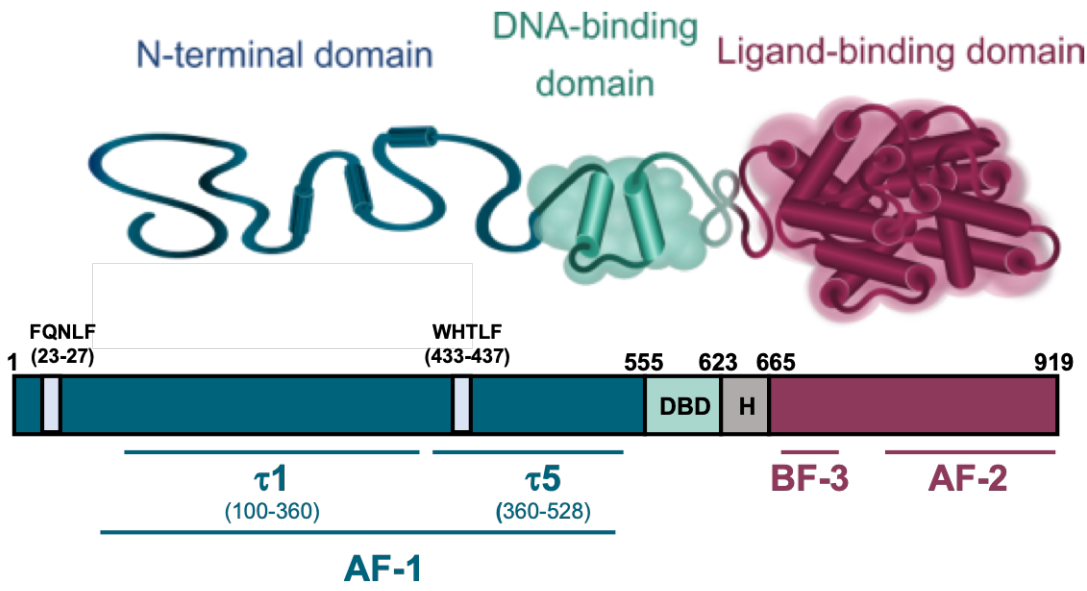

Figure 1.1: AR structure
Schematic represantation of the AR structure. The AR possesses multiple functional domains: the N-terminal domain (NTD, blue), the DNA-binding domain (DBD; green), a short hinge region and the ligand binding domain (LBD, red). The NTD contains the *activation function-1* which can further be subdivided into the transactivation units τ1 and τ5. The DNA-binding domain comprises two zinc finger motifs. The LBD encompasses the *activation function-2* as well the allosteric modulator *binding function 3*

AR-SV can arise from different mechanisms like alternative splicing or genomic rearrangements (Dehm *et al.*, 2008; Guo *et al.*, 2009; Hu *et al.*, 2009; Sun *et al.*, 2010). However, low androgen levels are required for AR-SV formation. Structurally, AR-V7 shares the conserved N-terminal AF-1 domain, the DNA-binding domain and part of the hinge region with the full-length AR (AR-FL). However, instead of the classical LBD, this AR variant possesses a unique C-terminal sequence composed of 16 amino acids termed cryptic exon 3 (Hu *et al.*, 2009).
On the cellular level AR-V7 is exclusively localized in the nucleus (Hu *et al.*, 2009). It was previously shown that AR-V7 co-localizes and forms heterodimers with AR-FL. Intriguingly, AR-V7 preferentially interacts with co-repressors and acts predominantly as a repressor of transcription for genes that limit CRPC proliferation (Cato *et al.*, 2019). This hints at a distinct role of AR-V7 compared to AR-FL in CRPC.

1.2.2 Androgen Receptor Action

The AR is a ligand-dependent transcription factor which regulates transcription of androgen-responsive genes (Mangelsdorf *et al.*, 1995). It plays a crucial role in the male sexual development and differentiation, as well as in different diseases such as *spinal and bulbar muscular atrophy*, androgen insensitivity syndrome and prostate cancer (Brinkmann *et al.*, 1995; Heinlein & Chang, 2002).
In the absence of hormone the AR forms a complex with heat-shock proteins, chaperones and cochaperones, which maintain the AR conformation relevant for ligand-binding (Cato & Peterziel,

1998; Peterziel *et al.*, 1999). In the ligand- bound state the AR adopts an active conformation, exposing the AF-2 region shaped by helices 3, 4 and 11 (Hur *et al.*, 2004). This conformational change induces dissociation of the AR from the chaperone complex, AR phosphorylation and N/C interaction of the AR. Subsequent exposure of the NLS (^{617}-RKCYEAGMTLGARKLKK-^{634}) allows nuclear import of the AR through binding to importin-α (Brinkmann *et al.*, 1999; Nazareth & Weigel, 1996).
Inside the nucleus the AR acts as a homodimer and recognizes AREs in the promotor or enhancer regions of AR target genes. Binding to the imperfect palindromic hexameric elements GG(A/T)ACAnnnTGTTCT enables the interaction of the AR with cofactor proteins as well as the basal transcription machinery (Roche *et al.*, 1992; Shang *et al.*, 2002; Burris & McCabe, 2000). Here the AR binds to components of the preinitiation complex (PIC), such as the *TATA-Box binding protein* (TBP) and helicase TFIIH (Transcription factor II H) (Mcewan & Gustafsson, 1997). Besides the classical ARE consensus sequence, more specific response elements for AR binding which are often partial replication of the canoncial hexamer $^{5'}$-TGTTCT-$^{3'}$ were identified in androgen-regulated genes (Rennie *et al.*, 1993; Adler *et al.*, 1993; Rundlett & Miesfeld, 1995; Claessens *et al.*, 1996; Verrijdt *et al.*, 2002)

1.2.2.1 Targeting AR signalling in PCa therapy

An early detection of prostate tumors ensures better prognosis for patients and allows for more treatment options. Early detection methods include tactile examinations of the prostate and the laboratory determination of blood PSA-levels. Increased PSA-levels, however, are only an indication but no definite proof for an existing tumor (Wirth *et al.*, 2009). To validate the results of PSA screenings and to determine the tumor stage, different instrument-based methods are employed, like the digital-rectal and transrectal ultrasound examination, follow-up punch biopsies of the prostate and x-ray examinations to rule out the existence of metastases (Wirth *et al.*, 2009).
At the time of diagnosis, most patients have usually developed a locally confined tumor. At this early stage patients can be monitored via active surveillance ("watchful waiting) to prevent unnecessary, overtreatment (Erbar, 2002). Furthermore, locally confined tumors are primarily treated by radical prostatectomy and/or radiation therapy and are well-managed this way. For metastatic or recurrent tumors androgen deprivation therapy (ADT) is the standard therapy. Here tumor growth is inhibited by (i) blocking androgen biosynthesis or by (ii) applying anti-androgens that compete with endogenous androgens for AR binding (Wirth *et al.*, 2009).
The former is achieved by a compound class comprising (LHRH) agonists and antagonists (Labrie *et al.*, 1982; Schally *et al.*, 1971), as well as abiraterone acetate (Castellan *et al.*, 2018), which inhibit important steps in androgen biosynthesis. While LHRH agonists and antagonists affect the release of luteinizing hormone (LH), which promotes testosterone production in the Leydig cells of the testis, abiraterone inhibits the enzyme CYP17, a key protein in testosterone synthesis (Rowlands *et al.*, 1995). Abiraterone is able to inhibit androgen production in the adrenal glands, testes as well as intratumorally (Rice *et al.*, 2019). Treatment with abiraterone decreases serum testos-

terone levels to 1–2 ng/dL, which is a 20- to 50-fold reduction compared to surgical castration, resulting in a state called "super-castrate" (Suzman & Antonarakis, 2014).
The latter is achieved via a compound class that includes steroidal (e.g. cyproterone acetate) and non-steroidal antiandrogens (flutamide, bicalutamide and nilutamide) (Neri *et al.*, 1967; Furr, 1988; Raynaud *et al.*, 1979). Steroidal antiandrogens are structurally related to testosterone, and bind the AR but show reduced capacity to activate the receptor (Migliari *et al.*, 1999). Furthermore, steroidal antiandrogens can reduce androgen levels (and also estrogen levels) by stimulating the negative feedback loop at hypothalamus level (Singh *et al.*, 2000). However, steroidal antiandrogens show off-target hormonal activity, activating progesterone and glucocorticoid receptors. These off-target effects together with suppression of estrogen levels and partial AR activation lead to an increase of unwanted side-effects such as liver changes, hepatotoxicity as well as depression, anxiety, and fatigue in patients (Singh *et al.*, 2000). Non-steroidal anti-androgens show no structural relation to testosterone and therefore do not express any off-target hormonal activity (Singh *et al.*, 2000). Non-steroidal antiandrogens specifically inhibit androgen binding to the AR and thereby affecting AR translocation and downstream signaling (Singh *et al.*, 2000; Migliari *et al.*, 1999) The second-generation (non-steroidal) anti-androgens enzalutamide (Tran *et al.*, 2010), apalutamide (Clegg *et al.*, 2012) and darolutamide (Moilanen *et al.*, 2015) bind AR with higher affinity than first-generation anti-androgens resulting in lower IC_{50} (Rice *et al.*, 2019). These compounds affect AR translocation, DNA-binding and co-activator recruitment to the DNA-bound AR, resulting in an increased efficacy and potency (Rice *et al.*, 2019; Tran *et al.*, 2010; Clegg *et al.*, 2012; Moilanen *et al.*, 2015). At the CRPC stage the only treatment options available are chemotherapy (docetaxel and cabazitaxel) or immunotherapy. However, these therapies usually prolong the patient lifes for only a few months (Petrylak *et al.*, 2004; Tannock *et al.*, 2004).
Efforts to develop drugs that target the AR NTD have led to identification of three compounds. The bispecific antibody 3E10-AR441 accumulates in the nucleus of prostate cancer cells, due to its high affinity to DNA. At the same time, it binds the N-terminus or the AR, thereby inhibiting AR activity. Immunoprecipitation assays showed that 3E10-AR441 binds full-length AR, as well as ARv7 in VCaP and 22Rv1 cells. Furthermore, it was shown that 3E10-AR441 inhibits AR function in a ligand-dependent manner (Goicochea *et al.*, 2017). However, so far no data regarding the effect of 3E10- AR441 on tumor growth has been published.
Furthermore, chlorinated peptides called Sintokamides, isolated from the marine sponge Dysidea sp., were identified in a screen for natural marine extracts that inhibit AR activity in reporter gene analyses. Sintokamides were also shown to inhibit growth of AR positive but not AR negative PCa cells (Sadar *et al.*, 2008). However, these compounds need further characterization. The first AR-NTD targeting compound to enter clinical trials for prostate cancer therapy was Ralaniten acetate (EPI-506) that specifically binds to the $\tau 5$ region in the AR NTD (Myung *et al.*, 2013). Ralaniten acetate is a prodrug of Ralaniten (EPI-002) one of the four stereoisomers of EPI-001 (Myung *et al.*, 2013; Andersen *et al.*, 2010). It was able to reduce PSA serum levels predominantly at higher doses in some patients. However, it was discontinued in favor of EPI-7386 due to a high drug burden (NCT02606123).

1.3 AR coregulators

Even though the AR is able to interact with the basal transcription machinery, other regulatory proteins are involved in the transcriptional regulation of AR target genes (Katzenellenbogen & Katzenellenbogen, 1996). The expression of coregulators is considered to play a crucial role for the specificity of AR action (Heemers *et al.*, 2009). Coregulators are recruited by nuclear receptors in response to ligand-binding to either activate (coactivators) or repress (corepressors) the transcription of target genes (Wang *et al.*, 2005; Heinlein & Chang, 2002; McKenna *et al.*, 1999). Coactivators can be subdivided in different groups: (i) proteins that connect parts of the preinitiation complex to the chromatin-bound receptor. (ii) proteins that modify chromatin via histone acetyltransferase (HAT) activity, in order to expose promotor regions and subsequently facilitate binding of transcription factors (McKenna & O'Malley, 2002; Glass & Rosenfeld, 2000). The best-characterized coactivators are the members of the p160-family and of the p300/CBP-family (Heinlein & Chang, 2002; Culig *et al.*, 2004). The p160 family comprises SRC-1/NCoA1, SRC-2/NCoA2/TIF2 and SRC-3/NCoA3/TRAM1, which interact with nuclear receptors and recruit transcriptional enzymes to chromatin to facilitate the assembly of general transcription factors for transcriptional activation (Xu *et al.*, 2009). The p300/CBP coactivator family consists of two closely related proteins, p300/EP300 and CBP (CREB-binding protein). Both proteins posses an intrinsic histone acetyltransferase (HAT) activity (Jin *et al.*, 2011) which allows the remodeling of chromatin at the promotor level. Both proteins further recruit the basal transcriptional machinery including RNA polymerase II to the promoter and act as adaptor molecules (Goodman & Smolik, 2000).

Most of classical NR coregulators, interact with the AF-2 in the AR LBD via a LxxLL motif in a hormone-dependent manner. Binding of androgens induces rearrangements of hydrophobic and charged amino acids in helix 11 of the LBD (He *et al.*, 2002; Estébanez-Perpiñá *et al.*, 2005). These hydrophobic clefts binds to the α-helix formed by the LxxLL motif (Darimont *et al.*, 1998). However, interactions with coactivator are not only mediated by LxxLL motifs. Phage display analysis demonstrated that the AR AF-2 preferentially binds to the related phenylalanine-rich motif FxxLF at the AR NTD, due to conformational constraints (Hsu *et al.*, 2003). This motif was originally identified at the AR NTD (^{23}FQNLF^{27}) as essential for mediating the intramolecular N/C interaction of he receptor. However, this motif is also present in other coactivators, such as ARA70/RFG, ARA55/Hic-5, and ARA54 (He *et al.*, 2002).

Other coactivators bind to the AR NTD independent of a LxxLL or FxxLF motif. For example, the co activator MED1 (*mediator of RNA polymerase II transcription subunit 1*) binds to the τ1 region in the AR NTD via two non-canonical α-helices (Jin *et al.*, 2012). Furthermore, some coactivators interact with the DBD/hinge-region of the AR, like BAF57 (BRG1-*associated factor 57*), which mediates its interaction through a proline-rich- and a high mobility group HMG (Link *et al.*, 2008). This shows that different coactivators use different domains to enhance AR transactivation.

Some AR coactivator are expressed in a cell- and tissue-specific manner. It is thought that these coactivators selectively enhance AF-2 accessibility for other coactivators. For example the coac-

tivators *Melanoma Antigen-11* (MAGE-A11) and Cyclin D1 bind to the ^{23}FQNLF^{27} motif and compete with the N/C interaction of the AR (Burd *et al.*, 2005; Bai *et al.*, 2005, 2008), thus enhancing the recruitment of coactivators of the p160- and p300/CBP-family to the exposed AF-2 region (Askew *et al.*, 2009, 2010).

1.3.1 AR coactivators in prostate cancer

Many coactivators of the p160-family as well as CBP are not only overexpressed in the primary prostate tumors but also in the metastatic tumor. Furthermore, expression of coactivators contributes to the specificity of AR action in prostate cancer and changes in coactivator expression drastically affect AR activity (Heemers *et al.*, 2009; Xu *et al.*, 2009).
Prostate cancer cells are able to adapt to an environment with low androgen concentrations in the progression to CRPC and it is reported that over-expression of different coactivators is one of the mechanisms to enhance AR sensitivity to low androgen concentrations. Furthermore, expression of some coactivators leads to resistance to antiandrogens (Huang *et al.*, 2018).
Coactivators are therefore interesting therapeutic targets for treatment of recurring prostate cancer (Chmelar *et al.*, 2007; Heemers & Tindall, 2005; Agoulnik *et al.*, 2003). The inhibition of coactivators that are specifically overexpressed in prostate tumors and that promote tumor growth and survival might be a promising strategy to overcome resistance in advanced PCa

1.4 BAG1 family of proteins

One protein that is known to modulate AR activity in PCa is Bcl-2 associated athanogene-1L. The term *Bcl-2 associated athanogene-1* (BAG1) is derived from the greek words a-/anti- meaning against and thanaton meaning death and can be ascribed to the fact that BAG1 proteins enhance the anti-apoptotic properties of BCL2 (Takayama *et al.*, 1995). In contrast to the known AR coregulators BAG1L does not possess a classical LxxLL- or FxxLF-motif for AR, which suggest that it must use other mechanisms to regulate AR activity. In pathological conditions BAG1 expression is correlated with different neurodegenerative diseases like Alzheimer's or cancers (Gamerdinger *et al.*, 2009; Takayama *et al.*, 1997). The first BAG1 coding gene was identified in a screen for interaction partners of Bcl2 using murine cDNA libraries of the mouse (Takayama *et al.*, 1995). Meanwhile, four more BAG proteins have been identified (BAG2-5), which all possess a conserved C-terminal BAG domain. However, BAG5 contains 5 tandem repeats of the BAG domain, but only the 5th repeat is functionally related to the classical BAG domain of BAG1 (Arakawa *et al.*, 2010). In humans, BAG1L belongs to a family of four proteins (BAG1L (50 kDa), BAG1M (46 kDa), BAG1 (36 kDa) and BAG1S (29 kDa)) derived from the same mRNA by alternative translation-initiation. This mechanism results in highly conserved C-terminal regions but variable N-terminal sequences. The translation of the largest isoform, BAG1L, begins at a non-canonical CUG-codon, while the other three isoforms are translated from AUG start-codon (Takayama *et al.*, 1997; Yang *et al.*, 1998). Alternative translational start sites such as the non-AUG start codon of BAG1L

are thought to regulate subcellular localization and/or distinct biological functions of the different isoforms (Touriol *et al.*, 2003). BAG1L is the only BAG1 isoform which possesses a complete NLS and is therefore localized in the nucleas, where it can regulate the activity of NR (Takayama *et al.*, 1998; Shatkina *et al.*, 2003).

The BAG domain consists of 110-124 amino acids and is composed of three antiparallel α-helices, which are organized by 30-40 amino acids (Takayama & Reed, 2001). The BAG domain is an important interaction surface for a variety of proteins, including the anti-apoptotic protein Bcl2, heat-shock proteins of the Hsp/Hsc70-family, as well as the serine/threonine kinase Raf-1, which plays an important role in *mitogen-activated protein kinase* (MAPK)-signaling pathways (Takayama *et al.*, 1997; Briknarová *et al.*, 2001; Sondermann *et al.*, 2001). BAG1 proteins furthermore possess a centrally located ubiquitin-like domain (ULD), which links the chaperone activity of Hsp70 to the degradation complex for misfolded proteins (Lüders *et al.*, 2000). The different BAG1 proteins possess varying number of copies of a TR/QSEEX-motif. This region can be targeted by several kinases, however, its exact function is so far unknown (Takayama *et al.*, 1997). The largest isoform BAG1L is the only BAG1 isoform that carries an entire nuclear localization signal (NLS) and is therefore localized in the nucleus (Takayama *et al.*, 1997; Shatkina *et al.*, 2003). The isoform BAG1M possesses a shorter version of the NLS motif and can also migrate to the nucleus under stress conditions (Zeiner *et al.*, 1999).

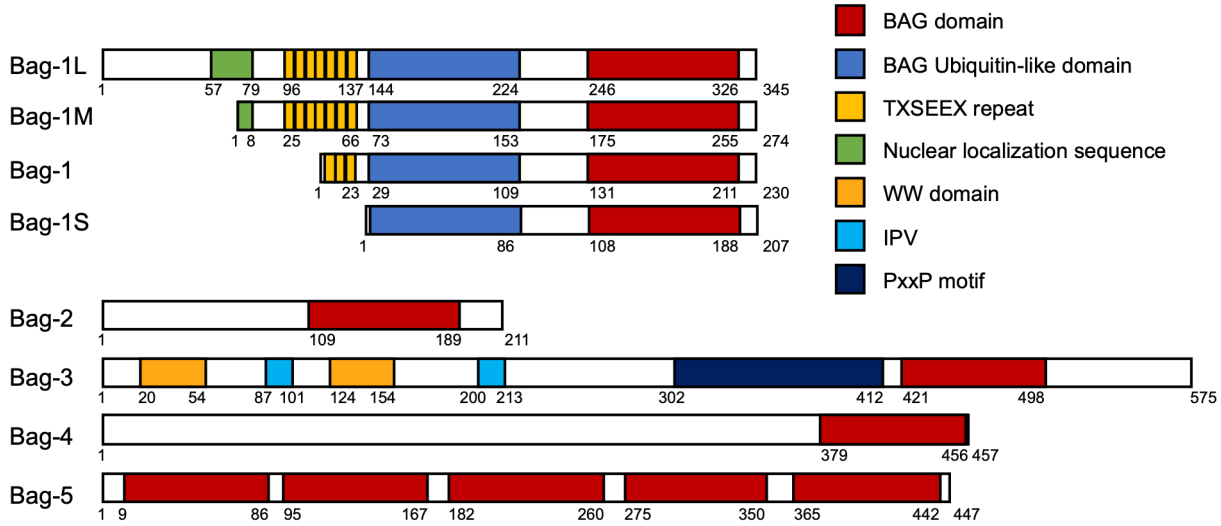

Figure 1.2: BAG proteins
Schematic diagram of the human BAG proteins representing the BAG domain, the ubiquitin-like domain, TXSEES repeats, the nuclear localization sequence, the WW domain, the IPV (Ile-Pro-Val) motifs and the PxxP motif. The domains of the proteins are derived from UniProt.

One of the best studied protein-protein interactions (PPI) of BAG1 proteins is with the molecular Chaperones Hsp70/Hsc70. Under stressful conditions, like heat shock or hypoxia, Hsp70/Hsc70 prevents the accumulation of misfolded proteins in the cytosol (Sondermann *et al.*, 2001). The ATPase-domain of Hsp70, which is important for ATP binding, hydrolysis and nucleotide exchange, was shown in NMR studies to bind helices two and three of the BAG domain of BAG1 (Briknarová *et al.*, 2001; Townsend *et al.*, 2003). Site-directed mutagenesis in the binding surface

confirmed these findings, resulting in a loss of binding of BAG1 to Hsc70 in yeast-two-hybrid and transfection experiment (Briknarová *et al.*, 2001). A 1.9 angstrom crystal structure of the BAG domain bound to Hsc70 has been resolved and showed that the three-helix bundle of the BAG domain induces conformational changes in the ATPase domain of Hsc70 to prevent nucleotide binding (Sondermann *et al.*, 2001). It is therefore thought that binding of the BAG domain to the nucleotide binding domain of Hsp70 enables ADP release, accelerates ATP cycle and promotes the refolding activity of Hsp70. Hence BAG1 is classified as a nucleotide exchange factor for Hsp70.

1.4.1 BAG1L regulation of AR activity

It has previously been shown that the BAG domain of BAG1L enhances the transactivation function of the AR through interaction with the AR NTD τ5 region (residues 360-528) (Shatkina *et al.*, 2003). This interaction is most likely transient, as NMR studies showed reduction in resonance intensities at the C-terminal part of AR τ5 in NMR experiments (Cato *et al.*, 2017). The residues that showed reduced resonance intensities were previously identified to be present in a partially folded region in the otherwise intrinsically disordered AR NTD (De Mol *et al.*, 2016). Additionally, triple alanine substitutions in helices one and two of the BAG domain abolished the changes in resonance intensities, showing that these residues are important for BAG domain binding to the AR NTD. These mutations also reduced BAG1L-mediated AR transactivation activity but had no effect on the interaction with Hsp70 (Cato *et al.*, 2017). This suggests that BAG domain has different binding sites for protein-protein interactions (PPIs) with AR and Hsp70. This would allow targeting the BAG domain-AR NTD interaction without interfering with its nucleotide exchanged factor function for the molecular chaperone Hsp70 (Cato *et al.*, 2017).
Besides the BAG domain another binding motif for the AR was identified in the N-terminal region of BAG1L. A duplicated hexapeptide motif, GARRPR (residues 6-11 and 66-71), was shown to interact with the allosteric *binding factor 3* (BF3) region in the AR LBD (Jehle *et al.*, 2014). The GARRPR motif is exclusive to BAG1L and was not identified in other cofactors that bind the AR NTD, such as members of p160 family or MED1 (Alen *et al.*, 1999; Bevan *et al.*, 1999; Christiaens *et al.*, 2002; Jin *et al.*, 2012). These findings suggest that BAG1L links the N- and C-terminal regions of the AR, however, there was so far no connection of BAG1L to other proteins, such as MAGE-A11, that modulate N/C interactions, suggesting a unique role of this protein in AR action (Liu *et al.*, 2011; Minges *et al.*, 2013).

1.4.2 BAG1L in prostate cancer

Given the fact that BAG1L regulates AR activity, its role in the development and progression of prostate cancer is therefore of great interest.
The connection between BAG1L and prostate cancer was reported when localization of BAG1L and AR in benign and malignant prostate tissue became evident. While AR was expressed in the epithelium of benign and malignant prostate tissue, BAG1L was found in the basal cells in benign

tissue and its expression was shifted to the secretory epithelium in malignant tissue, suggesting a colocalization of BAG1L and AR under tumor conditions (Shatkina *et al.*, 2003). Furthermore, in immunohistochemical studies BAG1L expression was increased in hormone refractory PCa compared to localized untreated tumors (Krajewska *et al.*, 2006; Maki *et al.*, 2007). Additionally, it was shown that BAG1 gene is amplified in 6 of 81 of hormone refractors patient samples, while no gene amplification was observed in 130 patient samples of untreated patients (Maki *et al.*, 2007). Recent studies showed that nuclear BAG1 (corresponding to BAG1L) is overexpressed in metatstatic CRPC patient samples compared to samples of hormone-sensitive PCa patients. Furthermore, expression levels of nuclear BAG1L correlated with a reduced clincal benefit from abiraterone (Cato *et al.*, 2017).

These findings suggest a role of BAG1L in advanced hormone-refractory PCa. As previously mentioned, the expression of AR-SV is one mechanism suggested for AR reactivation in CRPC. Given the fact that BAG1L regulates AR activity through interaction with the τ5 region in the AR NTD, BAG1L might also play a role in the regulation of AR-SV (Shatkina *et al.*, 2003; Cato *et al.*, 2017). Therefore, BAG1L might be suitable molecule to target for the treatment of CRPC patients. The BAG1 inhibitor Thio-2, an N-ethyl-4-(6- methyl-1,3-benzothiazol-2-yl)aniline compound was reported to bind the BAG domain of BAG1 in *in silico* analyses (Enthammer *et al.*, 2013). Accordingly, Thio-2 was shown to reduce BAG1L-mediated AR AF1 activity in mammalian-one-hydrid assays and reduced binding of BAG1L to the AR in a coimmunoprecipitation experiments. Furthermore, hormone-senstive LNCaP cells showed reduced proliferation upon treatment with Thio-2 with an IC_{50} of 17.5 μM (Cato *et al.*, 2017). Even though this effect was only observed at high concentrations (IC_{50}) the data suggest that BAG1L might be a promising target in overcoming resistance in CRPC.

1.5 Aim of this work

PCa is the most commonly diagnosed cancer in males. In the early stages of PCa, the tumors depend on androgens for proliferation and progression. Therefore, reducing androgen-mediated signaling is an effective strategy to reduce PCa growth in the early stages of the disease. Androgens exert their growth-promoting effects through binding to the AR. Upon ligand-binding the AR regulates the expression of genes that mediate growth and proliferation. During consecutive treatment the behavior of PCa cells changes and a shift to androgen-independent growth occurs. Mechanism contributing to the switch to androgen-independence include the overexpression of AR-SV. Most of these AR-SV lack the AR LBD but are constitutively active. Targeting the N-terminal domain of the AR would provide a promising alternative for treatment of CRPC patients. However, this approach has proven to be difficult to implement due to the intrinsically disordered region of the AR NTD.

Instead targeting regulatory proteins that bind the AR NTD is much more promising in order to overcome resistance in advanced PCa. One protein that is known to bind the AR NTD in the $\tau 5$ region and to regulate AR activity is the cochaperone BAG1L. BAG1L colocalizes with the AR in the secretory epithelium exclusively in PCa and BAG1L expression is enhanced in CRPC.

The aim of this work is to determine how BAG1L regulates AR activity at the AR NTD by systematic analysis of the sequences that constitute BAG1L interaction surface using NMR analysis, site-directed mutagenesis and transfection experiments. A further aim is to identify the downstream signaling pathway of BAG1L reguulated AR activity.

In addition, compounds that inhibit the BAG1L-AR interaction are to be identified for use as potential selective inhibitors of AR-NTD activity and AR dependent PCa growth.

2 Material and Methods

2.1 Materials

2.1.1 Chemicals

Table 2.1: Chemicals

Name	Source
Agarose	Peqlab, Erlangen, Germany
Ampicillin	Roth, Karlsruhe, Germany
Ammonium Persulfate (APS)	Roth, Karlsruhe, Germany
Bovine Serum Albumine (BSA)	PAA Laboratories GmbH, Pasching, Austria
Bacto-Agar	Otto Nordwald GmbH, Hamburg, Germany
Bacto-Trypton	Roth, Karlsruhe, Germany
Bacto-yeast extract	Roth, Karlsruhe, Germany
Dimethylsuloxide (DMSO)	Fluka, Neu Ulm, Germany
Dithiothreitol (DTT)	Gibco, Invitrogen, Karlsruhe; Germany
DNA Marker 1 Kb	PeqLab, Erlangen, Germany
Dulbecco's Modified Eagle Medium (DMEM)	Gibco, Invitrogen, Karlsruhe, Germany
Ethylenediamine Tetraacetic Acid (EDTA)	Roth, Karlsruhe, Germany
Ethanol (EtOH)	Roth, Karlsruhe, Germany
Ethidium Bromide	Roth, Karlsruhe, Germany
FBS (Fetal Bovine Serum)	Gibco, Invitrogen, Karlsruhe, Germany
G418 (Geneticin®)	Sigma Aldrich, Taufkirchen, Germany
Glycylglycerine	Roth, Karlsruhe, Germany
Glycine	Roth, Karlsruhe, Germany
Glycerol	Roth, Karlsruhe, Germany
Glucose	Roth, Karlsruhe, Germany
Glutamine	Sigma Aldrich, Taufkirchen, Germany
Hydrogen Chloride (HCl)	Roth, Karlsruhe, Germany
Isopropanol	Roth, Karlsruhe, Germany
Magnesium Chloride	Roth, Karlsruhe, Germany
Magnesium Sulfate	Roth, Karlsruhe, Germany
β-mercaptoethanol	Roth, Karlsruhe, Germany
Nonident P-40 (NP40)	Boehringer, Mannheim, Germany
1x Phosphate Buffered Saline (-$CaCl_2$/$MgCl_2$)	Gibco, Invitrogen, Karlsruhe, Germany
PMSF (phenyl methanesulphonyl fluoride)	Sigma Aldrich, Taufkirchen, Germany
Potassium Chloride	Merck, Darmstadt, Germany

Name	Source
Protein Marker	PeqLab, Erlangen, Germany
Rotiphorese (Acrylamide/bisacrylamide (30%) (w/v))	Roth, Karlsruhe, Germany
Rotisol	Roth, Karlsruhe, Germany
RPMI medium 1640	Gibco, Invitrogen, Karlsruhe, Germany
Sodium Chloride	Roth, Karlsruhe, Germany
Sodium Dodecyl Sulphate (SDS)	Roth, Karlsruhe, Germany
Sodium Hydroxide	Roth, Karlsruhe, Germany
Sodium N-lauryl sarcosinate (Sarkosyl)	Sigma Aldrich, Taufkirchen, Germany
Tetramethyl ethylen diamine (TEMED)	Roth, Karlsruhe, Germany
Tris-base	Roth, Karlsruhe, Germany
Tris-HCl	Roth, Karlsruhe, Germany
Triton-X-100	Sigma Aldrich, Taufkirchen, Germany
Trypsin (0,25%)-EDTA	Gibco, Invitrogen, Karlsruhe, Karlsruhe
Tween 20	Roth, Karlsruhe, Germany

2.1.2 Consumables

Table 2.2: Consumables

Name	Source
10 cm Bacto-petri dishes	Greiner Bio-One, Nürtingen, Germany
15 cm cell culture petri dishes	Greiner Bio-One, Nürtingen, Germany
10 cm cell culture petri dishes	Greiner Bio-One, Nürtingen, Germany
6-well multiwell plates	Greiner Bio-One, Nürtingen, Germany
12-well multiwell plates	Greiner Bio-One, Nürtingen, Germany
24-well multiwell plates	Greiner Bio-One, Nürtingen, Germany
48-well multiwell plates	Greiner Bio-One, Nürtingen, Germany
Corning T-75 CellBind Flask	Stein Labortechnik, Remchingen, Germany
50 ml reaction tube	Greiner Bio-One, Nürtingen, Germany
15 ml reaction tube	Greiner Bio-One, Nürtingen, Germany
2 ml reaction tube	Eppendorf, Hamburg, Germany
1,5 ml reaction tube	Eppendorf, Hamburg, Germany
96-well PCR Plate	Steinbrenner Laborsysteme GmbH Wiesenbach German
qPCR sealing film	Steinbrenner Laborsysteme GmbH Wiesenbach German
1 ml pipetttips (blue)	Stein Labortechnik, Remchingen, Germany
200 µl pipetttips (yellow)	VWR International, Bruchsal, Germany
3 ml syringes	Braun, Melsungen, Germany
Sterile filter (pore size 0,22 µm)	Carl Roth, Karlsruhe, Germany

2.1.3 Bacterias

Table 2.3: Bacteria strains

Name	Genotype	Application
E. coli DH5α	F-, endA1, hsdR17 (r_k^-, m_k^+), supE44, Δlac, U169 (ϕ80lacZΔM15), thi-1, λ-, recA1, gyrA96, relA1 (Meselson , Nature 1968)	Amplification of plasmid DNA
BL21 (DE3) pLysS	F-, ompT, hsdS_B (r_B^-, m_B^-), dcm, gal, DE3, pLysS (Cm^r) (Studier and Moffatt, J. Mol. Biol. 189 (1986)	Expression of proteins

2.1.4 Cell lines

Table 2.4: Mammalian cell lines

Name	Source & description
LNCaP	Human, androgen-sensitive prostate adenocarcinoma cell lines, which is derived from the left supraclavicular lymph node metastasis of a 50-year old caucasian man (Horoszewicz *et al.*, 1983)
Control LNCaP cells	Vector control for TALEN-induced BAG1L KO LNCaP cells (Cato *et al.*, 2017)
BAG1L KO LNCaP cells	LNCaP cell carrying a TALEN-induced Bag-1L KO (Cato *et al.*, 2017)
LNCaP95	Human prostate adenocarcinoma cell line derived from LNCaP cells cultured in phenol red-free RPMI-1640 with 10% (v/v) charcoal stripped FBS (Pflug *et al.*, 1999)
LNCaP95-shGFP	LNCaP95 cells that were lentivirally transduced with vector pLKO-Tet-On (Wiederschain *et al.*, 2009) expressing shRNA for targeting GFP (Cato *et al.*, 2019)
LNCaP95-shAR-FL	LNCaP95 cells that were lentivirally transduced with vector pLKO-Tet-On (Wiederschain *et al.*, 2009) expressing shRNA for targeting AR-FL (exon 8) (Cato *et al.*, 2019)
LNCaP95-shAR-V7	LNCaP95 cells that were lentivirally transduced with vector pLKO-Tet-On (Wiederschain *et al.*, 2009) expressing shRNA for targeting AR-V7 (cryptic exon 3) (Cato *et al.*, 2019)
LNCaP95-BAG1L	LNCaP cells transduced with an expression vector for BAG1L (pOZN) (Cato *et al.*, 2017)
LNCaP95-vector	LNCaP cells transduced with an empty vector construct (pOZN) (Cato *et al.*, 2017)

HeLa	Human epithelial cells derived from a cervix carcinoma of a 31-year old afro-american woman
COS-7	fibroblast-like cell line derived from kidney tissue of the African green monkey (Gluzman, 1981)

The prostate cancer cell line LNCaP, as well as Control and BAG1L KO LNCaP cells were cultured in RPMI 1640 (Gibco, Invitrogen, Karlsruhe, Germany) supplemented with 10% (v/v) FBS (PAA Laboratories, Pasching, Austria). The CRPC model cell line LNCaP95 and all cell lines derived from it, were cultured in phenol red-free RPMI 1640 medium supplemented with 10% (v/v) charcoal/dextran-stripped FBS, penicillin/streptomycin (100 u/ml) and L-glutamine (2 mM). Cells expressing pLKO-Tet-On backbones were selected with 1 µg/ml puromycin and shRNA expression was induced with 1 µg/ml doxycycline. The human cervical cancer cell line HeLa and the fibroblast-like cell line COS-7 from the african green monkey were cultured in DMEM medium supplement with 10% (v/v) FBS.

2.1.5 Oligonucleotides

All nucleotides were ordered from the company *metabion* (Planegg, Germany) and were ordered desalted.
The following oligonucleotides were used for QuikChange-PCR (Kunkel, 1985):

Table 2.5: Oligonucleotides used for QuikChange PCR

Name	Sequence (5'-3' direction)
Tau5_L391A_FW	TCAAGCTGGAGAACCCGGCGGACTACGGCAGCGCCT
Tau5_L391A_REV	AGGCGCTGCCGTAGTCCGCCGGGTTCTCCAGCTTGA
Tau5_W397A_FW	TGGACTACGGCAGCGCCGCGGCGGCTGCGGCGGCGC
Tau5_W397A_REV	GCGCCGCCGCAGCCGCCGCGGCGCTGCCGTAGTCCA
Tau5_C404A_FW	CGGCTGCGGCGGCGCAGGCCCGCTATGGGGACCTGG
Tau5_C40A_REV	CCAGGTCCCCATAGCGGGCCTGCGCCGCCGCAGCCG
Tau5_R405S_FW	GCGGCGCAGTGCAGCTATGGGGACC
Tau5_R405S_REV	GGTCCCCATAGCTGCACTGCGCCGC
Tau5_C404AR405A_FW	CCAGGTCCCCATAGGCGGCCTGCGCCGCCGCAG
Tau5_C404AR405A_REV	CTGCGGCGGCGCAGGCCGCCTATGGGGACCTGG
Tau5_W397C404A_FW	CGGCAGCGCCGCGGCGGCTGCGGCGGCGCAGGCCCG CTATGGGG
Tau5_W397C404A_REV	CCCCATAGCGGGCCTGCGCCGCCGCAGCCGCCGCGGC GCTGCCG
BAGD_FW (R305A/R308A/K309A)	GAACCTTTTTTACCAAGCCTGCCGCTTTCAATGCACTG TCTTTGAAATTTTCTGGCAGGATCAGTGTGTCAAT

Name	Sequence (5'-3' direction)
BAGD_REV (R305A/R308A/K309A)	ATTGACACACTGATCCTGCCAGAAAATTTCAAAGACA GTGCATTGAAAGCGGCAGGCTTGGTAAAAAAGGTTC

The following oligonucleotides were used for qRT-PCR:

Table 2.6: Oligonucleotides used for qRT-PCR

Name	Sequence (5'-3' direction)
Rib36B4_FW	CTCCTGAGCGCAAGTACTCC
Rib36B4_REV	GTCACCTTCACCGTTGTTCCA
F5_FW	TCCAGGCCGAGAATACACCTA
F5_REV	CGATTTGCTTGTCAAACGTCTTC
DUOX1_FW	GTGCTCCCTCTGTTGTTCGT
DUOX1_REV	GCTTCTCAGACACGATGCTCT
MICAL1_FW	ATGGGCAGCCTGATGTCTCT
MICAL1_REV	GGCGCCATGCTTCTCTTG
NNT_FW	TGGTCAAGCAGGGTTTTAATGT
NNT_REV	TCCTTTGCCCCTTGGATTTGG

2.1.6 Enzymes

All enzymes for *polymerase chain reaction*, restriction enzymes and enzymes for ligation of DNA-fragments were obtained from New Enland Biolabs (Beverly, USA), Promega (Mannheim, Germany) and Thermo Fisher Scientific/Fermentas (St. Leon-Rot, Germany).

2.1.7 Plasmids

Table 2.7: Plasmids

Name	Description
pcDNA3.1 (+)	Eukaryotic expression vector carrying a CMV (Cytomegalovirus)-Promotor. For selection in eukaryotes the vector contains a Geneticin (G418)-resistance gene. For selection in bacteria the vector contains an ampicillin-resistance gene (Invitrogen, Karlsruhe, Germany)

Name	Description
pcDNA3.1-BAG1L(cMut)	Eukaryotic expression vector, which contains the cDNA of the human BAG1L gene. Expression of BAG1L is favored due to mutation of the CUG start codon to AUG and expression is controlled by T7-promotor. The plasmid was kindly provided by John C. Reed, M.D. Ph.D.. Mutations in the residues K231/232/279 to alanine (referred to as cMut) were introduced by QuikChange PCR and validated by sequencing (Cato2017).
pcDNA3.1-BAG1M(NLS)	Eukaryotic expression vector, which contains the cDNA of the human BAG1M gene or the BAG1M gene fused to an NLS of simian virus 40. The plasmids were described in Shatkina *et al.* (2003)
pcDNA3.1-AR-FL	Eukaryotic expression vector, expressing the human AR-FL protein. The plasmid was kindly provided by Laura Cato, Ph.D.
pcDNA3.1-AR-V7	Eukaryotic expression vector, expressing the human AR-V7 protein. The plasmid was kindly provided by Laura Cato, Ph.D.
pM	Eukaryotic expression vector, which carries the cDNA of the DNA-binding domain (DBD) of the yeast-specific transcription factor Gal4 (Gal4DBD, amino acids 1-147) The Fusion-protein is translocated to the nucleus due to a Gal4 nuclear resistance sequence. Upstream of the Gal4DBD a multiple cloning site is located. For selection in bacteria the plasmid carries an ampicillin resistance gene.
pM-AR-AF1/AF2	Eukaryotic expression plasmid, which was used for Mammalian-One-Hybrid Assay. The plasmid contains the coding sequence of the human AR-AF1 region (amino acids 1-556) or the human AR-AF2 (amino acids fused to the Gal4DBD.
pM-AR-τ5	Eukaryotic expression plasmid, which was used for Mammalian-One-Hybrid and Mammalian-Two-Hybrid Assay. The plasmid contains the coding sequence of the human AR-AF1τ5 region (amino acids 360-548) fused to the Gal4DBD (Shatkina2003)
pVP-16	Eukaryotic expression vector encoding the transactivation domain of the *Herpes simplex virus* VP16 protein. The plasmid was kindly gifted by Karin Knudsen, PhD.

Name	Description
pVP-BAG1L	Eukaryotic expression vector, which carries the coding sequence of the human BAG1L. Upstream of the BAG1L cDNA the transactivation domain of the *Herpes simplex virus* VP16 protein is located.
pG5E4Δ38-Luciferase	Reporter construct carrying the coding sequence of firefly luciferase controlled by five copies of the Gal4-DNA-binding site (*upstream activation sequence* (UAS)) upstream of the adenovirus E4 promotor. This plasmid was used for Mammalian-One-Hybrid- and Mammalian-Two-Hybrid-Assays (Barrett *et al.*, 1988)
PSA-Enhancer-luc	Reporter construct carrying the coding sequence of the firefly luciferase driven by the -3935 to -4326 PSA core enhancer upstream of the E4TATA box. The plasmid was kindly provided by Elizabeth M. Wilson, PhD
Ubi-renilla luciferase	Reporter construct, which expresses the *Renilla reniformis* Luciferase cDNA (Promega, Mannheim, Germany) under control of the Ubiquitin promotor. The plasmid was used in Luciferase assay to check transfection efficiency.
pET28-Gb1a-BAGD	Prokaryotic expression plasmid, containing a histidin (His)-tag. C-terminally of the tag a multiple cloning site is located, in which the coding sequence of the human BAG domain was cloned. Additionally, expressed proteins are fused to Gb1a (B1 Immunoglobulin binding domain of streptococcus protein G, 56 amino acids) to increase protein yield. Proteinexpression is controlled by the lac operon and can be induced by IPTG. For selection in bacteria the plasmid contains a kanamycin resistance gene.

2.1.8 Equipment

Measuring devices:

StepOnePlus™ Real-Time PCR System, Applied Biosystems, Darmstadt, Germany
VICTOR Light 1420 Luminsecence Counter, PerkinElmer, Rodgau, Germany

Software:

Adobe Photoshop CS5.1, Adobe Systems Incorporated
GraphPad Prism 6, GraphPad Software, San Diego, California, USA

Microsoft Word for Mac, version 16.16.20, Microsoft Corporation
Microsoft Excel for Mac, version 16.16.20, Microsoft Corporation
Microsoft Powerpoint for Mac, version 16.16.20, Microsoft Corporation
StepOnePlus software v2.3, Applied Biosystems, Darmstadt, Germany
Wallac 1420 Manager, Version 3.0, PerkinElmer Life Sciences, Wallac Oy, Finnland

2.2 Methods

2.2.1 DNA and RNA methods

2.2.1.1 Preparation of plasmid DNA ("Miniprep" and "Maxiprep")

Small-scale and large-scale purification of plasmid DNA was performed using materials of the Plasmid Midi Kit (Qiagen, Hilden).
For small-scale purification of plasmid DNA transformed bacteria were incubated ON at 37°C in 3 ml of 1x LB medium (1% (w/v) tryptone, 0.5% (w/v) yeast extract, 0.5% (w/v) NaCl) supplemented with 0.1 mg/ml ampicillin or 50 µg/ml kanamycin (according to the antibiotic resistance of the plasmid) on a shaker at 280 ppm. Thereafter 2 ml of the bacteria culture were transferred into an 1.5 ml reaction tube and centrifuged at 13.000 rpm for 3 minutes (Heraeus Biofuge pico, rotor #3328). The Pellet was resuspended in 200 µl of Buffer P1 (Resuspension Buffer) and the equal volume of Buffer P2 (Lysis Buffer) was added. The mixture was gently inverted and thereafter, incubated for 5 minutes at room temperature. Afterwards 200 µl of Buffer P3 (Neutralization Buffer) was added and the suspension was gently mixed by inverting. After 20 min of incubation on ice the solution was centrifuged at 14.000 rpm at 4°C for 10 min (Eppendorf centrifuge 5417 R; rotor F45-30-11). The supernatant was transferred into a new 1.5 ml reaction tube and DNA was precipitated by adding 800 µl of isopropanol. After gently mixing the solution was centrifuged at 14.000 rpm for 10 minutes at 4°C (Eppendorf centrifuge 5417 R; rotor F45-30-11). The pellet was washed twice with 1 ml of 70 % (v/v) ethanol. Thereafter, ethanol was removed and the residual ethanol was allowed to evaporate. The DNA was resuspended in 30-50 µl nuclease-free water.
For the large scale purification of plasmid DNA transformed bacteria were incubated ON at 37°C in 100 ml of 1x LB medium (1% (w/v) tryptone, 0.5% (w/v) yeast extract, 0.5% (w/v) NaCl) supplemented with 0.1 mg/ml ampicillin or 50 µg/ml kanamycin (depending on the selection marker of the plasmid) on a shaker at 280 ppm. The overnight culture was centrifuged at 4.000 rpm for 15 min at 4°C (Centrifuge Hermle ZK 401, rotor A.14). The pellet was resuspended in 4 ml of Buffer P1 (Resuspension Buffer) and the equal volume of Buffer P2 (Lysis Buffer) was added. After gently inverting the mixture was incubated for 5 minutes at room temperature. Thereafter, 4 ml of Buffer P3 (Neutralization Buffer) was added and the suspension was gently mixed. After 20 minutes incubation on ice the suspension was centrifuged at 4.000 rpm for 30 minutes at 4°C (Eppendorf centifruge 5810, rotor A-4-62). In the meantime a QIAGEN-tip 100 was equilibrated with

Table 2.8: QuikChange PCR program

temperature	cycle	repeat
95°C	5 min	
95°C	30 sec	16-18x
55°C	1 min	
68°C	1 min/kb (~7 min)	
4°C	∞	

4 ml of Buffer QBT (Equilibration Buffer). The supernatant was applied to the QIAGEN-tip and allowed to flow through. The column was washed twice with Buffer QC which was also allowed to move through by gravity flow. The DNA was eluted using 5 ml of Buffer QF (Elution Buffer) into a new falcon tube. Precipitation was performed using 3.5 ml of isopropanol. The suspension was centrifuged at 4.000 rpm for 30 minutes at 4°C (Eppendorf centifruge 5810, rotor A-4-62). After discarding the supernatant the pellet was washed twice with 70 % ethanol. The pellet was air dried and dissolved in approximately 200-400 µl.

2.2.1.2 QuikChange Polymerase Chain Reaction

QuikChange *polymerase chain reaction* (PCR) was used for *site-directed mutagenesis* of plasmid DNA. This allows *inter alia* the exchange of specific amino acids of a double-stranded plasmid. Oligonucleotides were designed individually according to the desired mutation. The desired mutation was placed in the center of an otherwise homologues 25-45 base pair oligonucleotide. The oligonucleotides were designed that their melting temperature was higher than 78°C and the GC-content was at least 40 %.
The reaction was performed using 50 nm of the template plasmid, 125 ng of forward- and reverse primer, 10 mM dNTPs and 2,5 U PfuTurbo DNA-Polymerase. The PCR reaction was carried out in T100 Thermal Cycler (BioRad, Feldkirchen, Germany) with the following steps:
After PCR reaction DpnI (10 u) were added to the reaction mixture, which was incubated for 1 h at 37°C to digest methylated and hemi-methylated DNA. The PCR product was used for the transformation of *E. coli* DH5α.

2.2.1.3 Restriction digestion, extraction of DNA from agarose gels and ligation

In some cases mutated regions were subcloned into other plasmids after QuikChange PCR. Therefore, both plasmids were digested with the same restriction enzymes and the fragments (vector and insert) were separated in agarose gel electrophoresis, extracted from the gel and ligated with the desired fragment.
For restriction enzyme digestion 10 µg of DNA were incubated for 1 h at 37°C with 10-20 U of the respective enzymes (High-Fidelity Enzymes, New England Biolabs, Frankfurt or FastDigest Enzymes, Thermo Fisher Scientific, Karlsruhe, Germany) in an appropriate amount (up to 50 µl) of CutSmart or FastDigest Buffer. These enzymes are fully active in their universal buffer system and 1 µl of these enzymes is able to cut 1 µg of Lamda-DNA in 5 min at 37°C.
The digested DNA was then separated according to the fragment size by electrophoresis in 1-2 % (w/v) agarose gels. The fragment of interest was extracted with a scalpel under UV-light. The extraction of DNA fragments from agarose gels was performed by using PeqGold Gel Extraction Kit (PeqLab Biotechnologie GmbH, VWR, Bruchsal, Germany) according to manufacturer protocol. The weight of the piece of gel was determined and an equal volume of Binding Buffer was added. The gel was dissolved at 55°C for 7 min. The DNA/Agarose-solution was transferred into a PerfectBind-column which was then centrifuged at 10.000 rpm for 1 min (Eppendorf centrifuge 5417 R, rotor F45-30-11). The flow-through was discarded and the column was washed twice with 750 µl of completed GC wash buffer at 10.000 rpm for 1 min. The wash buffer was discarded after each washing step and the column was dried by empty centrifugation at 10.000 rpm for 1 min. The DNA was eluted through addition of 30 µl ddH_2O and subsequent centrifugation at 5.000 rpm for 1 min. Thereafter, the DNA-concentration was measured using a NanoDrop ND-1000 (Thermo Fisher Scientific, Karlsruhe, Germany).
For ligation 50-100 ng of vector and a threefold molar excess of insert were incubated over night at 4°C with 5 U of T4 DNA-Ligase (Thermo Fisher Scientific, Karlsruhe, Deutschland) in the according reaction buffer (50 mM Tris-HCl pH 7.5; 10 mM DTT; 1 mM ATP; 25 mg/ml BSA) (Thermo Fisher Scientific, Karlsruhe, Germany). The reaction was stopped by heat-inactivation at 65°C for 10 min. The ligation product was used for transformation of E. coli DH5α.

2.2.1.4 Separation of nucleic acids by agarose gel electrophoresis

Separation of DNA fragments was performed using horizontal agarose gel electrophoresis. Depending on the fragment size an agarose concentration ranging from 1-2% (w/v) was used. Therefore, the appropriate amount of agarose was dissolved in 1x TAE buffer (0.04 M Tris pH 7.2; 0.02 sodium acetate; 1mM EDTA). The mixture was boiled and after cooling down ethidium bromide was added to a final concentration of 0.4 mg/ml. The solution was transferred into a horizontal gel chamber and a comb was inserted to enable formation of pockets in which the samples could be placed. For the electrophoretic separation the gel was placed in a chamber filled with 1x TAE buffer and the samples, to which DNA sample buffer (5mM EDTA; 50% (v/v) glycerol; 0.01g bromophenolblue) was added, were loaded onto the gel. To validate fragment sizes the peqGOLD

1 kb DNA ladder (0.5 mg DNA/ml, for fragments ranging from 250 to 10000 bp) was loaded in a separate slot. The electrophoresis was performed at 120 V and the separated fragments were visualized under a UV light source until the colored marker reached about half of the gel. Pictures were taken on an Eagle-Eye camera system (Stratagene, Heidelberg, Germany).

2.2.1.5 Transformation of plasmid DNA

For transformation 50 µl of chemically competent bacteria DH5α were gently thawed on ice. Subsequently, 5 µl of the ligation mix or the purified plasmid DNA were added and the mix was incubated for 30 min on ice. Thereafter, the cells were thermically shocked at 42°C for 45 sec and then incubated on ice for 2 min. Afterwards, 500 µl of 1x SOC medium was added and the bacteria were incubated 1 h at 37ºC shaken gently.
During the incubation time, the antibiotic resistance could be expressed. In the meantime 1x LB agar plates (1% (w/v) tryptone, 0.5% (w/v) yeast extract, 0.5% (w/v) NaCl) 1.5% agar-agar), with 0.1 mg/ml ampicillin or 50 µg/ml kanamycin were pre-warmed at 37°C. Finally, the transformed bacteria were plated and incubated ON at 37ºC.

2.2.1.6 RNA extraction from eukaryotic cells

For RNA extraction 2 x 10^5 LNCaP were cultured in 6-well wells in phenolred free RPMI 1640 medium enriched with 3% (v/v) charcoal-stripped FBS (CCS) for three days. Thereafter, cells were treated with 10^{-8} M DHT or 0.1 % DHT for 16 h. If the effect of compounds was analysed in qRT-PCR cells were treated with 5 µM of compound 1 h prior to hormone treatment. For RNA extraction from eukaryotic cells the innuPREP RNA Mini Kit (Analytic Jena AG, Jena, Germany) was used. The cells were washed with 1x PBS (-$MgCl_2$/-$CaCl_2$) and subsequently 400 µl RL Buffer (Lysis buffer) was added to the cells. Samples were incubated for 3 min at room temperature. Cell lysates were pipetted into an Spin Filter D which was placed into a receiver tube and centrifuged at 11.000 rpm for 2 min (Eppendorf centifuge 5417R, rotor F45-30-11). Spin Filter D was discarded and the flow-through was transferred to a Spin Filter R column which was placed in a new receiver tube and centrifuged at 11.000 rpm for 2 min (Eppendorf centifuge 5417R, rotor F45-30-11). The flow-through was discarded. The Spin Filter D was placed in a new receiver tube and was washed with 500 µl of Washing Solution HS and centrifuged at 11.000 rpm for 1 min (Eppendorf centifuge 5417R, rotor F45-30-11). The filtrate was discarded and Spin Filter R was placed in a new receiver tube. In second washing step 700 µl of Washing Solution LS were added to the column and the column was centrifuged at 11.000 rpm for 1 min (Eppendorf centifuge 5417R, rotor F45-30-11). The flow-through was discarded again and the column was dried from residual ethanol by empty centrifugation with a fresh collection tube for 3 min at 11.000 rpm. The Spin Filter D was then placed in a new 1.5 ml collection tube and 30 µl of RNAse-free water (Promega, Mannheim, Germany) were put directly to the spin column membrane. RNA was eluted by centrifugation at 8.000 rpm for 1 min. RNA concentration was measured using a NanoDrop ND-1000 (Thermo Fisher Scientific, Karlsruhe, Germany).

2.2.1.7 Synthesis of complementary DNA (cDNA)

For cDNA synthesis 2 µg of the DNase-free, purified RNA was incubated with 200 ng of Random Primer at 70°C. For qualitative and quantitative control of cDNA synthesis the reaction mixtures were split equally. Afterwards, 1 mM dNTPS (VWR, Darmstadt, Germany) and M-MLV reaction buffer (Promega, Mannheim, Germany) was added to both samples. As a negative control one reaction mixture was incubated without reverse transcriptase, while 200 u of M-MLV (*Moloney Murine Leukemia Virus*) reverse transcriptase (Promega, Mannheim, Germany) were added to the sample. The cDNA synthesis was carried out in a T100 Thermal Cycler (BioRad, Feldkirchen, Germany) with the following protocol:

Table 2.9: Protocol for reverse transcription

temperature	cycle
60°C	10 min
42°C	60 min
70°C	10 min
4°C	∞

Table 2.10: Random Primer used for cDNA synthesis

Name	Sequence (5' - 3')
Random A	NNNNNNA
Random T	NNNNNNT
Random G	NNNNNNG
Random C	NNNNNNC

The cDNA was diluted by adding 100 µl of nuclease-free water (Promega, Mannheim, Germany).

2.2.1.8 Quality Control PCR (QC-PCR)

To check the quality and purity of the synthesized cDNA a PCR reaction using oligonucleotides for the housekeeping gene β-actin was performed. For this 4 µl of the cDNA were mixed with 10 pmol of forward- and reverse-primer, 0.25 mM dNTPs and 1.25 units GoTaq polymerase (Promega, Mannheim, Germany) in green GoTaq reaction buffer (Promega, Mannheim, Germany). The PCR reaction was performed according to following protocol:

Table 2.11: Protocol for quality control PCR

temperature	cycle	repeat
95°C	2 min	
95°C	30 sec	30x
55°C	40 sec	
72°C	45 sec	
72°C	10 min	
4°C	∞	

The transcription of β-actin was analyzed on a 1 % (w/v) agarose gel. The existence of a β-actin in the sample was interpreted as successful reverse transcription, while the existence of a β-actin band in the negative control without reverse transcriptase pointed towards contamination of other reagents. This would have led to an exclusion from the study.

2.2.1.9 Quantitative Real-Time PCR (qRT-PCR)

For quantitative Real-Time PCR 4 µl of cDNA were incubated with 10 pmol forward- and revers-primer, 10 µmol of 2x GoTaq qPCR Master Mix (Promega, Mannheim, Germany) and 4 µl of nuclease-free water (Promega, Mannheim, Germany). The reaction was performed with a final volume of 20 µl in a StepOnePlus Real Time PCR Reader with the following protocol:

Table 2.12: Protocol for quantitative Real Time PCR

temperature	cycle	repeat
95°C	15 min	
95°C	15 sec	40x
60°C	30 sec	
95°C	15 sec	
60°C	1 min	

The fluorescence after intercalation of SYBR Green to double stranded DNA was detected. For each experimental set up a fixed threshold was defined in the exponential phase between cycles 15 and 40, when the PCR product exactly duplicates, to obtain comparable threshold cycles (Ct values) for analysis. Differences in gene expression were determined in relation to the gene expression of the housekeeping gene Rib36B4 (human ribosomal subunit 36B4). For the analysis the ΔCt value was determined by subtracting the Ct value of the gene of interest from the Ct value of the housekeeping gene.

2.2.1.10 RNA sequencing

For transcriptomic analysis Control and BAG1L KO cells were hormone-starved for 96 h in phenol red-free medium supplemented with 3% (v/v) CCS. Subsequently, cells were treated for 16 h with 0.01% (v/v) EtOH or 10 mM DHT. The total RNA was extracted using innuPREP RNA Mini Kit (Analytic Jena AG, Jena, Germany), as described above (2.2.1.6). The mRNA libraries were generated using IlluminaTruSeq stranded mRNA sample kit with 1 mg of total RNA per sample. The library preparation and sequencing (HiSeq1500 Illumina platform) was performed at the NGS facility at the Institute of Biological and Chemical System at KIT. Data was analysed at the Dana-Farber Cancer Institute of the Harvard Medical School in Boston. Fastq files were processed with CASAVA and mapped against the human reference genome GRCh37 using TopHat 2.0.11 (Trapnell et al., 2009). Reads were quantified with HTSeq (Anders et al., 2015), using the reference gene annotation from Ensembl. Differential expression analysis was performed using DESeq2 (Love et al., 2014). AR target genes were defined as genes that were differentially expressed in

the presence of DHT (p(FDR) $\leq$ 0.05, fold change $\geq$ 2) and which harbor a DHT-responsive AR binding site within 50 kb of their transcription start site. Differentially expressed target genes were plotted in a Scatter Blot Matrix with differentially expression AR target genes of control cells on the x-axis and differentially expressed AR target genes of BAG1L KO cells on the y-axis. RNA-seq data have been deposited at the GEO depository under accession number GSE89939.

2.2.1.11 Quantification of nucleic acids

Quantification of DNA and RNA was performed with a NanoDrop ND-1000, which measures the extinction of the sample at 260, 280 and 230 nm. The concentration of RNA and DNA is calculated from the OD_{260} by the Beer-Lamber-equation. An OD_{260}=1 corresponds to 50 ng/µl of double-stranded DNA. The ratio of OD_{260}/OD_{280} is used to determine potential contaminations of proteins and a value of 1.8 indicates a pure nucleic acid preparation. The ratio of OD_{260}/OD_{230} is used to determine potential contaminations of organic chemicals and solvents and a value greater than 1.6 is accepted a contamination-free. For RNA a ratio of OD_{260}/OD_{280} greater than 1.8 is acceptable with very pure RNA typically showing a ratio of 2.1. The OD_{260}/OD_{230} should as well be greater than 2 for RNA.

2.2.2 Cell culture and transfection methods

2.2.2.1 Cell culture

All mammalian cell lines were cultured in standard conditions at 37ºC, 5% of CO_2 and 95% of humidity in an incubator (Steri Cult 200, Forma Scientific Labortech GmbH, Göttingen, Germany). All cell lines were cultured in sterile Cellstar Petri dishes (Greiner Bio-One, Nürtingen, Germany). Cells were confirmed to be mycoplasma-negative using the VenorGeM Classic Mycoplasma Detection Kit for conventional PCR machines (Minerva Biolabs, Berlin, Germany).
Cells were cultured until confluency of 80-90% was reached. The cell culture medium was then removed and cells were carefully washed with 1x PBS (-$MgCl_2$/-$CaCl_2$). To detach cells from the culture vessel 0.5-1 ml of 0.25% Trypsin-EDTA were added to the cells and incubated for 5 min at 37°C. Trypsination was stopped by adding at least the tenfold volume of fresh medium to the cells. Cells were then transferred into a falcon tube and Trypsin was removed by centrifugation at 800 rpm for 3 min. Cells were picked up in fresh medium and were seeded at the desired dilution. For long-term storage all mammalian cells were cultured on 15 cm^2 cell culture plates until 80-90% of confluency were reached. The cells were then washed with 1x PBS (-$MgCl_2$/-$CaCl_2$) and were detached from the plate using 1 ml of 0.25% Trypsin-EDTA for 5 mi at 37°C. Trypsination was stopped by adding at least the tenfold volume of fresh medium to the cells. Cells were then transferred into a falcon tube and Trypsin was removed by centrifugation at 800 rpm for 3 min. Cells were resuspended up in 2 ml of 90% (v/v) FCS and 10% (v/v) DMSO and 1 ml each was transferred in cryotube. The cells were slowly frozen at -80°C in freezing containers filled with isopropanol.

To take frozen cells into culture cryotubes were thawed quickly (maximum 1 min) at 37°C in a waterbath. Cells were then transferred into fresh medium and centrifuged at 800 rpm for 3 min (Biofuge Heraeus pico, rotor # 3328) to remove residual DMSO. Cells were taken up in fresh medium and plated onto new cell culture plate.
The human cervical cancer cell line HeLa and the fibroblast-like cell line COS-7 from the african green monkey were cultured in DMEM medium enriched with 10% (v/v) FBS. The human lymphnode metastasis LNCaP cell line, as well as the derived Control and BAG1L KO cell lines, were cultured in RPMI 1640 enriched with 10% (v/v) FBS. The CRPC model cell line LNCaP95, which is derived from LNCaP, was cultured in phenol red-free RPMI 1640 supplemented with 10% (v/v) CCS, 100 u/ml (v/v) penicillin/streptomycin and 1% (v/v) L-Glutamine (Gibco, Invitrogen, Karlsruhe, Germany). LNCaP95 cells were cultured in 75 cm^2 flasks with a CellBind surface.

2.2.2.2 Transfection with FuGene

For transfection with FuGene HeLa or COS-7 cells were seeded at a densitiy of 2 x 10^5 cells per well in 6-well plates. For all reportgene assays the following DNA amounts were used:

Table 2.13: General Transfection mixture

plasmid	amount
Reporter luciferase	0.8 µg
renilla luciferase	0.2 µg
AR construct	0.2 µg
BAG1 construct	1 µg

The transfection mix was then diluted in 100 µl of serum-free medium and 4,4 µl of FuGene were added. The solution was gently mixed by inverting and incubated for 15 min at room temperature. Finally the solution was dropwise added into the cell culture medium and distributed evenly by gentle swirling. If the effect of compounds was analyzed, cells were treated with compound 24 h after transfection and hormone was added 1 h after compound application. The cells were usually harvested 48 h after transfection.

2.2.2.3 Luciferase assay

For the analysis of AR-FL and AR-V7 activity HeLa cells were seeded in 6-well cell culture plates at a density of 2 x 10^5 in RPMI 1640 supplemented with 10% (v/v) FBS. One day post seeding cell culture medium was changed to phenol red-free RPMI 1640 supplemented with 3% (v/v) CCS and cells were transfected with FuGene 6. The effect of BAG1L on AR-FL and AR-V7 activity was investigated by transfection of 0.2 µg of pcDNA3.1 AR-FL or pcDNA3.1 AR-V7, 0.8 µg of PSA-Enhancer-luciferase and 0.2 µg of Ubi-renilla construct. The PSA-Enhancer-luciferase contains the -3935 to -4326 PSA core enhancer upstream of the E4TATA box driving the expression of a firefly luciferase. The expression of the luciferase takes place after activation of AR and its binding to the promotor region. The transfection efficiency was determined with the help of a

renilla luciferase construct. The expression of the renilla luciferase is controlled by a Ubiquitin promotor, which is independent of AR transactivation.
The cells were treated 24 h post transfection with 10 nM DHT or ethanol for 16 h. Afterwards, cells were washed once with 1x PBS (-$MgCl_2$/-$CaCl_2$) and lysed with 200 µl 1x *Passive lysis buffer* (Promega, Mannheim, Germany). For each sample 20 µl of lysates were measured in duplicates in a 96-well luminometer plate. The relative luciferase activity was calculated by dividing firefly luciferase activity through renilla luciferase activity.

2.2.2.4 Mammalian-One-Hybrid and Mammalian-Two-Hybrid

To examine *in vivo* transactivation and protein-protein interactions *Mammalian-One-Hybrid* and *Mammalian-Two-Hybrid* Assays were performed. For the investigation of the effect of AR τ5 mutations on the transactivation activity as well as on interaction with BAG1L the cervical carcinoma cell line HeLa was used. To examine the effect of benzothiazole derivatives on AR AF1 activity the fibroblast like cell line COS-7 from the African green monkey was used, due to its low expression of endogenous BAG1L. In both cases 1 x 10^5 cell were seeded per 6-well in DMEM medium supplemented with 10% (v/v) FBS. For the analysis of benzothiazol derivates on AR-AF2 activity cells were transfected in phenol red-free medium supplemented with 3% (v/v) CCS. Cells were transfected in suspension with FuGene 6.
The transactivation of AR τ5 mutations was examined by *Mammalian-One-Hybrid*-Assay with HeLa cells transfected with 0.2 µg of Gal4DBD-AR-τ5 and increasing concentrations of pcDNA3.1.-BAG1L balanced with pcDNA3.1 empty vector to 1 µg. The effect of AR τ5 mutations on interaction with BAG1L was investigated by transfecting HeLa cells with 0.2 µg of Gal4DBD-AR-τ5, -τ5ΔPro-C404A or -τ5-C404AR405A and 1 µg of VP16-BAG1L or VP-16 empty vector. For the analysis of the benzothiazole derivatives on AR-AF1/AF2 transactivation COS-7 cells were transfected with 0.2 µg of Gal4DBD-AR-AF1 or pM-AR-AF2 and 1 µg pcDNA3.1.-BAG1L. The transactivation of the Gal4DBD was detected through cotransfection of 0.8 µg of a pG5E4Δ38 luciferase construct, which comprises five copies of a Gal4-DNA-Binding site (*upstream activation sequence* (UAS)), upstream of the Adenovirus E4 promotor. Transactivation of the Gal4DBD leads to binding to the UAS and subsequently to the expression of the firefly luciferase. Transfection-efficiency was analyzed through transfection of 0.2 µg of renilla luciferase, which was controlled by the constitutively active Ubiquitin-promotor. Cells transfected with Gal4DBD-AR-AF2 were treated with ethanol or 10^{-8} M DHT 24 h post transfection.
The cells were harvested 48 h post transfection after washing once with 1x PBS (-$MgCl_2$/-$CaCl_2$) and addition of 200 µl 1x *Passive lysis buffer* (Promega, Mannheim, Deutschland). For each sample 20 µl of lysates were measured in duplicates in a 96-well luminometer plate. The relative luciferase activity was calculated by dividing firefly luciferase activity through renilla luciferase activity.
For the measurement of the firefly-luciferase activity 70 µl of Gly-Gly-Buffer (25 mM Glyglycin, 15 mM $MgSO_4$, 1 mM DTT and 0.1 mM ATP) and 20 µl of luciferin solution (1 mM firefly

luciferin, 25 mM Glyglycin, 15 mM $MgSO_4$, 4 mM EGTA) were autoinjected per well and the luciferase activity was measured in a *Victor Light 1420 Luminscence Counter* (PerkinElmer, Rodau, Deutschland).
For the measurement of renilla luciferase activity 100 µl of Coelenterazin-Buffer (0.1 M KPi (0.2 M KH_2PO_4, 0.2 M K_2HPO_4), 0.5 M NaCl, 1 mM EDTA, pH 7.6, 0.2 nM Coelenterazin) were autoinjected and luciferaserase activity was measured in *Victor Light 1420 Luminscence Counter* (PerkinElmer, Rodau, Deutschland).

2.2.2.5 Proliferation Assay in 2D cell culture

To examine the proliferation of PCa cell lines in the presence of different compounds Control and BAG1L KO LNCaP cells or LNCaP95 cells overexpressing vector or BAG1L were seeded at a density of 4 x 10^4 cells/well into 12-well plates in their standard culture medium. For each treatment and time point triplicates were seeded. The baseline cell number was determined one day after seeding by counting in a Neubauer chamber. Afterwards, cells were treated with the indicated concentration of the compounds. Cells were counted on the indicated days and the mean of three triplicates was calculated. Proliferation factor was determined by normalizing the mean for each sample to day 0.

2.2.2.6 Proliferation Assay in 3D cell culture

For the generation of 3D cell culture cryogels, poly(ethylene glycol) diacrylate (PEGda, MW 575, Sigma-Aldrich, Munich, Germany) was diluted in 1x PBS (-$MgCl_2$/-$CaCl_2$) (11.2 w/v %). To remove any particles the solution was filtered through a 0.22 µm filter (Roth, Karlsruhe,Germany). Subsequently, the mixture was precooled at -20°C for 5 min. Afterwards, 100 mg Ammonium persulfate (APS) (Roth, Karlsruhe, Germany) and tetrametyhlethylenediamine (TEMED) (0.075 w/v %) (Merck, Darmstadt, Germany) were added. The mixture was taken up in a 3 ml syringe (Braun, Melsungen, Germany) and was polymerization was allowed at -20°C for 3 h. After thawing, the PEGda cryogels were cut into 3 mm thick discs.
Cryogels slices were inserted into the wells of conventional 12-well cell culture plates, washed with 70% (v/v) ethanol for 5 min and ethanol was removed by three washing steps with 1x PBS (-$MgCl_2$/-$CaCl_2$). After the last washing step PBS was removed and cryogels were air dried under a laminar flow cabinet for at least 30 min. Afterwards, LNCaP95 cells were seeded at a density of 2.5 x 10^5 in 20 µl of culture medium. The cells were allowed to attach to the scaffold at 37°C for 2 h and subsequently each well was filled with 1 ml of cell culture medium. One day post seeding 1 µg/ml doxycycline and 1 µg/ml puromycin were added to the medium.
To analyze growth cryogels were removed from the medium 7 days post seeding, incubated ON at 56 °C in lysis buffer (10×10^{-3} M Tris-HCl pH 7.5; 1×10^{-3} M EDTA, 1% (w/v) sodium dodecyl sulfate) containing 200 µg/ml Proteinase K (Sigma-Aldrich, Munich, Germany). Proteinase K digestion was stopped at 95 °C for 10 min and DNA was precipitated through addition of isopropanol. After washing with 70% (v/v) ethanol DNA was dissolved in $10 \times 10_{-3}$ M Tris-HCl pH

7.5, 1×10^{-3} M EDTA. The concentration was measured spectro-photometrically at a NanoDrop ND-1000 (Thermo Fisher Scientific, Karlsruhe, Germany).
To analyze cell morphology in *scanning electron microscopy* cells were fixed in 2.5 % (v/v) glutaraldehyde for 1 h and followed by sequential washes with 50%, 70%, 95%, and 100% ethanol (v/v) for 5 min each. Thereafter, the samples were dried under vacuum before silver sputtering. Measurements were performed at a scanning electron microscope (Zeiss Supra 60 VP, Carl Zeiss NTS company, Oberkochen, Germany) with an accelerating voltage of 3 kV. Cell clusters were colored in photoshop CS 5.1.

2.2.3 Protein methods

2.2.3.1 Protein Preparation from BL21

For the generation of purified BAG domain the plasmid pET28.GB1a.BAGDfl was used for transformation of the *E. coli* strain BL21 (DE3). For the generation of a a ^{15}N-labelled BAG domain bacteria were grown ON in 100 ml of M9 minimal medium supplemented with 0.5 g/l $^{15}NH_4Cl$. For the production of an unlabelled BAG domain bacteria were grown ON in 1x LB medium (1% (w/v) tryptone, 0.5% (w/v) yeast extract, 0.5% (w/v) NaCl). The next morning the ON cultured was diluted 1:10 with the corresponding medium and bacteria were grown to an OD_{600} of 0.8. Subsequently, production of the His-tagged protein was induced by adding 0.5 mM IPTG. Bacteria were allowed to grow ON at 16°C on a shaker. Bacteria culture was centrifuged at 4.000 rpm for 30 min (HERMLE ZK 401, rotor A.9) and pellets were resuspended in lysis buffer (50 mM $NaHPO_4$, pH 8.0; 10 mM Imidazole; 300 mM NaCl) supplemented with 1% (v/v) µl of Triton X-100, 0,2 mM PMSF, 5 mM β-Mercaptoethanol and 1 mM DTT. After resuspension 1.5% (w/v) of N-Laurylsarcosine and 100 µg/ml Lysozyme was added to the suspension. Bacteria were lysed for 30 min on ice while gently shaking. To ensure complete lysis bacteria were additionally sonificated twice for 30 sec (2 Hz). The lysates were cleared by centrifugation at 8.000 rpm for 20 min and proteins were coupled to Ni-NTA beads (Expedeon, Heidelberg, Germany) rotating at 4°C over night. The beads were washed three times with 20 ml of wash buffer (50 mM $NaHPO_4$, pH 8.0; 20 mM Imidazole; 300 mM NaCl) supplemented with 5 mM β-Mercaptoethanol, and 1 mM DTT. Multiple fractions (300µl) of proteins were eluted with elution buffer (50 mM $NaHPO_4$, pH 8; 250 mM Imidazole; 300 mM NaCl, 2 mM PMSF) supplemented with 5 mM β-Mercaptoethanol, 1 mM DTT. The fractions were analyzed on a coomassie-stained SDS-Gel (Laemmli, 1970) and the fractions containing the highest amount of proteins were pooled. Pooled fractions were transferred to a dialysis tube and dialysed twice against 1x PBS (-$MgCl_2$/-$CaCl_2$) with 1 mM DTT for several hours at 4°C. The dialysed proteins were analysed on a coomassie-stained SDS-Gel and the concentration was determined using Bradford reagent. The His.Gb1-tag was cleaved off the ^{15}N-labelled BAG domain using 1µg TEV proteinase per 100 µg of protein. The cleaved His.Gb1-tag was removed from the solution by Ni-agarose beads (Biozol, Eching, Germany).

2.2.3.2 Separation of protein by SDS PAGE (Polyacrylamide gel electrophoresis)

Proteins were separated according to their size by SDS-PAGE (*sodium dodecylsulfate polyacrylamide gel electrophoresis*) (Laemmli, 1970). Therefore 10% (v/v) polyacrylamide gels (10% (v/v) Rotiphorese Gel 30; 375 mM Tris-HCl, pH 8.8; 0.1% (v/v) SDS; 0.1% (v/v) APS; 0.4% (v/v) TEMED) were cast in SDS-PAGE apparatus (BioRad, Mini-PROTEAN® Tetra Vertical Electrophoresis Cell, Feldkirchen, Germany). To ensure straight edges the separating gel was overlaid with Isopropanol, which was removed after polymerization of the gel. On top of the separating gel a 5% (v/v) stacking gel (5% (v/v) Rotiphorese Gel30; 125 mM Tris-HCl, pH 6.8; 0.1% (v/v) SDS; 0.1% (v/v) APS; 1% (v/v) TEMED) was cast and a comb was placed on top to allow the formation of sample pockets. The electrophoretical separation was performed in 1x Laemmli-Buffer (25 mM Tris Base, 200 mM Glycin, 0.1% (w/v) SDS) in the running chamber. The desired amount of cell lysate was diluted in sample buffer, boiled at 95°C for 5 min and was loaded onto the SDS gel. The electrophoretical run was performed at 25 mA per small gel.

2.2.3.3 Quantification of protein extract

The concentration of proteins from lysates was determined via Bradford method (Bradford MM, 1976). For this, 100 µl of 1x Bradford solution (5x stock solution; Bio-Rad, Munich, Germany) in H_2O was mixed with 1 µl of lysate. For the generation of a calibration line 100 µl of 1x Bradford were mixed with increasing concentrations (0 µg µl, 2 µg µl, 4 µg µl, 8 µg µl)of BSA in lysisbuffer. The Lysis buffer was used as zero value. Determination of the protein content was carried out by measuring the optical density at 595 nm and concentration was calculated with the aid of the calibration line.

2.2.3.4 Differential Scanning Fluorimetry

Binding of compounds to the purified unlabelled BAG domain protein was monitored using differential scanning fluorimetry. As a fluorescent probe SYPRO orange (Thermo Fisher Scientific, Karlsruhe, Germany) was used. The protein was used at a final concentration of 0.11 µg/µl and SYPRO orange (final concentration 50×) in buffer (HEPES pH 7.0, 150 mM NaCl). Indicated concentrations of the compounds dissolved in DMSO were added to the protein mixture. Melting curve analysis was performed on a StepOnePlus real-time qPCR thermocycler (ThermoFisher Scientific, Karlsruhe, Germany), ranging from 25 to 99 °C with a ramp of 1%. The melting temperature (T_m) of the protein in the presence of compounds was determined from the inflection point of the melting curve. Melting temperatures were plotted against compound concentration to identify concentration-dependent increase in the melting temperature.

2.2.3.5 NMR

To check binding of AR τ5 peptides to the ^{15}N-labelled BAG domain the peptides were dissolved in either phosphate buffer or DMSO. Peptides were dialyzed over night against 1x PBS with 2 mM

DTT. The peptides were added to 50 µM ^{15}N-labelled BAG domain to reach a final concentration of 300 µM in PBS/DTT and the mixture was transferred to a 5 mm NMR tube. ^{1}H^{15}N-HSQC spectra were measured with a Avance III 600 MHz spectrometer (Bruker BioSpin GmBH, Rheinstetten, Germany), which was equipped with a TXI-cryoprobe and Z-gradient. Spectra were acquired with 16 scans per increment, 2048 points in the direct and 256 points in the indirect dimension at a temperature of 26.7°C. Calibration, processing and analysis of spectra was performed using Topspin ((Bruker BioSpin GmbH, Rheinstetten, Germany). Chemical shift changes were calculated with the following formula: For interaction studies, peptides were dissolved at 1.5. mM concentration in either phosphate buffer or DMSO and dialysed over night against phosphate buffered saline (PBS) buffer with 2 mM DTT. The peptides were added to 50 µM 15N-BagD in PBS/DTT to a final concentration of 300 µM and transferred to a 5 mm NMR tube. 1H15N-HSQC spectra were measured on an Avance III 600 MHz spectrometer (Bruker BioSpin GmBH, Rheinstetten, Germany) equipped with a TXI-cryoprobe and Z-gradients. Spectra were acquired with 16 scans per increment, 2048 points in the direct and 256 points in the indirect dimension. The temperature was set to 26.7 °C. Spectra were calibrated, processed and analysed with Topspin (Bruker BioSpin GmbH, Rheinstetten, Germany). Chemical shifts changes (CSP) were calculated with the following formula: CSP=$\sqrt{(\delta CS(^{1}H)^{2} + (0.1CS(^{15}N)^{2}))}$ (CS = chemical shifts in Hz of 1H and 15N resonances).

2.2.3.6 MARCoNI assay

For the analysis of coregulator binding to the AR in the presence and absence of BAG1L, control and BAG1L KO LNCaP cells were hormone-starved in phenol red-free RPMI 1640 medium supplemented with 3% (v/v) CCS for 96 h. The cells were then treated with 10^{-8} M DHT for 4 h or 16 h. The cells were harvested by trypsination and pellets were frozen. Pellets were further processed at PamGene B.V. ('s-Hertogenbosch, The Netherlands). AR-containing lysates were incubated on a PamChip (PamGene) with 154 coregulator-derived NR-binding motifs. After washing of PamChip bound AR was detected via a fluorescently labeled antibody and quantified using BioNavigator software (PamGene). Experiments were performed in technical quadruplicates.

2.2.3.7 Reduced 2´7-dichlorofluorescein (DCF) diacetate oxidation assay

For the determination of ROS levels Control and BAG1L KO LNCaP cells were hormone-starved for 48 h in phenol red-free RPMI 1640 medium supplemented with 4% (v/v) CCS and 1% (v/v) FCS. The cells were then plated at a density of 1.5 x 10^{4} cells/well in 96-well plates in phenol red-free medium supplemented with 5% (v/v) CCS for 48 h. Thereafter, the cells were treated with 10^{-8} M R1881 or ethanol for 96 h. For detection of ROS 10 µM H_2DCF-DA in phenol red-free medium was added for 40 min at 37°C. Afterwards, cells were washed with phenol red-free medium and incubated at room temperature for 120 min prior to measuring the fluorescence at 485 nm excitation and 530 nm emission in a multi-well fluorescence reader (SpectraMax iD3, Molecular Devices with SoftMax Pro 7 software, Biberach an der Riss, Germany). The detected fluorescence was

then normalized to the total cell number, which was determined by counting Hoecht-stained nuclei. Therefore, cells were incubated with Hoechst dye (0.3 µg/ml final concentration) for 30 min at 37°C and imaged using the tenfold objective of the automated fluorescence microscope IX81 (Olympus, Germany). For each well four pictures were taken and automated image analysis was performed with the Olympus scanR̂ analysis software.

2.2.3.8 *in silico* analysis

To investigate sequence homology of the AR τ5 region, a multiple sequence alignment was performed using the online software tool MultAlin (http://multalin.toulouse.inra.fr/multalin) using the alignment parameter Blosum62-12-2.
AR protein sequences of mammalians, birds, fish and amphibians were taken from the National Center of Biotechnology Information (https://www.ncbi.nlm.nih.gov/protein/) with the following accesion numbers: Homo sapiens NP_000035.2; Canis lupus familiaris NP_001003053.1; Rattus norvegicus NP_036634.1; Gallus gallus NP_001035179.1; Mus musculus NP_038504.1; Sus scrofa NP_999479.2; Taeniopygia guttata NP_001070156.1; Ovis aries NP_001295513.1; Bos taurus NP_001231056.1; Macaca mulatta NP_001028083.1; Pan troglodytes NP_001009012.1; Equus caballus NP_001157363.1; Danio rerio NP_001076592.1; Oryctolagus cuniculus NP_001182653.1; Pongo abelii XP_009233214.1; Macaca mulatta NP_001028083.1;

2.2.4 Synthesis of benzothiazole derivatives

All benzothiazole derivatives were synthesized at the Compounds Platform (ComPlat) at KIT. Benzothiazole derivatives were synthesize according to the general procedures GP1 and GP2.
GP1: The aldehyde (1.20 equiv) was dissolved in toluene and a 2-amino-benzenethiol (1.00 equiv) as well as p-toluene sulphonic acid monohydrate (0.1 equiv) were added. The reaction was stirred for 18 h at 70 °C. To prepare the reaction mixture for purification by column chromatography (dryload method), silica gel was added and the mixture of combined organic phases and silica gel was evaporated. The crude reaction products were purified by flash chromatography followed by HPLC purification when necessary.
GP2: 4-Fluorobenzaldehyde (1.00 equiv), the amine (1.50 equiv), tetrabutylazanium;bromide (0.300 equiv) and potassium carbonate (1.00 equiv) were stirred at 95 °C for three days. Water was added to the reaction and the resulting mixture was extracted three times with ethyl acetate. The combined organic phases were washed with brine and dried over Na2SO4 and filtered. As preparation for column chromatography (dryload), silica gel was added (6 g) and the mixture of combined organic phases + silica gel was evaporated.

2.2.5 Statistics

All experiments were performed with at least three replicates. Differences between two groups were analyzed by Student's t test and multiple comparison were determined by one-way ANOVA followed by a post-hoc test. If there were two factors (such as dose and time) investigated, data were analyzed by two-way ANOVA followed by a post hoc test. Data was expressed as means $\pm$ SEM, and $p \leq 0.05$ was considered significant. All analyses were performed using Microsoft Excel 2010 and GraphPad Prism 6 software.

3 Results

3.1 Proliferation of LNCaP95 PCa cells is reduced upon knockdown of AR-FL or AR-V7

During the progression to castration-resistant prostate cancer (CRPC), tumor growth and proliferation remain critically dependent on AR activity (Visakorpi *et al.*, 1995b; Watson *et al.*, 2015). However, the molecular basis responsible for reactivation of AR transcriptional activity are so far poorly understood. One of the mechanisms suggested to be accountable for AR reactivation in CRPC is the increased expression of AR splice variants (AR-SV) which lack the ligand-binding domain (LBD) and are constitutively active. The most common and so far best characterized AR-SV is AR-V7. AR-V7 is generated by cryptic exon exclusion and therefore shares the N-terminal *activation function-1* (AF-1) domain, the DNA-binding domain (DBD) and a partial hinge region with the full-length AR (AR-FL) but possesses a unique 16-amino-acid sequence (CE3) at the C-terminus instead of the classic LBD. The expression of AR-V7 is thought to contribute to CRPC (Hu *et al.*, 2009) but its exact role is not known. To determine the contribution of AR-V7, the CRPC model cell line LNCaP95 which endogenously expresses both AR-FL and AR-V7 was employed. LNCaP95 cells were lentivirally transduced with doxycycline (dox)-inducible short hairpin RNAs (shRNAs) that selectively down-regulated the expression of AR-FL (shAR-FL), AR-V7 (shARv7) or GFP as a control (shGFP). Effective down-regulation of both receptor types was confirmed by Western blotting (Cato *et al.*, 2019).

Cells were seeded into a 3D scaffold of polyethyleneglycol diacrylate to mimic the physical properties of malignant prostate tissue (Göppert *et al.*, 2016) and cultured in medium containing doxycycline and puromycin for selection. Cells in the scaffold were visualized at the end of the study by scanning electron microscopy and proliferation was determined by quantification of the DNA content of cells in the matrix. The cells expressing both AR variants (shGFP) formed large spheroids that invaded the pores of the scaffold and covered a larger area, whereas knockdown of either AR-FL or AR-V7 resulted in the formation of smaller globular spheroids that were mostly focused (Figure 3.1A). This suggested that the knockdown of AR-FL or AR-V7 resulted in decreased proliferation, a result that could be confirmed by the determination of the DNA content in the bar chart (Figure 3.1B).

These results suggest that AR-FL and AR-V7 can both promote proliferation of LNCaP95 cells.

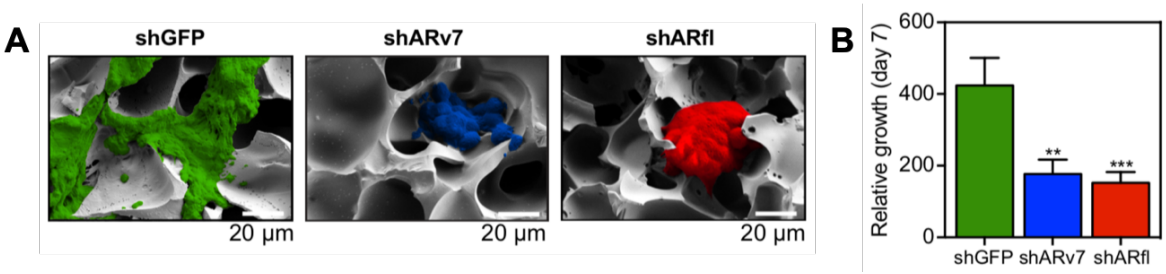

Figure 3.1: LNCaP95 proliferation is hampered upon knock-down of AR-FL or AR-V7
(A) LNCaP95 cells expressing shAR-FL, shAR-V7 or shGFP were cultured in 3D PEGda575-Cryogels. After 7 days spheroids were fixed in glutaraldehyde and cryogels were dehydrated by ascending alcohol series, prior to visualization via SEM. Representantive images are shown. (B) Growth of LNCaP95 cell lines expressing shAR-FL, shAR-V7 or shGFP was analyzed by determination of the total DNA amount isolated from spheroids after 7 days of culture in 3D PEGda575-Cryogels. Data shows the mean of four independent experiments normalized to day 0 ±SEM. Significance was calculated using students t-test $**$ p ≤ 0.01; $***$ p ≤ 0.001

3.1.1 BAG1L regulates the activity of AR-FL and AR-V7

The findings that that the expression of AR-FL as well as AR-V7 is needed for the growth of CRPC cells suggests that targeting both AR variants is crucial to overcome resistance in advanced PCa. Therefore, regulatory proteins required for the activity of both receptors might be promising targeting options. The hypothesis of this work is that the cochaperone BAG1L which is overexpressed during the progression to CRPC and which enhances the activity of the AR by binding its N-terminal domain might function by regulating the activity of both proteins.
To test this hypothesis a reporter-gene assay was carried out in HeLa cells using as reporter gene a PSA-Enhancer-luciferase construct that contains the -3935 to -4326 PSA core enhancer upstream of the E4TATA box driving the expression of a firefly luciferase. PSA (*prostate-specific antigen*) is a glycoprotein enzyme which is present at low concentrations in the serum of healthy men but is often increased in the presence of prostate tumors and is clinically used as an early marker for PCa. HeLa cells were additionally transfected with a renilla luciferase being driven by a ubiquitin promoter for control of transfection efficiency and ARwt or AR-V7 expression vectors as well as increasing amounts of BAG1L. Solvent (ethanol) or 5α-dihydrotestorene (DHT) was added to the cells. Luciferase activity was measured and firefly luciferase activity was normalized to renilla activity. The results showed that increasing amounts of BAG1L hormone-dependently enhanced the relative luciferase activity in AR-FL expressing cells significantly. A similar trend was observed in ARv7 transfected cells, however, the enhancing effect of BAG1L was less strong and occurred in a hormone-independent way confirming the hypothesis that BAG1L positively regulates the activities of both AR-FL and AR-V7. (Figure 3.2)

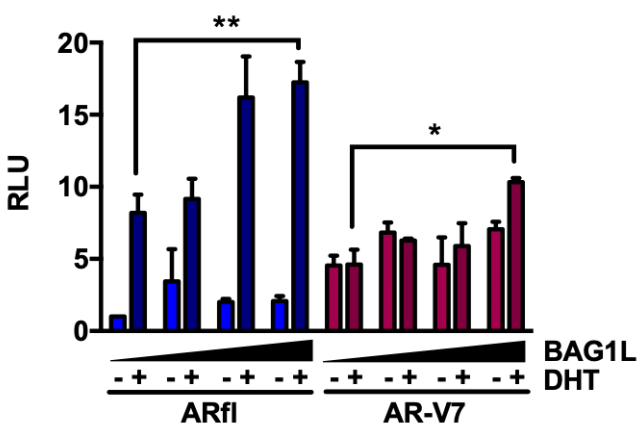

Figure 3.2: BAG1L enhances activity of AR-FL and AR-V7
Hela cells were transiently transfected with PSA-enhancer-luciferase, Ubiquitin-Renilla, pcDNA-AR-FL or pcDNA-AR-V7 and increasing amounts of pcDNA-BAG1L. Cells were treated with solvent (ethanol) or DHT 24 h post transfection. Samples were harvested and luciferase activity was presented as relative luciferase units (RLU) which is the ratio of firefly over renilla luciferase activity. Bar charts represent the mean of 3 independent experiments; each experiment was measured in duplicates and the mean of duplicates was used as one independent experiment. Error bars represent SEM. Significances were calculated using students t-test with $* \ p \leq 0.05$, $** \ p \leq 0.01$

3.2 Identification of BAG1L binding sites in the AR-NTD

As BAG1L enhances the hormone-dependent activity of the full-length AR as well as the hormone-independent action of AR-SV to the same extent, the action of BAG1L must therefore occur via the N-terminus of the AR, that is present in both AR isoforms. To gain more insights into the potential binding site at the AR NTD, a heteronuclear single quantum coherence (HSQC) NMR titration approach was carried out using a purified ^{15}N-labelled BAG domain and seven unlabelled peptides that span the complete tau5 region, which was formerly reported to be important for binding of BAG1L to the AR (Figure 3.3A). (Cato *et al.*, 2017). The NMR experiments were performed by PD Dr. Claudia Muhle-Goll.

The results showed that the longest peptide PM206 which comprises the polyproline region and a folded polyalanine region, but not the classical WHTLF binding motif, which is known to be important for ligand-independent AR activity (Dehm *et al.*, 2007), caused small but distinct chemical shifts (biggest chemical shift differences of 40 Hz) in the BAG domain sequence (especially at E283, V325, E326 and N328) (Figure 3.3B and C). Peptide PM205 that covers the polyproline region and upstream sequences was however not able to induce chemical shifts (Figure 3.3B). Interestingly, peptide PM153 which possesses the partially folded poly-alanine stretch adjacent to the poly-proline region produced the same weak chemical shifts as PM206 (Figure 3.3B). The other peptides that contained sequences downstream of the poly-alanine stretch including the classical WHTLF binding motif did not induce chemical shifts. This identified the sequence of PM153 ('HAR IKL ENP LDY GSA WAA AAA QCR YGD LA') as potential motif for BAG domain binding however it has to be considered a low affinity binding because of the weak chemical shifts produced in the NMR experiments.

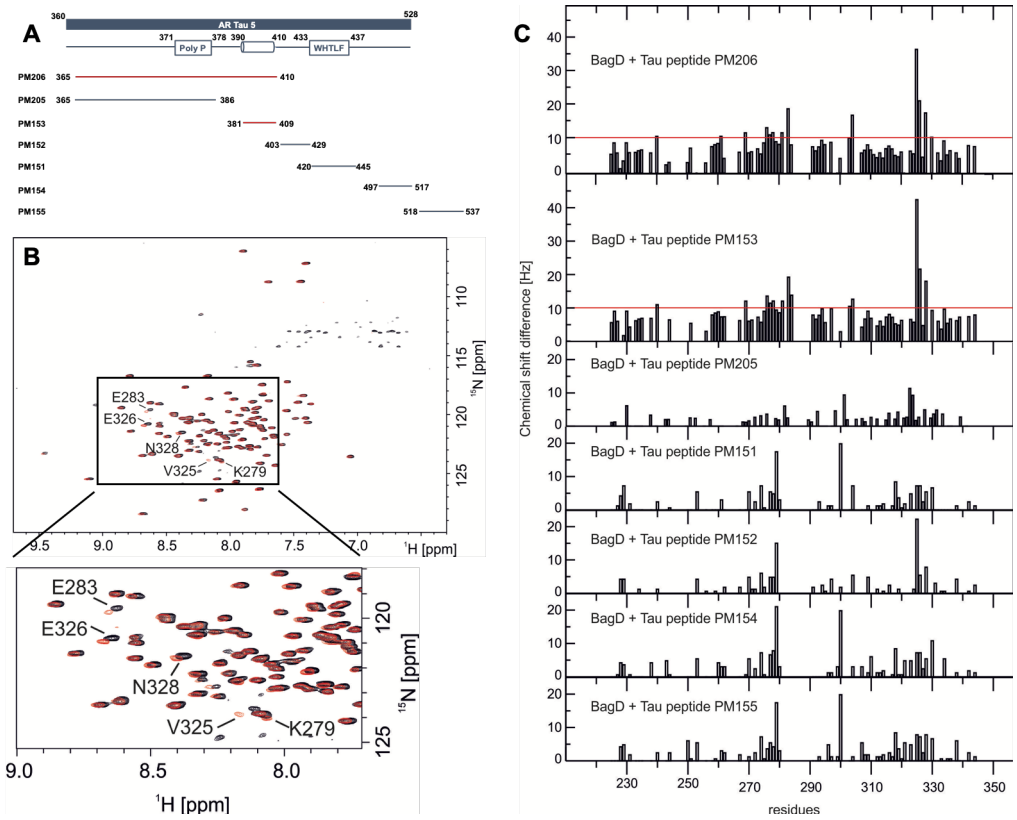

Figure 3.3: Identification of the BAG1L binding sites in the τ5 region
(A) Schematic illustration of the different peptides spanning the τ5 region of the AR NTD that were used in HSQC NMR studies. (B) Complete (top) and close-up (bottom) HSQC spectra of 50 µM ^{15}N-labelled BAG domain alone (black) and in the presence of 300 µM peptide PM206 (red). (C) Chemical shift differences of amino acid residues in the ^{15}N-labelled BAG domain (50 µM) upon addition of 300 µM of the indicated ARt5 peptides.

3.2.1 Multiple sequence alignment of AR τ5 region shows high sequence conservation

The information that BAG1L binds to a poly-alanine region in the AR τ5, which has so far not been reported to be important for protein-protein interactions, led to question whether this motif is evolutionary conserved amongst different species. To investigate this, a multiple sequence alignment was performed using the online software tool MultAlin (http://multalin.toulouse.inra.fr/multalin) and AR protein sequences of mammalians, birds, fish and amphibians were taken from the National Center of Biotechnology Information (https://www.ncbi.nlm.nih.gov/protein/).
The multiple sequence alignment showed that the AR tau5 sequence is highly conserved in mammalian species. The highest degree of conservation was found *inter alia* in the poly-proline region, the adjacent 'HARIKLEN' motif present in peptide PM153, the partially folded poly-alanine stretch and the 'WHTLF'-motif. However, there was little consensus to the AR protein sequence of *Xenopus laevis* and almost no sequence homology to sequences of *Danio rerio*, *Gallus Gallus* and *Taeniopygia guttata* (Figure 3.4).
These results hint at a conserved, regulatory function of the BAG1L binding sides in mammalian AR action, which is not present in fish, bird and amphibians.

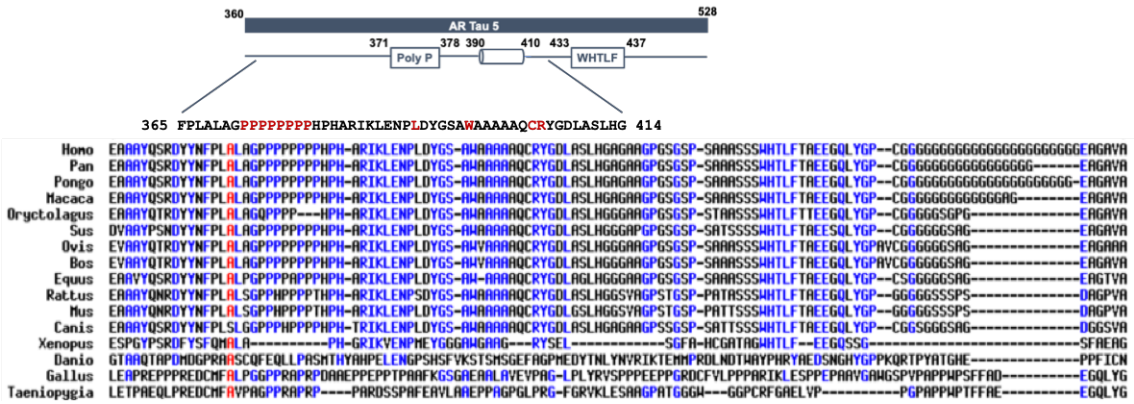

Figure 3.4: Identification of conserved BAG1L regulatory elements in the τ5 region
Top: Schematic representation of the ARτ5 region. Bottom: Multiple sequence alignment of AR protein sequences from different species showing conserved residues in the BAG1L binding site. The alignment was performed with the online software tool MultAlin (http://multalin.toulouse.inra.fr/multalin/). The sequences were taken from the National Center of Biotechnology Information (https://www.ncbi.nlm.nih.gov/protein/) with the following accesion numbers: Homo sapiens NP_000035.2; Canis lupus familiaris NP_001003053.1; Rattus norvegicus NP_036634.1; Gallus gallus NP_001035179.1; Mus musculus NP_038504.1; Sus scrofa NP_999479.2; Taeniopygia guttata NP_001070156.1; Ovis aries NP_001295513.1; Bos taurus NP_001231056.1; Macaca mulatta NP_001028083.1; Pan troglodytes NP_001009012.1; Equus caballus NP_001157363.1; Danio rerio NP_001076592.1; Oryctolagus cuniculus NP_001182653.1; Pongo abelii XP_009233214.1; Macaca mulatta NP_001028083.1; Oryctolagus cuniculus NP_001182653.1.

3.2.2 Mutations in the BAG1L binding site affect AR τ5 activity

BAG1L has been reported to upregulate AR activity through the interaction with the AR τ5 (Shatkina *et al.*, 2003; Cato *et al.*, 2017). However, it has previously been difficult to identify a distinct interaction site for BAG1L on the AR. In order to test the hypothesis that the binding motif identified in the NMR studies mediates BAG1L activity at AR τ5, a *mammalian-one-hybrid* assay with wild-type and mutant AR τ5 constructs was performed. The principal of *mammalian-one-hybrid* assays is based on the fact that transcriptional activators consist of two distinct units, a DNA-binding unit (here: GAL4-DBD) and a transactivation unit (here: AR-τ5). Only activation of the transactivation unit enables binding of the GAL4-DBD of *Saccharomyces cervisiae* to the *upstream activation sequence* (UAS) (here: GAL4 binding sites) in the nucleus and subsequent expression of the reporter gene firefly-luciferase.

For this experiment alanine substitution in single amino acid residues were inserted via QuikChange site-directed mutagenesis into a wild-type AR τ5 construct and an AR τ5 construct in which the poly-proline stretch was deleted (ΔPro). The single amino acid residues that were substituted in this experiment showed reduced resonance intensities (L391, W397 and C404) in a NMR study (Cato et al, 2017) or had previously been identified in a SPOT analysis by a former PhD student in the laboratory using different AR τ5 peptides and a GST-BAG1L C-terminal protein, (W397, C404 and R405). To study potential collective effects of the mutations, combinations of the alanine substitutions were inserted. Additionally, ΔPro was combined with L391A, W392A and C404A or ΔPro with C404A and R405A or just a combination of C404A and R405A. Furthermore, the effect

of mutation in the WHTLF motif to AHTAA was analyzed.

HeLa cells were transfected with a firefly luciferase construct under control of a GAL4-DNA binding site and a renilla luciferase construct controlled by a Ubiquitin promoter. Additionally, wild-type ARτ5 and the different mutants described above fused to a GAL4-DBD were cotransfected along with increasing amounts of BAG1L. Luciferase activity was measured and presented as firefly luciferase activity relative to renilla luciferase activity (Figure 3.5).

The results showed that overexpression of BAG1L in the presence of wild-type ARτ5 construct resulted in a 14-fold increase of AR τ5 activity. Single amino acid substitutions of the residues L391, W392, C404 and R405 had only moderate effects on the BAG1L-mediated AR τ5 activity. Similarly, the mutation of the WHTLF motif to AHTAA mutant did not significantly change BAG1L effect at the AR τ5. In contrast to the NMR results, deletion of the poly-proline region significantly reduced the BAG1L effect on AR τ5 activity inducing luciferase activity only 6-fold in comparison to basal activity. This inhibitory effect was more evident when an alanine substitution in residues L391 or C404 was inserted in addition to deletion of the poly-proline region. However, alanine substitution in residue W397 in the ΔPro context did not significantly change BAG1L-mediated AR τ5 activity compared to the wild-type AR τ5 construct. Intriguingly, combinations of the alanine substitutions in the wild-type or in the ΔPro backbone increased the BAG1L-mediated AR τ5 activity compared to the basal activity tremendously (C404A/R405A)(Figure 3.5).

The findings that single alanine substitutions in the amino acid residues had no effect on BAG1L-mediated AR τ5 activity but that deletion of the poly-proline region, significantly reduced BAG1L-mediated AR τ5 activity, particularly in combination with mutation L391A and C404A, suggests that BAG1L action at the AR τ5 region appears rather through a specific conformation than via single amino acid sequences. This hypothesis is further supported by the results that the peptide containing the polyproline region alone did not show chemical shifts in the NMR experiments, suggesting that polyproline region alone is not sufficient for mediating BAG1L effect at the AR tau5. The result that mutation in the WHTLF motif did not affect BAG1L action at the AR τ5 region validates that the poly-proline and poly-alanine regions are mainly required for BAG1L interaction with the AR NTD.

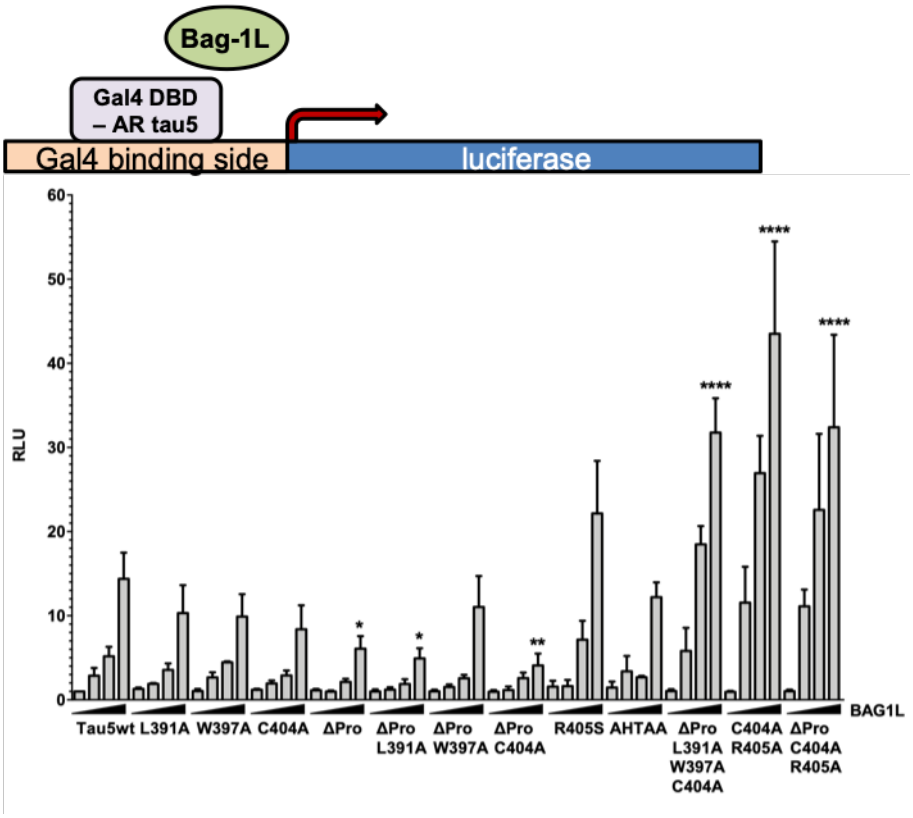

Figure 3.5: Mutations in the potential BAG1L binding sites affect AR τ5 activity
Mammalian-one-hybrid assay in HeLa cells transiently transfected with pG5ΔE4-38-luciferase, Ubiquitin-Renilla, the indicated pM-AR-τ5 constructs fused to Gal4 DBD and increasing amounts of pcDNA-BAG1L. Samples were harvested 48 h after transfection and luciferase activity was measured in duplicates. The mean of duplicates was used as one independent experiment. The bar charts are the mean of at least three independent experiments ± SEM, relative to the empty BAG1L expression vector. p-values were calculated using one-way ANOVA and Dunnett's test: $*$ $p \leq 0.05$, $**$ $p \leq 0.01$ and $****$ $p \leq 0.0001$

To examine whether the observed inhibitory or enhancing effects of mutations in the τ5 region on BAG1L action were brought about by decreased or facilitated binding of BAG1L to the mutants, a *mammalian-two-hybrid* experiment was performed. The principle of *mammalian-two-hybrid* assays is similar to *mammalian-one-hybrid* assays. However, in this type of interaction study the DNA-binding unit (here: GAL4-DBD) and the transactivation unit (here: VP16) are seperated. Only interaction of the VP-16 fusion construct with the GAL4 fusion construct enables expression of the firefly luciferase. In this experiment mutant ΔProC404A, which showed the strongest negative effect, and C404R405A, which showed the most enhancing effect on AR τ5 activity were further analyzed.
In this assay, HeLa cells were transfected with the firefly luciferase construct controlled by a GAL4 DNA binding site, a renilla luciferase construct under control of an ubiquitin promoter, the different pM-ARτ5 constructs and the herpes virus activation domain VP-16 or VP-16 fused to BAG1L. Luciferase activity was measured and firefly activity was normalized to renilla luciferase activity (Figure 3.6 Top). The empty vector pM, which expresses yeast Gal4-DBD alone, did not increase the activity of the Gal4-luciferase fusion protein and neither did cotransfection with the activator protein VP-16 or the BAG1L-VP-16 fusion protein. Also neither the activity of the Gal4-ARτ5

construct nor mutants thereof were enhanced in the presence of VP-16. Cotransfection of pM-ARτ5 and VP-16 BAG1L enhanced luciferase activity 55-fold compared to the basal activity of pM-ARτ5, which is due to interaction of BAG1L to the wild-type τ5 region. BAG1L-mediated luciferase activity was reduced to 34-fold increase compared to the basal activity, when the AR τ5ΔProC404 mutant was expressed. Overexpression of the C404A/R405A mutant resulted in an increased BAG1L effect showing a 64-fold increase of luciferase activity compared to the basal activity (Figure 3.6 Bottom).

Together these results suggest that mutations in the BAG1L binding site lead to changes in the interaction of BAG1L with the ARτ5 and these changes in interaction affect the transactivation activity of the AR τ5 region.

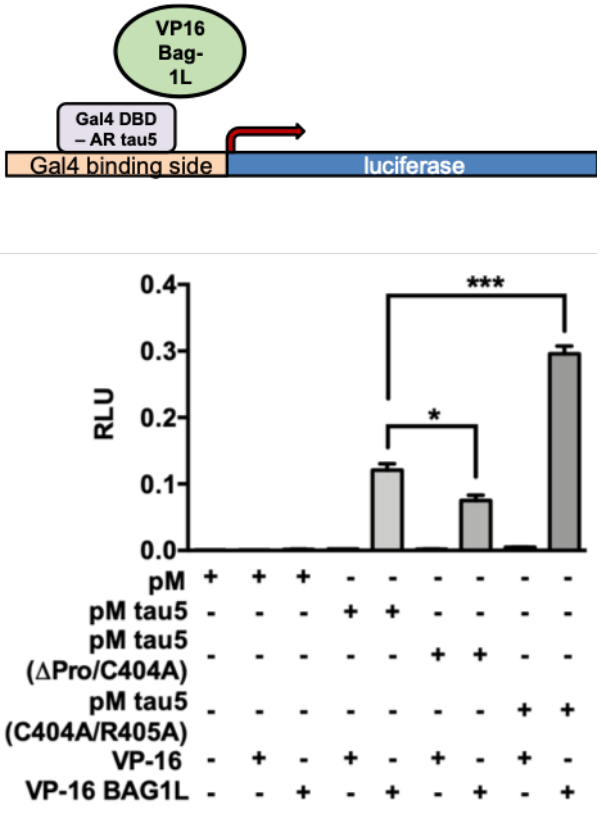

Figure 3.6: Mutations in the BAG1L binding sites affect BAG1L binding to AR τ5 region
Mammalian-two-hybrid assay with HeLa cells transiently transfected with pG5ΔE4-38-Luciferase, Ubiquitin-Renilla, the indicated ARτ5 constructs fused to Gal4-DBD (pM) and a VP16-BAG1L construct or the VP16 empty vector as a control. Samples were harvested 48 h after transfection and luciferase activity was measured in duplicates. The mean of duplicates was used as one independent experiment. The bar charts are the mean of three independent experiments ∓ SEM, relative to the Gal4-DBD (pM) vector control. p-values were calculated using student's t-test: $* \; p \leq 0.05$, $*** \; p \leq 0.001$

3.3 Knock-out of BAG1L leads to reduced co-regulator recruitment to AR

BAG1L is not a classical AR coactivator as it does not mediate histone acetyltransferase (HAT) activity. Its effect on AR gene expression is thought to be through a change in conformation of the receptor upon binding which results in the recruitment of coactivators to the AR (Cato *et al.*, 2017). To identify which coactivators are recruited to the AR by BAG1L, a *Microarray Assay for Real-time Coregulator-Nuclear receptor Interaction* (MARCoNI) was carried out in order to determine the interaction of coactivator peptides with the AR in the presence and absence of BAG1L. To this end, LNCaP control and BAG1L KO cells (Cato *et al.*, 2017) were hormone-starved and then treated with vehicle or hormone (DHT). Cell lysates were further analyzed on a PAMchip, which carries immobilized peptides encompassing the LxxLL or FxxLF binding motifs of known coregulators, and binding of the AR to those peptides was detected with an AR-specific antibody. Treatment with DHT effectively enhanced binding of the AR to the coregulators CBP, GELS, NCOA1/2/3 and 4, PAK6, PRGC1, RAD9A and ZHNI3 with association factors (AF) between 250 and 3000. Lysates of BAG1L KO cells showed a significant reduction of AR binding to the cofactor motifs reaching approximately 50 % in some cases compared to the control cells in the presence and absence of hormone (Figure 3.7 Bottom and Table 3.1). However this reduced effect was more noticeable in the 16 h DHT treatment than in the 4 h DHT treatment.
These results identify the coactivators that may play a role in BAG1L-mediated activation of AR action.

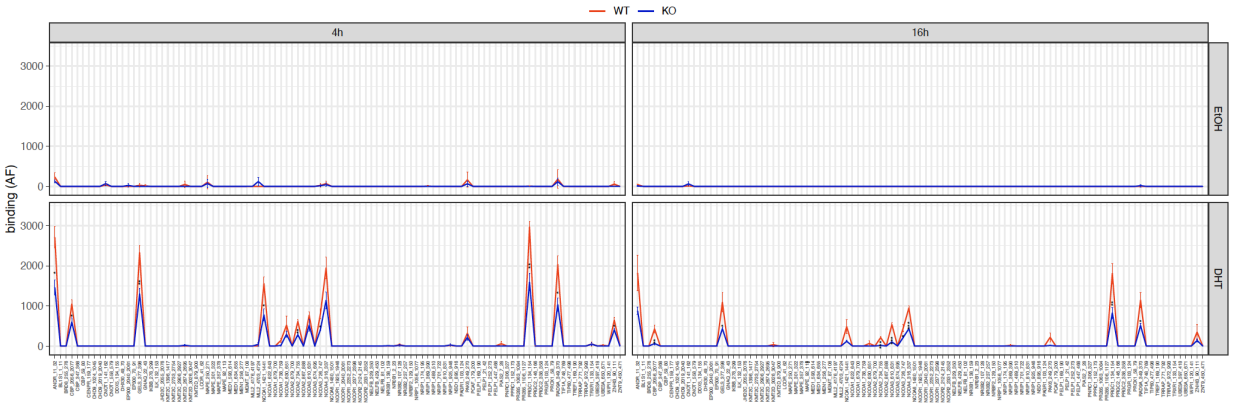

Figure 3.7: Knock-out of BAG1L reduces binding of Co-factors to the AR
Control and BAG1L KO LNCaP cells were starved for 72 h and treated with vehicle or hormone (DHT) for 4 h or 16 h. Cells were harvested and lysed and the total protein amount was determined via Bradford assay. Input was normalized to total protein amount. Lysates were applied to a Chip carrying co-activator binding sites. After incubation excess lysates were removed and binding of AR to the peptides was detected with a specific AR antibody. Each sample was measured in quadruplets

Table 3.1: AR affinity (AU) to coregulator motifs in the abscence or presence of BAG1L

Coregulators	4 h DHT (AU)		16 h DHT (AU)	
(Residues)	Control	BAG1LKO	Control	BAG1LKO
CBP (347-368)	∼ 1000	∼ 500	∼ 500	∼ 10
GELS (377 - 398)	∼ 2500	∼ 1500	∼ 1000	∼ 500
NCOA1 (1421-1441)	∼ 1750	∼ 1000	∼ 500	∼ 100
NCOA2 (630 - 651)	∼ 500	∼ 300	∼ 75	0
NCOA2 (734 - 755)	∼ 600	∼ 300	∼ 200	0
NCOA3(610 - 631)	∼ 750	∼ 500	∼ 500	∼ 100
NCOA3 (726 - 747)	∼ 750	∼ 500	∼ 500	∼ 250
NCOA4 (316 - 337)	∼ 2000	∼ 1000	∼ 1000	∼ 500
PAK6 (249-270)	∼ 250	∼ 200	∼ 250	0
PRGC1 (134-154)	∼ 3000	∼ 1600	∼ 2000	∼ 1000
RAD9A (349 - 370)	∼ 2000	∼ 1000	∼ 1000	∼ 500
ZNHI3 (90 - 111)	∼ 600	∼ 450	∼ 450	∼ 150

3.4 Knock-out of BAG1L affects AR target gene profile

Many of the coregulators that showed differential binding to the AR upon BAG1L KO in the MAR-CoNI experiments are involved in transcriptional regulation of the AR (Xu *et al.*, 2009; Goodman & Smolik, 2000; Broustas *et al.*, 2019). This suggested that loss of BAG1L would also alter the expression of AR target genes. To identify BAG1L regulated AR target genes and pathways previously generated RNA-seq results (Cato *et al.*, 2017) were re-analyzed by calculating the differences in fold change for androgen-responsive gene in the control and BAG1L KO cells. The androgen responsive genes were then plotted in a Scatter Plot Matrix. Here, differentially regulated genes of LNCaP control cells on the x-axis (vehicle (EtOH) vs DHT). Genes which were strongly regulated by DHT in these cells can be found in the far left and far right area of the Matrix and genes that moderatly regulated by DHT can be found in the center of the Matrix. Differentially, regulated genes of LNCaP BAG1L KO cells were blotted on the y-axis (vehicle (EtOH) vs DHT). Genes which were strongly regulated by DHT in the BAG1L KO cells can therefore be found in the top and the bottom area of the Matrix. 3.8).

Gene ontology analysis was then performed using the Broad Institute Molecular Signature Database (MSigDB) to identify AR-regulated signaling pathways controlled by BAG1L. These studies-revealed, as expected, that most of the genes were linked ton androgen response. Additionally the BAG1L regulated androgen response genes were associated with oxidative stress and metabolic processes (Figure 3.8B). Some of those genes were highlighted in purple in the Scatter Blot Matrix (Figure 3.8A). Analysis of the RNA-seq results was performed by Irene Lee and Jaice Rottenberg at the Dana-Farber-Institute in Boston.

To validate the findings of the RNA-seq results, four of the BAG-1L regulated AR target genes were chosen for quantitative RealTime-PCR analysis. Hormone-treated control and BAG1L KO LNCaP cells were compared in terms of the expression of the AR target gene transcripts of *MICAL1*, *DUOX1*, *NNT* and *F5*. MICAL1 and DUOX1 code for NAD(P)H oxidases and NNT codes for a NAD(P)H transhydrogenase. These proteins are directly involved in maintaining ROS levels in the cell. The gene F5 codes for the Proaccelerin protein, which is involved in blood coaggulation and represents a potential prostate cancer marker. The expression of all four genes was significantly induced in control cells in response to DHT treatment. BAG1L KO resulted in a significantly reduced expression of MICAL1, DUOX1 and F5 in absence as well as in the presence of hormone. Expression levels of NNT in BAG1L KO cells were comparable to the expression in control cells under vehicle conditions. However, no hormone effect was observed in the absence of BAG1L. Together these results validated the findings of the RNA seq analysis, showing that loss of BAG1L reduces the expression of several AR target genes, some of which are associated with oxidative stress.

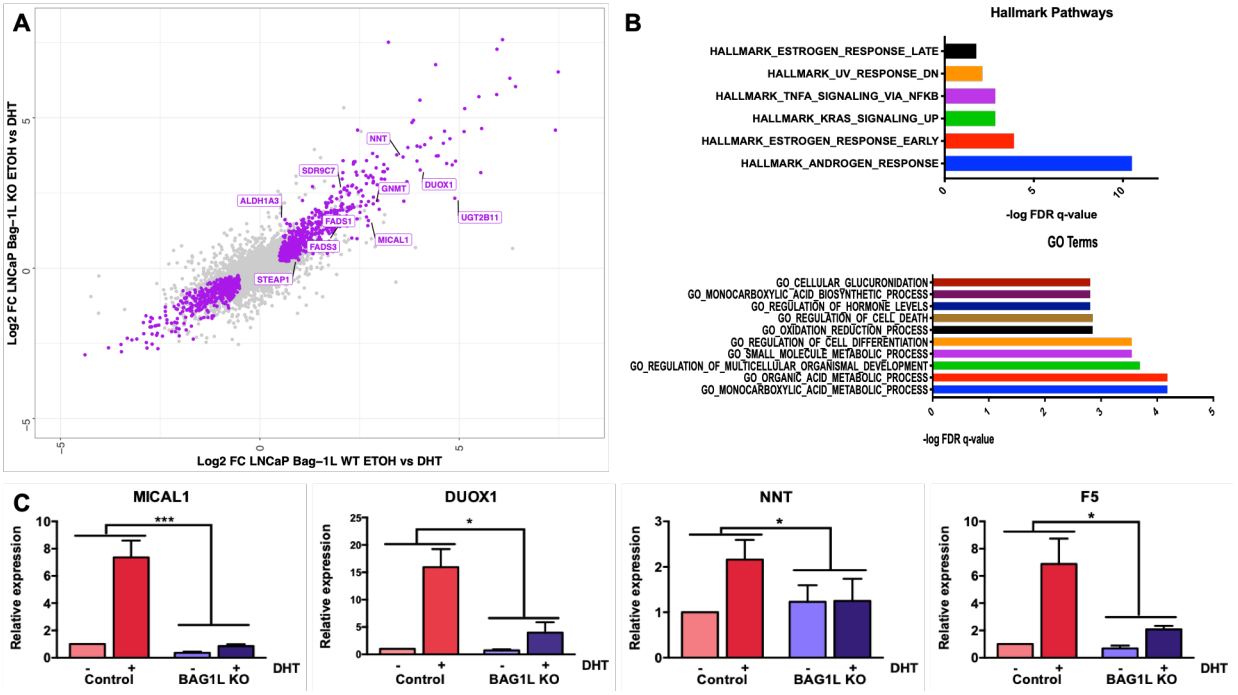

Figure 3.8: Identification of BAG1L-regulated AR target genes
(A) Analysis of RNA-seq data from LNCaP control and BAG1L KO cells. Scatter Plot Matrix represents genes of interest in LNCaP Control cells (ethanol vs DHT) on x-axis and LNCaP BAG1L KO cells (ethanol vs DHT) on y-axis. (B) Hallmark Pathways (GSEA; Top) and GO Terms (Bottom) associated with BAG1L-regulated direct AR-target genes. (C) Validation of BAG1L-responsive direct AR target genes. LNCaP Control and BAG1L KO cells were hormone-starved for 72 h and treated with vehicle (ethanol) or DHT for 16 h. RNA was extracted and transcribed into cDNA. The expression of target genes was analyzed using specific primers for the indicated genes. Significance was calculated by Two-Way ANOVA and Sidak's test * $p \leq 0.05$, *** ≤ 0.001

3.5 BAG1L plays a role in the regulation of androgen-mediated oxidative stress

The analysis of RNA-seq results hinted at a role of BAG1L in AR-mediated regulation of oxidative stress. Oxidative stress describes an imbalance of elevated reactive oxygen species (ROS) levels and the 'antioxidant' defense mechanisms in the cell. Oxidative stress can be indirectly determined by measuring oxidative stress marker such as the levels of DNA/RNA damage, lipid peroxidation or protein oxidation/nitration or by direct measurement of cellular reactive oxygen species using fluorescent dye-based methods (Abcam, 2020). To further examine the role of BAG1L in the regulation of oxidative stress, ROS production was measured in the androgen-responsive control and BAG1L KO LNCaP cells. The fluorescent probe 2´,7´-dichlorofluorescein diacetate (DCF), which is *inter alia* a reporter for hydrogen peroxide and hydroxyl radicals, was used for this purpose. LNCaP control and BAG1L KO cells were subjected to H_2DCF and subsequently treated with 10^{-8}M androgen (R1881) for 96 h. The cells were subjected to H_2DCF for 40 minutes and H_2DCF oxidation was measured at 485 nm excitation and 530 nm emission.
H_2DCF oxidation was slightly increased in control cells after treatment with R1881 compared to the vehicle control. In the BAG1L KO cells the basal H_2DCF oxidation was reduced compared to the vehicle treated control cells. Additionally, treatment of R1881 did not enhance H_2DCF oxidation (Figure 3.9A).
This suggests that BAG1L indeed contributes to the production of ROS in PCa cells in the presence and absence of hormone.
Classically the production of ROS is associated with cell stress and apoptosis. However, it has been reported that low levels of ROS can also enhance cell growth and proliferation, especially in a tumor context (Day & Suzuki, 2005). To asses if that BAG1L can enhance the production of ROS to promote proliferation of PCa cells a proliferation assay with the NAD(P)H oxidase inhibitor diphenyleiodonium (DPI) was performed. NAD(P)H oxidases are membrane-bound enzyme complexes that catalyze the production of superoxide (O_2^-) radicals. DPI inhibits the activity of those enzymes, resulting in reduction of superoxide radicals in the cells. Control and BAG1L KO LNCaP cells were seeded one day prior to treatment with DPI. The basal cell number was determined by counting on the day of treatment. Additionally, cells were counted one, three and five days post treatment. One day post application no significant differences in proliferation was observed between the two cell lines. After three days of treatment, proliferation of control cells and BAG1L KO was slightly reduced in the presence of DPI compared to solvent treated cells. Five days post application, DPI treatment reduced proliferation of control cells by half compared to the vehicle treated cells. BAG1L KO cells proliferated less under vehicle conditions compared to control cells. However, addition of DPI did not further inhibit proliferation of BAG1L KO cells. (Figure 3.9B).
Together these results suggest that production of ROS in PCa cells promotes proliferation and is regulated by AR and BAG1L.

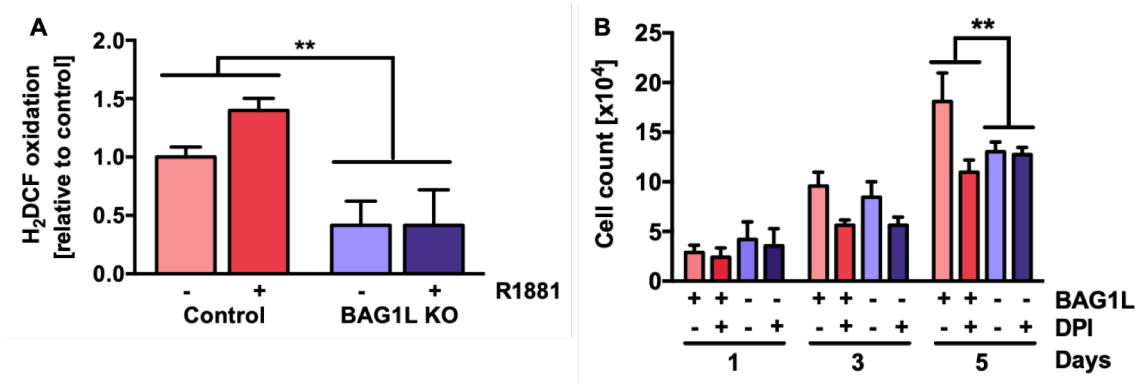

Figure 3.9: Loss of BAG1L reduces production of reactive oxygen species (ROS) in LNCaP cells
(A) Control and BAG1L KO LNCaP cells were starved for 4 days and subsequently treated with 10^{-8}M androgen (R1881) for 96 h. Cells were then subjected to H_2DCF for 40 minutes and thereafter H_2DCF oxidation was measured at 485 nm excitation and 530 nm emission. The results represent the averages of H_2DCF oxidation $\pm$ SEM (** $p \leq 0.01$, n = 6) (B) NAD(P)H oxidase inhibitor inhibits proliferation of LNCaP control cells but not of BAG1L KO cells. Proliferation of control and BAG1L KO LNCaP cells was determined in the absence and presence of 0.1 µM of the NAD(P)H oxidase inhibitor diphenyleneiodonium (DPI). Cell number was assessed by counting on days 0, 1, 3 and 5 post treatment. Data shows the average of three independent experiments $\pm$ SEM, normalized to day 0; p-values were calculated using students t-test ** ≤ 0.01

3.6 Identification of small molecule AR-AF-1 inhibitors

After the site and mode of action of BAG1L was clarified, it was considered appropriate to apply this knowledge to search for inhibitors that would function through the BAG1L-AR-AF1 interaction. The small molecule 2-arylbenzothiazole Thio-2 (A1B1) had previously been reported to inhibit BAG1 action and was predicted in *in silico* analyses to bind the C-terminal BAG domain (Enthammer *et al.*, 2013; Papadakis *et al.*, 2016). However, in subsequent studies, Thio-2 was shown to be a non-selective inhibitor (unpublished data of our group). In collaboration with the Compounds Platform (ComPlat) of the KIT, 47 derivatives of Thio-2 were synthesized. In this process different substituents were introduced into the benzothiazole (building block A) and aryl (building block B) parts of the core structure to improve its pharmacological effects. The resulting compounds can be sorted into five different classes A1B (17 compounds) plus A1B20, A2B (14 compounds), A3B (5 compounds) and A4B (11 compounds) (Figure 3.10).
The derivatives were then analyzed for their efficacy to reduce AR target gene expression in quantitative real-time PCR (qPCR) experiments. To this end, the BAG1L-regulated AR target gene *F5*, which was identified in the RNA-seq reanalysis (Figure 3.8C) was used. Hormone responsive LNCaP cells were hormone-starved for three days and subsequently treated with 5 µM of each compound, DMSO as negative control or the classical antiandrogen enzalutamide as positive control. One hour post application, DHT was added to the cells and the samples were incubated for 16 h. Expression of Proaccelerin was analyzed using specific primers.
DHT-treatment in the absence of compounds increased F5 expression tenfold compared to vehicle treated cells. Application of Thio-2 (A1B1) inhibited DHT-mediated F5 expression only slightly. However, a number of the Thio-2 derivatives were able to inhibit F5 expression by approximately

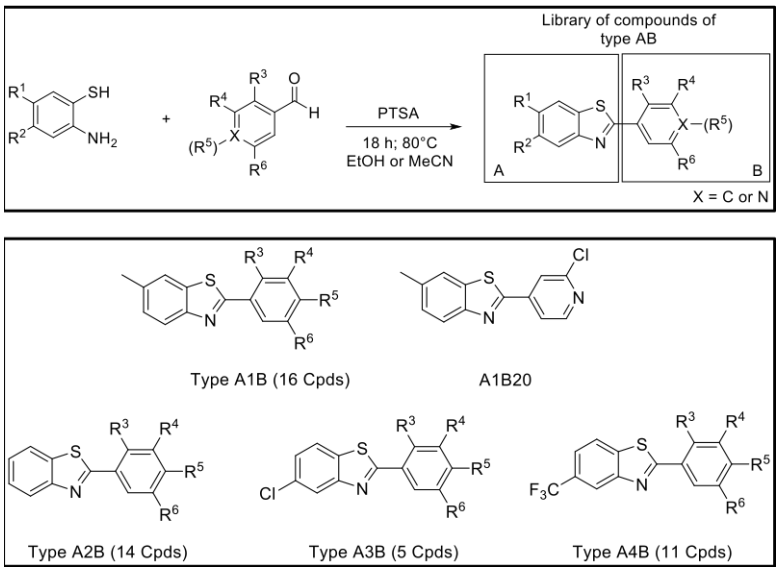

Figure 3.10: Synthesis of benzothiazole derivatives.
Schematic description of the synthesis of different 2-arylbenzothiazoles. Reaction was performed with different aldehydes and 2-aminoaryl thiols resulting in five different classes of benzothiazoles: A1B, A1B20, A2B, A3B and A4B. PTSA: p-Toluene Sulphonic Acid, ETOH: ethanol and MeCN: acetonitrile.

60 % or more showing an inhibitory effect comparable to the classical antiandrogen enzalutamide (Enza). The most prominent inhibitions were achieved by compounds with an aryl building blocks B11, B17, B18 or B20. The different substitutions on the the benzothiazole ring did not show consistent effects. Six of the compounds, A1B17, A1B18, A1B20, A2B17, A2B18 and A4B17 (highlighted in dark grey), which showed improved inhibition were chosen for further analysis (Figure 3.11 B and C).

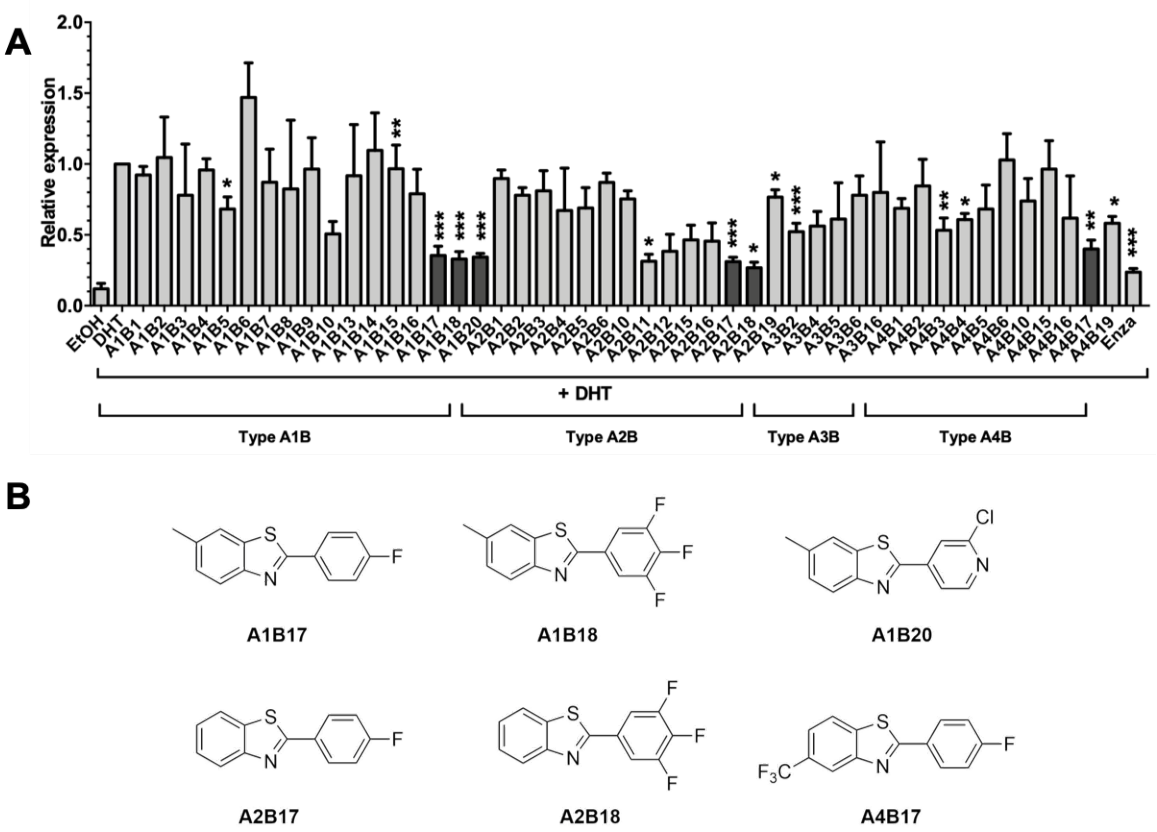

Figure 3.11: Identification of benzothiazole derivatives that inhibit BAG1L-regulated AR target gene expression.
(A) Efficacy of different benzothiazole compounds to down-regulate androgen-mediated gene expression of the Proaccelerin gene (F5) determined in quantitative RT-PCR studies. LNCaP cells were starved for 72 h and subsequently treated with 5 µM of the indicated compounds, DMSO as a negative control or enzalutamide (Enza) as positive control. One hour post application, DHT was added to the samples. Total RNA was extracted and RT-PCR was carried out with the F5 primer and a control ribosomal RNA primer. The bar chart shows F5 expression relative to the housekeeping gene Rib36B4 and normalized to DHT-treated control ± SEM (n = 3-23; student's t-test * $p \leq 0.05$, ** $p \leq 0.01$, *** $p \leq 0.001$). (B) The structures of the six 2-arylbenzothiazole derivatives selected as inhibitors of AR activity.

3.7 Small molecule AR-AF-1 inhibitors selectively inhibit BAG1L-mediated AF1 activity

To determine whether the compounds that effectively downregulated *F5* expression selectively function through the BAG1L-AR-AF1 interaction, a series of *mammalian-one-hybrid* assays (see section 3.2.2) was performed. In these experiments the potency of the compounds in the presence of different BAG1 variants was assessed. Furthermore, their effects on basal AR-AF1 activity and on the AR AF-2 activity were analyzed. All experiments were performed as described in the following:

To exclude the possibility that endogenous BAG1L levels could influence the potency of the compounds the experiments were performed in COS-7 cells, that do not express BAG1L. For each experiment COS-7 cells were transfected with a firefly luciferase construct under control of the

GAL4 binding sites and a renilla luciferase controlled by an ubiquitin promoter to check the transfection efficiency. Furthermore, cells were transfected either with the AR-AF1 or AR-AF2 fused to the GAL4-DBD. Cells transfected with AR-AF2 were additionally treated with ethanol or DHT 24 h after transfection.
To first demonstrate the effect of the BAG1 variants on AR-AF1/AF2 activity cells were transfected with increasing concentration of BAG1L, BAG1L-cMut, BAG1M or BAG1M-NLS (DNA-amount was equalized with empty vector).
For investigation of the compounds, cells were transfected with one concentration of BAG1L, BAG1L-cMut, BAG1M or BAG1M-NLS. Cells were treated with the compounds one day post transfection and luciferase activity was measured 48 h post transfection. The firefly luciferase activity was normalized to renilla luciferase activity.

3.7.1 Small molecule AR-AF-1 inhibitors that reduce AF1 activity in the presence of BAG1L but not mutant BAG1L

In the first experiment, all compounds were tested for their potency of inhibition of the BAG1L-AR-AF1-interaction. Therefore, their dose-dependent effect on AR-AF1 transactivation was tested in the presence of BAG1L or a C-terminal Triple mutant of BAG1L (cMut), which is deficient for AR binding.
First it was shown that AR-AF1 activity significantly increases with transfection of increasing amounts of BAG1L. However, expression of the C-terminal BAG1L mutant did not increase AR-AF-1 activity as expected (Figure 3.12).

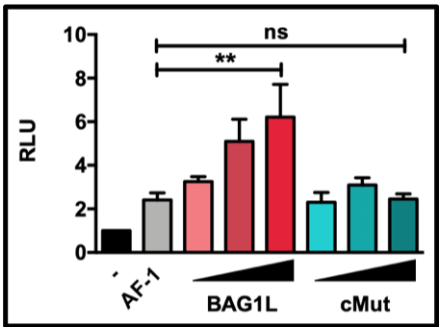

Figure 3.12: Overexpression of BAGL1 but not BAG1L cMut enhances AR-AF1 activity
Mammalian one-hybrid assays in COS-7 cells transfected with pG5ΔE4-38 luciferase, Ubi-Renilla luciferase, pM-AR AF-1 and increasing amounts of pcDNA-BAG1L or pcDNA-BAG1LcMut. Samples were harvested 48 h after transfection and luciferase activity was measured in duplicates. The mean of duplicates was used as one independent experiment. The bar charts are the mean of four independent experiments ± SEM, relative to the empty BAG1L expression vector. p-values were calculated using one-way ANOVA and Dunnett's test: ** $p \leq 0.01$; ns: not significant.

The effect of the compounds was calculated from the firefly luciferase activity normalized to renilla luciferase activity. This showed that the compounds A1B1, A1B17, A2B18 and A4B17 inhibited BAG1L-mediated AR-AF1 activity with IC_{50} in the µM and nM ranges (Figure 3.13). The compounds A1B18, A1B20 and A2B17 did not affect BAG1L-mediated AR-AF1 activity, meaning that they most likely inhibited *F5* gene expression through a different mechanism. For this reason, these compounds were excluded from further analyses (Figure 3.13).

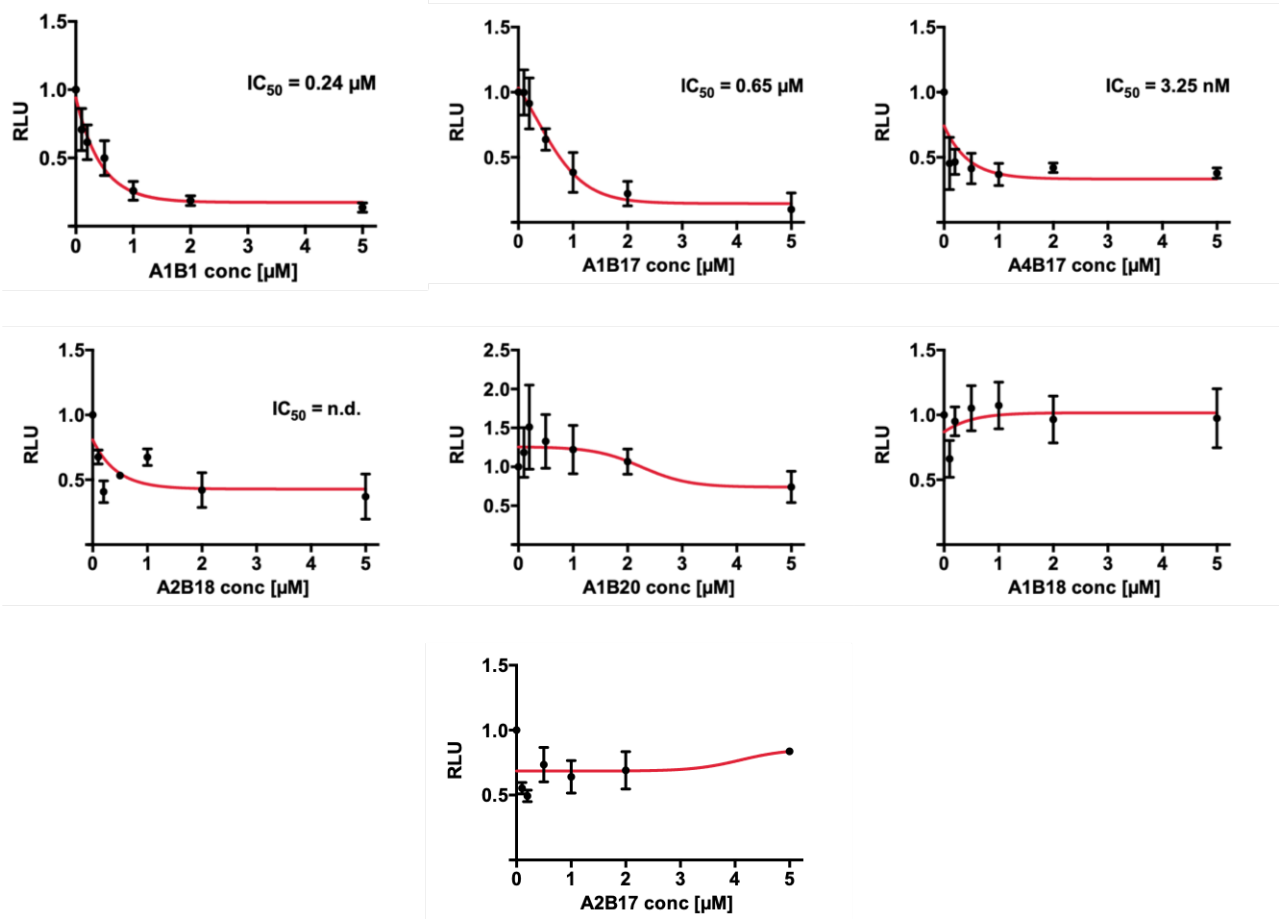

Figure 3.13: Identification of benzothiazoles that inhibit BAG1L-AR-AF-1 activity
Mammalian one-hybrid assay to assess the effect of the indicated compounds in COS-7 cells transfected with pG5ΔE4-38 luciferase, Ubi-Renilla luciferase, pM-AR-AF1 and pcDNA-BAG1L. Samples were harvested 48 h after transfection and luciferase activity was measured in duplicates. The results are the mean of at least three independent experiments ± SEM, relative to the solvent control (0 µM)

Assuming that the compounds function through selective inhibition of BAG1L-AR-AF1 interaction the selected compounds should not affect AF-1 activity in the presence of BAG1L cMut. Nonetheless, compound A1B17 as well as the parental compound A1B1 did inhibit AR-AF1 activity in the presence of BAG1L cMut (IC_{50} = 0.65 µM and 0.54 µM), suggesting that these compounds function through a different pathway. Regarding efficacy, increasing concentrations of the compound A4B17 also reduced AR-AF1 activity in the presence of BAG1L cMut. However, this inhibitory effect was brought about by higher concentrations compared to wild-type BAG1L transfected cells, resulting in an IC_{50} of 1.2 µM, which indicates a reduced potency of the compound in the presence of mutant BAG1L and suggests that compound A4B17 has a higher degree of selectivity compared to A1B1 or A1B17. Compound A2B18 did not affect AF-1 activity in the presence of BAG1L cMut indicating a high degree of selectivity for the BAG1L-AR-AF1 interaction (Figure 3.14).

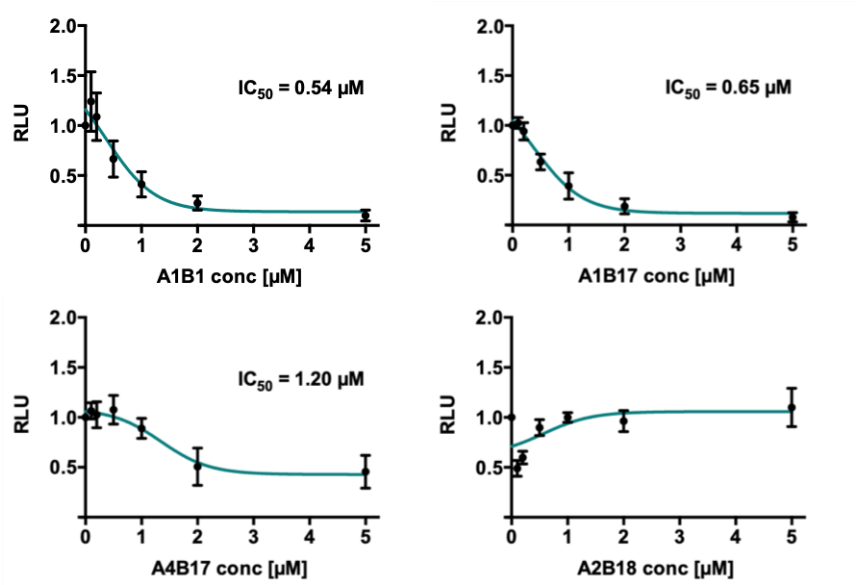

Figure 3.14: Effect of benzothiazoles on AR-AF-1 activity in the presence of BAG1L cMut.
Mammalian one-hybrid assay to assess the effect of the indicated compounds in COS-7 cells transfected with pG5ΔE4-38 luciferase, Ubi-Renilla luciferase, pM-AR-AF1 and pcDNA-BAG1L cMut. Samples were harvested 48 h after transfection and luciferase activity was measured in duplicates. The results are the mean of at least three independent experiments ± SEM, relative to the solvent control (0 µM)

These results identify A2B18 and A4B17 as compounds that inhibit expression of the AR target gene *F5* and selectively target BAG1L-AR-AF1 activity and were therefore selected for further characterization.

3.7.2 Small molecule AR AF-1 inhibitors do not affect AF1 activity in the presence of cytoplasmic BAG1 isoforms

The interaction with the AR-AF1 takes place at the C-terminal BAG domain of BAG1L. The BAG1 family consists of four proteins derived from the same mRNA by alternative translation and therefore all four isoforms possess a conserved C-terminal BAG domain that interacts with the AR. However, only the largest, nuclear isoform BAG1L is able to regulate AR action in the nucleus. To test whether the identified compounds also inhibit AR activity mediated by other BAG1 isoforms their effect on AR-AF1 transactivation was analyzed in the presence of the cytoplasmic BAG1 isoform BAG1M and the nuclear form of this protein BAG1M-NLS, where the simian virus SV40 is N-terminally fused to the BAG1M sequence (Shatkina et al, 2003).
Overexpression of the cytoplasmic BAG1 isoform BAG1M showed that BAG1M has only marginal effects on AR-AF1 activity. However, overexpression of the NLS-BAG1M fusion protein significantly enhanced activity of the AR-AF1, which validates that nuclear localisation of the BAG protein is important to regulate AR activity. Treatment with the compounds A2B18 and A4B17 showed that neither of the two benzothiazole derivatives had an effect on BAG1M or NLS-BAG1M-mediated AR-AF1 activity (Figure 3.15B). On the contrary A1B1 inhibited the activity of AR-AF1 in the presence of BAG1M as well as BAG1M NLS (Figure 3.15C).

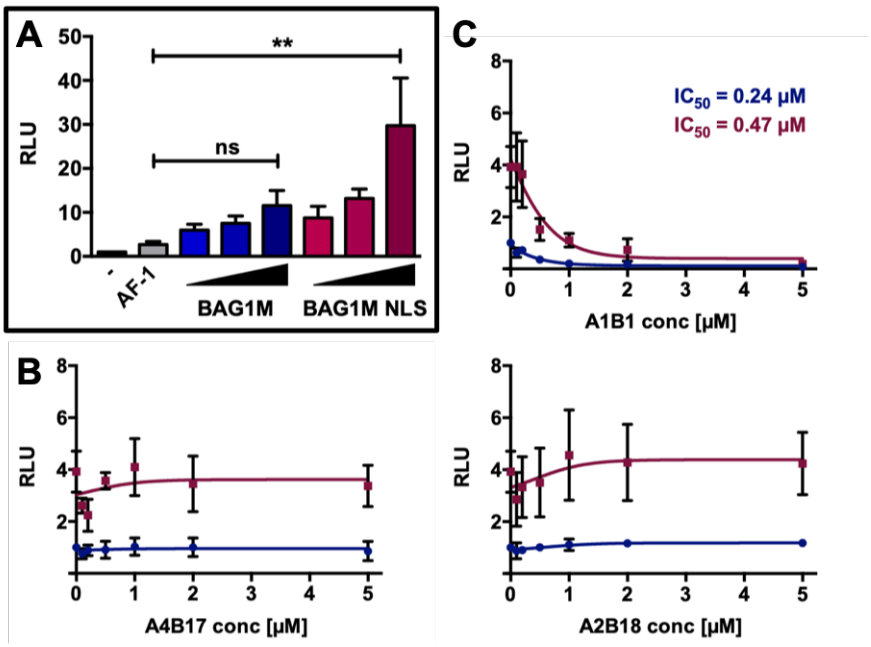

Figure 3.15: Benzothiazole derivative do not affect AF1 activity in the presence of other cytoplasmic or nucelar BAG1 isoforms.
Analysis of the specificity of the identified compounds for BAG1L. (A) Mammalian one-hybrid assays were carried out in COS-7 cells transfected with pG5ΔE4-38 luciferase, Ubi-Renilla luciferase, pM-AR and increasing amounts of pcDNA-BAG1M or pcDNA-BAG1MNLS. Samples were harvested 48 h after transfection and luciferase activity was measured in duplicates. The mean of duplicates was used as one independent experiment. The bar charts show the mean of three independent experiments. p-values were calculated using one-way ANOVA and Dunnett's test; ns: not significant; ** $p \leq 0.01$ (B) + (C) Mammalian-one-hybrid Assay to asses the effect of increasing concentrations of the indicated compounds on BAG1M and BAG1MNLS-mediated AR-AF1 activity. COS-7 cells were transfected with pGΔDE4-38 luciferase, Ubi-Renilla luciferase, pM-AR-AF1 and pcDNA-BAG1M or pcDNA-BAG1MNLS. Samples were treated with increasing amounts of the indicated compound after 24 h post transfection. Samples were harvested 48 h after transfection and luciferase activity was measured in duplicates. The mean of duplicates was used as one independent experiment. The results are the mean of at least three independent experiments ± SEM, relative to the solvent control (0 µM)

3.7.3 Small molecule AR AF-1 inhibitors do not affect AR AF-1 activity in the abscence of BAG1L

It was further assessed whether the compounds might affect basal AR AF-1 activity. For this their effect in empty vector transfected cells was analyzed.
In this experiment the effect of the compounds A2B18 and A4B17 on basal AR-AF1 activity was examined. The parental compound A1B1 was used as a control. In contrast to the derivatives A2B18 and A4B17, which showed no effect on AR-AF-1 activity in the absence of BAG1L , A1B1 inhibited AR-AF-1 activity with an IC_{50} of 0.27 µM (Figure 3.16).

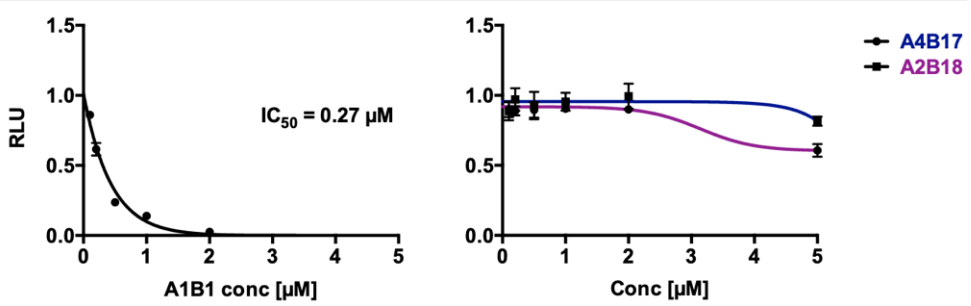

Figure 3.16: Small molecule AR AF-1 inhibitors do not affect AR AF-1 activity in the abscence of BAG1L.
Effect of increasing concentrations of the indicated compounds on basal AR-AF1 activity in Mammalian one-hybrid assay. COS-7 cells were transfected with pG5ΔE4-38 luciferase, Ubi-Renilla luciferase and pM-AR-AF1. Samples were treated with increasing amounts of the indicated compound 24 h post transfection. Samples were harvested 48 h after transfection and luciferase activity was measured in duplicates. The mean of duplicates was used as one independent experiment. The results are the mean of at least three independent experiments ± SEM, relative to the solvent control (0 µM)

3.7.4 Small molecule AR AF-1 inhibitors do not inhibit BAG1L-mediated AR AF-2 activity

Most of the clinically used therapeutics for prostate cancer act exclusively on the AR-AF2 in the LBD by either blocking biosynthesis of endogenous androgens or by competing with endogenous androgens for LBD binding. It was previously shown in mammalian-one-hybrid assays that BAG1L also enhances the activity of not only the AR NTD but also the AR LBD in the presence of DHT (Cato *et al.*, 2017). In the following experiments the compounds A2B18 and A4B17 were tested for their ability to inhibit BAG1L-mediated AR-AF2 activity.

In this experiment previous findings were validated (Cato *et al.*, 2017) showing that overexpression of BAG1L did not alter AF2 activity in the absence of hormone. Yet, in the presence of DHT BAG1L significantly enhanced AR-AF2 activity.
Treatment with A1B1 inhibited AR-AF2 activity both in the presence or absence of DHT with an IC_{50} of 0.26 µM, validating previous findings that A1B1 is an unselective inhibitor. The two compounds A2B18 and A4B17 however had no effect on AR-AF2 activity neither in the absence nor presence of hormone.
Taken together these finding suggest that in contrast to the parental compound A1B1, the two compounds A2B18 and A4B17 inhibit BAG1L-AR-AF1 activity more selectively. However, for further analysis A4B17 was selected because of its IC_{50} in the nanomolar range for BAG1L-mediated activity as opposed to A2B18, for which no IC_{50} was detectable.

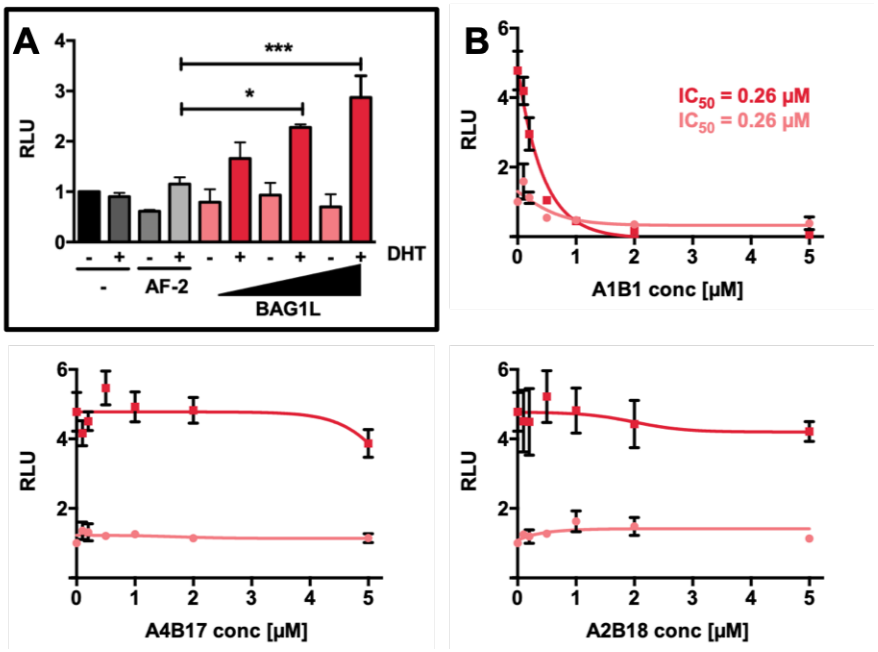

Figure 3.17: Small molecule AR-AF1 inhibitors do not affect BAG1L-mediated AF-2 activity.
Effect of increasing concentrations of the indicated compounds on BAG1L-mediated AF-2 activity in mammalian-one-hybrid experiments. (A) COS-7 cells were transfected with pG5ΔE4-38 luciferase, Ubi-Renilla luciferase construct and pM-AR AF2 and increasing concentrations of BAG1L. After 24 h, the transfected cells were treated with solvent (ethanol) or 10 nM DHT. Cells were harvested 48 h after transfection and luciferase activity was measured in duplicates. The mean of duplicates was used as one independent experiment. The bar charts show the mean of three independent experiments. p-values were calculated using one-way ANOVA; * $p \leq 0.05$; *** $p \leq 0.001$. (B) Mammalian one-hybrid assay to assess the effect of increasing concentrations of the indicated compounds on BAG1L-mediated AR-AF2 activity. COS-7 cells were transfected with pG5ΔE4-38 luciferase, Ubi-Renilla luciferase, pM-AR AF2 and pcDNA-BAG1L. Samples were treated 24 h post transfection with increasing amounts of the indicated compound. Solvent (ethanol) or DHT (10 nM) was added 1h later. Cells were harvested 48 h after transfection and luciferase activity was measured in duplicates. The mean of duplicates was used as one independent experiment. The results are the mean of at least three independent experiments ± SEM, relative to the solvent control (0 µM)

3.8 Compound A4B17 binds weakly to the BAG domain of BAG1L

Using computational modelling approaches based on the X-ray crystal structure of the BAG domain of BAG1L (Res: 1.9Å) the intramolecular interactions between compound A4B17 and the BAG domain was analyzed by Dr. Ravi Munuganti. Molecular docking studies showed that A4B17 forms arene-cation interactions with charged residues Arg305, Arg308 and Lys309 of the BAG domain. Additionally, the CF3 group at the 5th position of the benzothiazole ring interacts with the Leu306. However, with a docking score of -4.05 it was considered weak binding which is probably caused by the flatness of the BAG domain (Figure 3.18A).

To learn about the binding affinity of A4B17 to the BAG domain a differential scanning fluorimetry experiment was performed. This method is based on the ability of the fluorescent dye SYPRO Orange to bind non-specifically to hydrophobic residues of a protein, which are exposed during denaturation. The fluoresence of SYPRO Orange is quenched by water and therefore binding to

hydrophobic sites enhances fluoresence by excluding water from the complex. Increased binding of a ligand to the protein (e.g. at higher concentrations of the ligand) results in an enhanced stability of the protein, even at higher temperatures leading to higher melting temperatures. Here SYPRO Orange was added to an unlabelled BAG domain (Tm = 37.3 °C). Increasing concentration of A4B17 was then added to the protein mixture and a melting curve analysis was performed using a StepOnePlus Real-Time PCR System. Binding of the compound to the BAG domain resulted in the stabilization of protein which was reported by an increased melting temperature (Tm). The experiment showed that A4B17 interacts with the BAG domain with a thermal shift from 37 °C to 48 °C. However binding affinity was low resulting in a Kd of 13.1 mM (Figure 3.18B).
To demonstrate that A4B17 indeed interacts with the BAG domain the amino acid residues identified in the computational analysis (R305, R308 and K309) as putative interaction sites were exchanged to alanines in the BAG1L expression vector. This construct as well as a wild-type BAG1L construct was used in mammalian-one-hybrid experiments to determine their effect on AR-AF1 activity. COS-7 cells were transiently transfected with a firefly luciferase sequence under control of the GAL4 DNA binding site and a Ubiquitin-Renilla luciferase construct along with AR-AF1 fused to GAL4-DBD and the wild-type or mutant BAG1L (R305A/R308A/K309A) to examine the dose-dependent effect of A4B17. This results demonstrated that mutations in the putative binding sites of A4B17 in the BAG domain abolish BAG1L-mediated AR-AF1 activity suggesting that these residues are critical for AR-AF1 enhancement by BAG1L. Furthermore treatment with increasing amounts of A4B17 did not further inhibit AF1 activity, supporting the findings that A4B17 binds to the BAG domain.

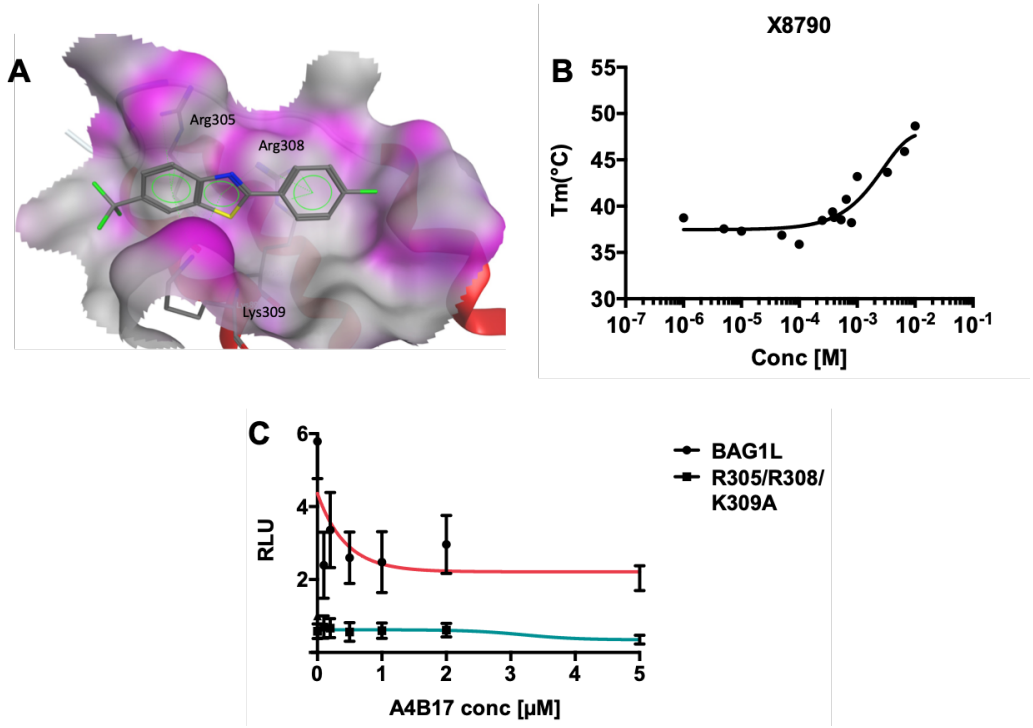

Figure 3.18: Binding of A4B17 to BAG1 domain.
(A) Docking results of A4B17 in the BAG domain identify amino acid residues Arg305, Arg308 and Lys309 as important for binding to compound A4B17. (B) Binding of compound A4B17 to the BAG domain was confirmed by a thermal shift assay in the presence of SYPRO Orange and increasing amounts of A4B17. Data shows Tm in response to different concentrations of A4B17. Data is a representative of three experiments that showed the same trend. The results are the mean of an experiment carried out in triplicates ± SEM. (C) Mutations in the BAG domain of BAG1L impair BAG1L effect on AR-AF1 activity. Effect of increasing concentrations of A4B17 in COS-7 cells transfected with pG5ΔE4-38 luciferase, Ubi-Renilla luciferase, pM-AR-AF1 and BAG1L or BAG1L-R305A/R308A/K309A. The results are the mean of at three independent experiments

3.9 Compound A4B17 affects proliferation of PCa cell lines in a BAG1L-dependent manner

BAG1L had previously been shown to promote the proliferation of PCa cell lines (Cato *et al.*, 2017). Given the findings that A4B17 binds weakly to the BAG domain of BAG1L and thereby reduces BAG1L-mediated AR-AF1 activity, it was necessary to determine whether A4B17 inhibits proliferation AR positive PCa cell lines.

LNCaP cell lines which carry a transcription activator-like nuclease (TALEN) induced knock-out of BAG1L (BAG1L KO cells) and control cells were cultured in medium containing vehicle (acetone) or 5 µM of A4B17. Proliferation was determined by counting cells daily over a period of six days. This demonstrated that in the presence of A4B17 proliferation of LNCaP control cells was delayed by four days and in general reduced by half compared to vehicle treated cells (AUC = 12.90 vs AUC = 24.96). In contrast, LNCaP BAG1L KO cells, which showed decreased proliferation compared to the control cells under vehicle conditions (AUC = 20.37 vs AUC = 24.96), even showed a slightly increase proliferation in the presence of A4B17 (AUC = 27.69

vs AUC = 20.37). These results suggest that A4B17 selectively inhibits PCa cell growth in the presence of BAG1L (Figure 3.19A).

To test whether the negative effect of A4B17 on proliferation of cells was dependent on the cellular levels of BAG1L, LNCaP95 cells transduced with a BAG1L lentiviral vector or empty vector were used. The cells were cultured in serum-reduced medium (standard culturing medium for LNCaP95) in the presence or absence of 5 µM A4B17. This showed that growth of vector expressing cells was only slightly decreased in the presence A4B17 (AUC = 14.71) compared to the vehicle treated cell (AUC = 22.20). However, overexpression of BAG1L enhances proliferation of LNCaP95 cells under vehicle conditions (AUC = 34.95). Intriguingly the growth inhibitory effect of A4B17 was more notable in the BAG1L overexpressing cell (AUC = 12.60) compared to the vector transfected cells, further demonstrating that A4B17 acts thorugh BAG1L and that the cellular content of BAG1L is important for the action of this compound (Figure 3.19B).

Together these results demonstrate that A4B17 might be an option for treatment of advanced PCa due to its alternate mode of action.

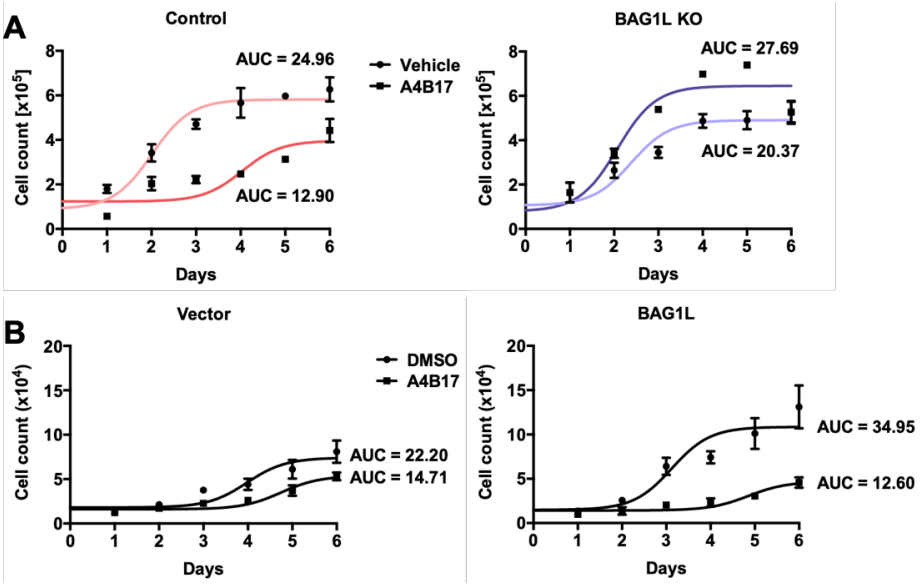

Figure 3.19: A4B17 inhibits proliferation of PCa cell lines in a BAG1L- and AR- dependent manner. (A) Proliferation experiments with control and Bag-1L KO cell lines in the presence and absence of 10^{-5} M A4B17. Cells were counted in triplicates daily over 6 days (B) Effect of A4B17 on the proliferation of LNCaP95 cells overexpressing BAG1L or an empty vector as control. Cells were cultured in triplicates in the presence or absence of 10^{-5} M A4B17 and counted daily over 6 days (n = 2).

4 Discussion

Prostate cancer is the most of commonly diagnosed cancer in men (Robert-Koch-Institut, 2016). Androgens are essentially involved in the development and progression of PCa. They exert their growth-promoting action through binding and activating the AR. Current PCa therapies aim at reducing AR signaling by lowering endogenous androgen levels or by inhibiting AR signaling through antiandrogens (Debes & Tindall, 2002). These kinds of therapies, referred to as Androgen Deprivation Therapies (ADT) are initially effective in reducing prostate tumor growth. However, in the course of treatment, prostate cancer cells adapt to low androgen levels, leading to an androgen-independent type of PCa, called castration-resistant PCa (CRPC). One of the suggested mechanisms thought to enhance AR sensitivity to low androgen concentrations is the overexpression of AR coregulators and the expression of some coactivators correlates with resistance to antiandrogens. Coactivators that are specifically overexpressed in CRPC and promote tumor growth and survival might therefore represent interesting therapeutic targets for treatment of resistant prostate tumors (Chmelar *et al.*, 2007; Heemers & Tindall, 2005; Agoulnik *et al.*, 2003). One of these proteins is BAG1L, which is not only expressed in primary prostate tumors but its expression increases in the progression to CRPC (Maki *et al.*, 2007; Cato *et al.*, 2017). In contrast to many known AR coregulators that regulate AR activity through binding to the AR via LxxLL- or FxxLF-motifs, BAG1L does not carry any of these sequences, suggesting that it must use other mechanisms to regulate AR activity.

One aim of the present work was to determine how BAG1L regulates AR action in CRPC. This led to the identification of a partially folded region in the τ5 region of the intrinsically disordered AR NTD as the binding motif for BAG1L. On the one hand, mutations in this region impaired BAG1L action at the AR τ5 region. On the other hand, a complete deletion of BAG1L further impaired the recruitment of other coregulators to the AR and altered the gene expression profile of AR target genes. BAG1L mainly regulated genes involved in androgen response. Additionally, genes involved in oxidative stress were regulated by BAG1L. With this as background information, small molecule BAG1L inhibitors were sought that would disrupt the BAG1L-AR interaction and inhibit the BAG1L-mediated enhancement of AF1 activity. One of these inhibitors that was identified in this work decreased the proliferation of AR positive PCa cells as well as PCa cell lines resistant to the clinically used antagonist, enzalutamide.

4.1 BAG1L regulates AR activity through interaction with the AR-NTD

Of the many mechanisms that have been postulated to contribute to resistance to hormonal therapies in PCa is the expression of AR-SV that lack the AR LBD but are constitutively active (Dehm *et al.*, 2008; Hu *et al.*, 2009; Guo *et al.*, 2009). The most commonly detected AR-SV is AR-V7,

which is overexpressed in bone-metastases of CRPC patients and its expression is correlated with androgen-independent proliferation (Dehm *et al.*, 2008; Hörnberg *et al.*, 2011; Qu *et al.*, 2015). However, it was not clear to which extent AR-V7 contributes to the growth of CRPC as opposed to AR-FL.

In this work, it was demonstrated that silencing of either AR-FL or AR-V7 is sufficient to reduce growth of the CRPC model cell line LNCaP95. Thus both AR subtypes are needed to promote androgen-independent growth of CRPC cell lines. This is consistent with previous studies, showing that overexpression of AR-FL enables growth of LNCaP cells at low androgen concentrations (Chen *et al.*, 2004), as well as studies showing that AR-V7 promotes androgen-independent cell growth (Guo *et al.*, 2009). Furthermore, these results suggest an interdependent role of AR-V7 and AR-FL, which is in line with previous reports that AR-V7 primarily heterodimerizes with AR-FL to mediate AR target gene expression (Watson *et al.*, 2010; Cao *et al.*, 2014; Cato *et al.*, 2019). In contrast to the above reported studies that monitored the proliferation of PCa in a 2D culture on plastic plates, the studies reported in this work analyzed the growth of the prostate cells in a 3D scaffold with lumen and elasticity akin to that of prostate tumor. These results therefore establish that both AR-FL and AR-V7 need to be targeted if one aims to overcome resistance to antihormone therapy in CRPC.

One of the ways of targeting both AR-FL and AR SVs that lack the C-terminal LBD is to focus on regulatory factors that enhance the activity of both receptor types. In this work the focus was on the cochaperone BAG1L that was reported previously (Shatkina *et al.*, 2003; Cato *et al.*, 2017) to enhance the NTD activity of the AR. In reporter gene experiments using a luciferase construct controlled by the PSA core enhancer element, it was shown that overexpression of the cochaperone BAG1L enhanced the activity of both AR- FL and AR-V7. A striking feature of the AR NTD is its intrinsic disordered structure, that prevents it from adopting a secondary or tertiary structure. Yet about 16% of the AR NTD has α-helical structure which makes it likely that those regions could form brief interactions with regulatory proteins that may control the activity of the AR. This awakes reminiscences of the function of short linear motifs (SLiMs) that have been described in intrinsically disordered proteins. SLiMs acts as small interaction modules and provide a wide range of functionality to proteins. Depending on their interaction partner they can influence subcellular location, modification state and stability of a protein, and regulate the context-dependent activity of proteins (Van Roey *et al.*, 2014). Therefore, they play crucial roles in cell regulation and aberrant SLiM function has been associated with cancer (Uyar *et al.*, 2014)

Therefore, this work focused on the BAG1L-AR-NTDτ5 interaction. HSQC NMR titration experiments led to the identification of a partially folded sequence (De Mol *et al.*, 2016) containing a polyalanine stretch as the binding motif for BAG1L. Intriguingly, alanine exchanges in sequences surrounding this motif (increasing the length of the alanine sequences) further enhanced the activity of BAG1L. This is most likely due the fact that polyalanine sequences adopt α-helical structures and the mutations therefore increase the α helicity of the AR sequence making it more prone to interaction with BAG1L. It has previously been shown that polyalanine stretches consisting of seven or more alanine residues are likely to form α-helices and the tendency of α-helix formation

rises with extension of the polyalanine stretch (Bernacki et al, 2011). This suggests that BAG1L might recognize the structure of the AR τ5 region rather than the primary aminoacid sequence. A decrease in BAG1L-mediated increase in AR $\tau 5$ activity was only observed with the deletion of a polyproline region preceding the polyalanine stretch, in particular in combination with single amino acid substitutions in the polyalanine stretch. This is contradictory to the NMR studies that did not indicate binding of the BAG domain to the polyproline site using purified protein yet in the reporter gene assay the polyproline sequence seems to be relevant. The polyproline sequence has been reported to bind another regulator of AR NTD activity, SH3LY1 (Blessing *et al.*, 2015). Interaction of SH3LY1 with BAG1L in vivo could potentiate the action of BAG1L. Furthermore, it was shown that a sequence of four or more proline residues is able to form a helical structure, called polyproline II helix (Williamson, 1994). This helical conformation could contribute to the overall structure of the τ5 region required for BAG1L to bind.

BAG1L is not considered a classical coactivator because of its lack of histoneacetyl transferase (HAT) activity. Classical coactivators which recruit HATs to acetylate lysine residues on histone proteins, which aids the formation of euchromatin and enhance transacriptional activity (McKenna & O'Malley, 2002; Glass & Rosenfeld, 2000). The mode of action of BAG1L is thought to be through changing AR conformation, which would result in the recruitment of classical coactivators (Cato *et al.*, 2017). To explore this hypothesis a Microarray Assay for Real-time Coregulator-Nuclear Receptor Interaction (MARCoNI) with 153 coregulator peptides of classical coactivators was performed with lysates from hormone-responsive control and BAG1L KO LNCaP cells. The assay showed that in the absence of BAG1L binding affinity of the DHT-bound AR to 12 coregulator motifs was significantly reduced. All coregulators that interact with the DHT-bound AR in the presence of BAG1L have previously been reported to be AR coactivators, except for PAK6 that acts as a corepressor (Comuzzi *et al.*, 2003; Chen *et al.*, 2003; Yang *et al.*, 2001; Shiota *et al.*, 2010; Wang *et al.*, 2004; Gao *et al.*, 2019). It is know that upon androgen stimulation AR regulates transcription of its target genes in the nucleus, a process that is modulated both by AR coactivators and corepressors (Wang *et al.*, 2005). It is known that coregulators are recruited to the ARE-bound AR in a gene-specific and context-dependent manner and that AR coregulators preferentially control subsets of AR target genes (Liu *et al.*, 2017), mediating AR specificity. The fact that mainly coactivators are affected by BAG1L loss supports findings that BAG1L is positive regulator of AR activity. Some of these coactivators with reduced binding in the abscence of BAG1L, NCoA1/2/3/4, PRCG1 and CBP interact not only with AR-LBD (with their LxxLL motif) but also with the AR NTD, suggesting a role of these coactivators in the regulation of ligand-independent AR activity. Indeed, coactivators of the p160-family, CBP, PRCG1, RAD9A, ZNHIT3 and Gelsolin are associated with progression to CRPC (Comuzzi *et al.*, 2004; Xu *et al.*, 2009; Chen *et al.*, 2003; Dasgupta *et al.*, 2015; Gao *et al.*, 2019). The finding that binding of the liganded AR to these coactivators is reduced in the absence of BAG1L suggests a role of the cochaperone in the recruitment of coactivators that are involved in the progression to CRPC. Previous studies comparing the effect of the AR antagonist enzalutamide with other AR targeting compounds (UT-34, BPA, BPAF; BPS) showed differential binding of the AR to coregulators in the presence of differ-

ent compounds, suggesting conformational differences in the AR in the presence of the different compounds (Ponnusamy *et al.*, 2019; Perera *et al.*, 2017). These further substantiate the notion that BAG1L also alters AR conformation to enable interaction with other coregulators.

4.2 BAG1L regulates pathways involved in the regulation of oxidative stress in prostate cancer

As AR coregulators play an important role in the transcriptional activity of the AR, changes in the recruitment of AR coregulators would lead to changes in gene expression pattern. To investigate whether decreased expression of BAG1L affects AR target gene expression, previously established RNA-seq data was reassessed. This demonstrated that KO of BAG1L impaired the expression of a subset of genes involved in "AR response". This confirms the role of BAG1L in AR action (Shatkina *et al.*, 2003; Cato *et al.*, 2017; Jehle *et al.*, 2014). Furthermore, loss of BAG1L affected the expression of genes that are involved in oxidative stress and metabolism. Oxidative stress defines an imbalance between increased levels of reactive oxygen species (ROS) and the antioxidative defense mechanism of the cells (Patlevič *et al.*, 2016). Traditionally, oxidative stress is associated with tissue injury, DNA damage and apoptosis. However, it was shown that increased ROS levels also function as secondary messengers in cell growth and proliferation as well as in the control cellular energy metabolism and growth (Kumar *et al.*, 2008; Sauer *et al.*, 2001; Sullivan & Chandel, 2014; Gough & Cotter, 2011). Additionally, it was demonstrated that increased ROS levels also play a role in prostate carcinogenesis (Shiota *et al.*, 2010) and that androgen levels in the serum can promote the production and accumulation of ROS in PCa cells.
A Reduced 2´7-dichlorofluorescein (H_2DCF) assay (Carter *et al.*, 1994), which measures intracellular hydrogen peroxide and superoxide anions with control and BAG1L KO LNCaP cells further showed an increase in ROS production upon treatment of control cells with androgen in agreement with a previous report (Basu *et al.*, 2011). However, in the absence of BAG1L, the basal ROS levels as well as the androgen-induced ROS levels were reduced supporting a role of BAG1L in the regulation of ROS production both in the presence and absence of hormone. In support of these findings, it was shown in this study that the NAD(P)H inhibitor Diphenyliodonium (DPI) significantly inhibited cell proliferation of control but not of BAG1L KO LNCaP cells. DPI has been reported to reduces growth of LNCaP cells through the inhibition of the NAD(P)H oxidases NOX that is involved in membrane-derive ROS production Kumar *et al.* (2008).
Taken together these results suggest a role for BAG1L in the generation of reactive oxygen species (ROS) to enhance growth of prostate cancer cell lines.

4.3 Identification of small molecule compounds that inhibit BAG1L-mediated AR-AF1 activity

With the site and mode of action of BAG1L fully clarified, it was considered appropriate to use that knowledge to search for BAG1L inhibitors that would function through the AR NTD. Targeting the AR NTD is of great interest to many investigators interested in overcoming antiandrogen resistance in advanced prostate cancer patients.

This has so far been difficult, as the AR NTD is intrinsically disordered and it is not accessible to target by structural based drug design. Some of the attempts made have not been further developed or have failed to pass the proof of efficacy. For example, a bispecific antibody 3E10-AR441 which accumulates in nucleus and inhibits the activity of AR and AR-V7 in a ligand-dependent manner through interaction with the AR NTD (Goicochea *et al.*, 2017). However, there are no reports on 3E10-AR441 effect on tumor growth so far (Goicochea *et al.*, 2017). Secondly, chlorinated peptides termed Sintokamides, isolated from the marine sponge *Dysidea sp.,* were shown to inhibit AR activity in reporter gene assays and to reduce growth of AR positive but not AR negative PCa cell lines (Sadar *et al.*, 2008). However, so far these compounds have not been further characterized. The first AR-NTD targeting compounds to enter clinical trials were Ralaniten acetate (EPI-506), which directly binds the AR τ5 region and inhibits growth of PCa cells in xenograft mouse model as well as Niphatenones, which inhibit transactivation of AR-FL and AR variants (Andersen *et al.*, 2010; Myung *et al.*, 2013; De Mol *et al.*, 2016; Banuelos *et al.*, 2014). However, phase 1/2 clinical trials for Ralaniten acetate have been discontinued due to lack of efficacy and a high patient burden of pill intake (NCT02606123). Clinical trials for Niphatenones were as well discontinued due to lack of efficacy and poor absorption (NCT02532114) (Schweizer *et al.*, 2018).

In this work a further attempt has been made to reduced AR NTD activity based on a systematic collection of data on the regulation of this activity by the cochaperone BAG1L. A benzothiazole compound, Thio-2, that had previously been reported to bind to the BAG domain of BAG1 (Enthammer *et al.*, 2013) to provide moderate and unselective effects was used as a starting compound. Following the synthesis and analysis of several derivatives of Thio-2, the compound A4B17 was identified that effectively inhibited the expression of the BAG1L-regulated AR target genes and performed well as an AR NTD inhibitor. A4B17 further inhibited growth of PCa cells in a BAG1L-dependent manner. In light of previous studies that showed that BAG1L levels increased during the progression of PCa to CRPC and increased BAG1L is associated with resistance to antiandrogen treatment (Cato *et al.*, 2017), A4B17 would be a good therapeutic agent for these group of patients (see results Fig. 3.11B for the schematic description of the BAG1L inhibitors).

A4B17 like Thio-2 is a benzothiazole derivative. Benzothiazoles have generally been described for a variety of medicinal applications (Sharma *et al.*, 2012). Analogs of these compounds have been shown to be selective, as for example rhodacyanine benzothiazoles that selectively bind an allosteric region of Hsp70 and interrupt protein-protein interactions with nuclear exchange factors (Li *et al.*, 2016).

A4B17 could therefore be put into the class of selective benzothiazoles that presents a suitable parent structure for further optimization to improve efficacy and potency in the inhibition of AR action in PCa.

4.4 Conclusion

In this study, structural biological approaches, global transcriptome analysis and different screening methods were combined to characterize the regulation of AR activity through the BAG1L-AR-AF1 activity and to identify an inhibitor of this interaction. This led to the discovery of a compound A4B17, which selectively inhibits BAG1L-mediated AR activity and PCa cell proliferation in a BAG1L-dependent manner. Taken into account that BAG1L colocalizes with the AR in malignant but not in benign prostate tissue and that BAG1L is overexpressed in CRPC, A4B17 as a selective inhibitor for BAG1L action, might present a promising compound to develop further for the treatment of antihormone resistant PCa patients.

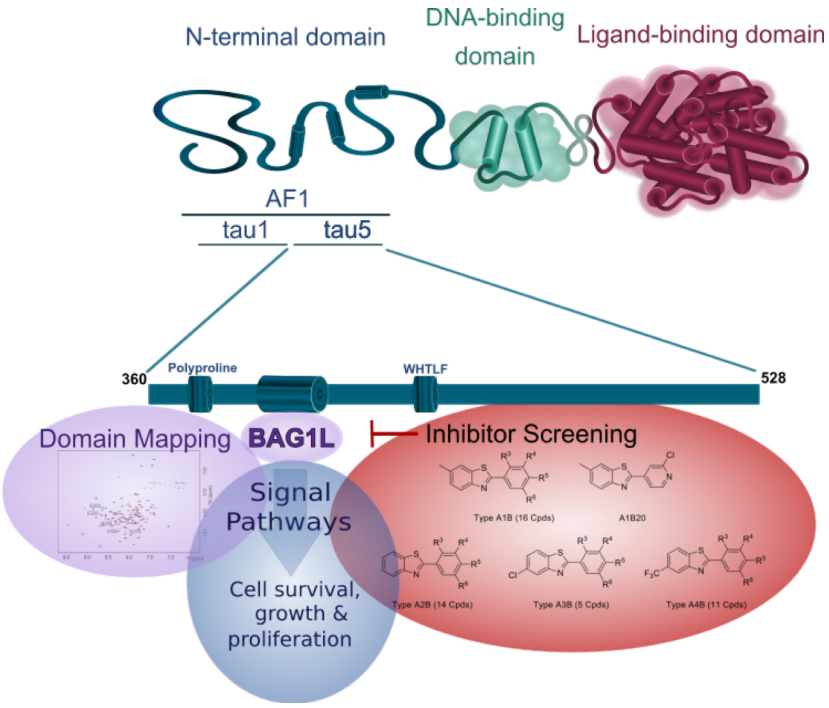

Figure 4.1: In this work the regulation of AR activity by the cochaperone BAG1L was extensively characterized. Therefore structural biological approaches (domain mapping), global transcriptome analysis were combined. This led to identification of a partially folded region in the AR NTD as binding site for BAG1L. Furthermore, odixative stress pathways was shown to be regulated by BAG1L-mediated AR activity. The acquired findings were used to screen for selective inhibitor of the BAG1L-AR-interaction. This led to the identification of a small compound A4B17 as selective inhibitor for BAG1L action

References

Abcam (2020). Oxidative stress assays and oxidative stress markers.

Adams, J. (1853). The case of scirrhous of the prostate gland with corresponding affliction of the lymphatic glands in the lumbar region and in the pelvis. *Lancet*, *1*(1), 393.

Adler, A. J., Scheller, A., & Robins, D. M. (1993). The stringency and magnitude of androgen-specific gene activation are combinatorial functions of receptor and nonreceptor binding site sequences. *Molecular and Cellular Biology*, *13*(10), 6326–6335.

Agoulnik, I. U., Krause, W. C., Bingman, W. E., Rahman, H. T., Amrikachi, M., Ayala, G. E., & Weigel, N. L. (2003). Repressors of androgen and progesterone receptor action. *Journal of Biological Chemistry*, *278*(33), 31136–31148.

Alen, P., Claessens, F., Schoenmakers, E., Swinnen, J. V., Verhoeven, G., Rombauts, W., & Peeters, B. (1999). Interaction of the putative androgen receptor-specific coactivator ARA70/ELE1alpha with multiple steroid receptors and identification of an internally deleted ELE1beta isoform. *Molecular endocrinology (Baltimore, Md)*, *13*(1), 117–128.

Andersen, R. J., Mawji, N. R., Wang, J., Wang, G., Haile, S., Myung, J. K., Watt, K., Tam, T., Yang, Y. C., Bañuelos, C. A., Williams, D. E., McEwan, I. J., Wang, Y., & Sadar, M. D. (2010). Regression of Castrate-Recurrent Prostate Cancer by a Small-Molecule Inhibitor of the Amino-Terminus Domain of the Androgen Receptor. *Cancer Cell*, *17*(6), 535–546.

Arakawa, A., Handa, N., Ohsawa, N., Shida, M., Kigawa, T., Hayashi, F., Shirouzu, M., & Yokoyama, S. (2010). The C-Terminal BAG Domain of BAG5 Induces Conformational Changes of the Hsp70 Nucleotide- Binding Domain for ADP-ATP Exchange. *Structure*, *18*(3), 309–319.

Askew, E. B., Bai, S., Blackwelder, A. J., & Wilson, E. M. (2010). Transcriptional synergy between melanoma antigen gene protein-A11 (MAGE-11) and p300 in androgen receptor signaling. *Journal of Biological Chemistry*, *285*(28), 21824–21836.

Askew, E. B., Bai, S., Hnat, A. T., Minges, J. T., & Wilson, E. M. (2009). Melanoma antigen gene protein-A11 (MAGE-11) F-box links the androgen receptor NH2-terminal transactivation domain to p160 coactivators. *Journal of Biological Chemistry*, *284*(50), 34793–34808.

Bai, S., Grossman, G., Yuan, L., Lessey, B. A., French, F. S., Young, S. L., & Wilson, E. M. (2008). Hormone control and expression of androgen receptor coregulator MAGE-11 in human endometrium during the window of receptivity to embryo implantation. *Molecular Human Reproduction*, *14*(2), 107–116.

Bai, S., He, B., & Wilson, E. M. (2005). Melanoma Antigen Gene Protein MAGE-11 Regulates Androgen Receptor Function by Modulating the Interdomain Interaction. *Molecular and Cellular Biology*, *25*(4), 1238–1257.

Banuelos, C. A., Lal, A., Tien, A. H., Shah, N., Yang, Y. C., Mawji, N. R., Meimetis, L. G., Park, J., Kunzhong, J., Andersen, R. J., & Sadar, M. D. (2014). Characterization of Niphatenones that Inhibit Androgen Receptor N-Terminal Domain. *PLoS ONE*, *9*(9), e107991.

Barrett, J. C., Press, E. C. R. C., Newbold, R. F., Overell, R. W., Carey, M., Leatherwood, J., & Ptashne, M. (1988). Potent GAL4 Derivative. *Science*, *585*(1961), 1–3.

Basu, H. S., Mahlum, A., Mehraein-Ghomi, F., Kegel, S. J., Guo, S., Peters, N. R., & Wilding, G. (2011). Pretreatment with anti-oxidants sensitizes oxidatively stressed human cancer cells to growth inhibitory effect of suberoylanilide hydroxamic acid (SAHA). *Cancer Chemotherapy and Pharmacology*, *67*(3), 705–715.

Bennett, N. C., Gardiner, R. a., Hooper, J. D., Johnson, D. W., & Gobe, G. C. (2010). Molecular cell biology of androgen receptor signalling. *The International Journal of Biochemistry & Cell Biology*, *42*(6), 813–827.

Bevan, C. L., Hoare, S., Claessens, F., Heery, D. M., & Parker, M. G. (1999). The AF1 and AF2 Domains of the Androgen Receptor Interact with Distinct Regions of SRC1. *Molecular and Cellular Biology*, *19*(12), 8383–8392.

Blessing, A. M., Ganesan, S., Rajapakshe, K., Ying Sung, Y., Reddy Bollu, L., Shi, Y., Cheung, E., Coarfa, C., Chang, J. T., McDonnell, D. P., & Frigo, D. E. (2015). Identification of a Novel Coregulator, SH3YL1, That Interacts With the Androgen Receptor N-Terminus. *Molecular endocrinology (Baltimore, Md.)*, *29*(10), 1426–1439.

Briknarová, K., Takayama, S., Brive, L., Havert, M. L., Knee, D. A., Velasco, J., Homma, S., Cabezas, E., Stuart, J., Hoyt, D. W., Satterthwait, A. C., Llinás, M., Reed, J. C., & Ely, K. R. (2001). Structural analysis of BAG1 cochaperone and its interactions with Hsc70 heat shock protein. *Nature structural biology*, *8*(4), 349–352.

Brinkmann, A. O. (2011). *Molecular Mechanisms of Androgen Action – A Historical Perspective*, (pp. 3–24). Totowa, NJ: Humana Press.

Brinkmann, A. O., Blok, L. J., de Ruiter, P. E., Doesburg, P., Steketee, K., Berrevoets, C. A., & Trapman, J. T. (1999). Mechanisms of androgen receptor activation and function. *J Steroid Biochem Mol Biol.*, *69*((1-6)), 07–313.

Brinkmann, A. O., Jenster, G., Ris-Stalpers, C., van der Korput, J. A., Brüggenwirth, H. T., Boehmer, A. L., & Trapman, J. (1995). Androgen receptor mutations. *Journal of Steroid Biochemistry and Molecular Biology*, *53*(1-6), 443–448.

Broustas, C. G., Hopkins, K. M., Panigrahi, S. K., Wang, L., Virk, R. K., & Lieberman, H. B. (2019). RAD9A promotes metastatic phenotypes through transcriptional regulation of anterior gradient 2 (AGR2). *Carcinogenesis*, *40*(1), 164–172.

Brown, C. J., Goss, S. J., Lubahn, T. D. B., Joseph, D. R., Wilson, E. M., French, F. S., & Willard, H. F. (1989). Androgen Receptor Locus on the Human X Chromosome: Regional Localization to Xql 1-12 and Description of a DNA Polymorphism. *Receptor*, *44*, 264–269.

Burd, C. J., Petre, C. E., Moghadam, H., Wilson, E. M., & Knudsen, K. E. (2005). Cyclin D1 binding to the androgen receptor (AR) NH2-terminal domain inhibits activation function 2 association and reveals dual roles for AR corepression. *Molecular Endocrinology*, *19*(3), 607–620.

Burris, T. P., & McCabe, E. R. (2000). *Nuclear Receptors and Genetic Disease*. American Press.

Cai, C., Chen, S., Ng, P., Bubley, G. J., Nelson, P. S., Mostaghel, E. A., Marck, B., Matsumoto, A. M., Simon, N. I., Wang, H., Chen, S., & Balk, S. P. (2011). Intratumoral De Novo steroid synthesis activates androgen receptor in castration-resistant prostate cancer and is upregulated by treatment with CYP17A1 inhibitors. *Cancer Research*, *71*(20), 6503–6513.

Callewaert, L., Van Tilborgh, N., & Claessens, F. (2006). Interplay between two hormone-independent activation domains in the androgen receptor. *Cancer Research*, *66*(1), 543–553.

Cao, B., Qi, Y., Zhang, G., Xu, D., Zhan, Y., Alvarez, X., Guo, Z., Fu, X., Plymate, S. R., Sartor, O., Zhang, H., & Dong, Y. (2014). Androgen receptor splice variants activating the full-length receptor in mediating resistance to androgen-directed therapy. *Oncotarget*, *5*(6), 1646–1656.

Carter, W., Narayanan, P., & JP, R. (1994). ntracellular hydrogen peroxide and superoxide anion detection in endothelial cells. *I J Leukoc Biol.*, *2*(55), 253–258.

Castellan, P., Marchioni, M., Castellucci, R., Francesco, P. D., Schips, L., & Cindolo, L. (2018). Abiraterone acetate for early stage metastatic prostate cancer : patient selection and special considerations. *Therapeutics and Clinical Risk Management*, *14*, 2341–2347.

Cato, A. C., & Peterziel, H. (1998). The androgen receptor as mediator of gene expression and signal transduction pathways. *Trends in Endocrinology and Metabolism*, *9*(4), 150–154.

Cato, L., de Tribolet-Hardy, J., Lee, I., Rottenberg, J. T., Coleman, I., Melchers, D., Houtman, R., Xiao, T., Li, W., Uo, T., Sun, S., Kuznik, N. C., Göppert, B., Ozgun, F., van Royen, M. E., Houtsmuller, A. B., Vadhi, R., Rao, P. K., Li, L., Balk, S. P., Den, R. B., Trock, B. J., Karnes, R. J., Jenkins, R. B., Klein, E. A., Davicioni, E., Gruhl, F. J., Long, H. W., Liu, X. S., Cato, A. C., Lack, N. A., Nelson, P. S., Plymate, S. R., Groner, A. C., & Brown, M. (2019). ARv7 Represses Tumor-Suppressor Genes in Castration-Resistant Prostate Cancer. *Cancer Cell*, *35*(3), 401–413.e6.

Cato, L., Neeb, A., Sharp, A., Buzón, V., Ficarro, S. B., Yang, L., Muhle-Goll, C., Kuznik, N. C., Riisnaes, R., Rodrigues, D. N., Armant, O., Gourain, V., Adelmant, G., Ntim, E. A., Westerling, T., Dolling, D., Rescigno, P., Figueiredo, I., Fauser, F., Wu, J., Rottenberg, J. T., Shatkina, L., Ester, C., Luy, B., Puchta, H., Troppmair, J., Jung, N., Bräse, S., Strähle, U., Marto, J. A., Nienhaus, G. U., Al-Lazikani, B., Salvatella, X., De Bono, J. S., Cato, A. C., & Brown, M. (2017). Development of bag-1L as a therapeutic target in androgen receptor-dependent prostate cancer. *eLife*, *6*, 1–27.

Chamberlain, N. L., Whitacre, D. C., & Miesfeld, R. L. (1996). Delineation of two distinct type 1 activation functions in the androgen receptor amino-terminal domain. *J Biol Chem*, *271*(43), 26772–26778.

Chandrasekar, T., Yang, J. C., Gao, A. C., & Evans, C. P. (2015). Mechanisms of resistance in castration-resistant prostate cancer (CRPC). *Translational Andrology and Urology*, *4*(3), 365–380.

Chen, C. D., Welsbie, D. S., Tran, C., Baek, S. H., Chen, R., Vessella, R., Rosenfeld, M. G., & Sawyers, C. L. (2004). Molecular determinants of resistance to antiandrogen therapy. *Nature Medicine*, *10*(1), 33–39.

Chen, G., Nomura, M., Morinaga, H., Matsubara, E., Okabe, T., Goto, K., Yanase, T., Zheng, H., Lu, J., & Nawata, H. (2003). Modulation of Androgen Receptor Transactivation by Gelsolin: A Newly Identified Androgen Receptor Coregulator. *Cancer Research*, *62*, 4888–4894.

Chmelar, R., Buchanan, G., Need, E. F., Tilley, W., & Greenberg, N. M. (2007). Androgen receptor coregulators and their involvement in the development and progression of prostate cancer. *International Journal of Cancer*, *120*(4), 719–733.

Christiaens, V., Bevan, C. L., Callewaert, L., Haelens, A., Verrijdt, G., Rombauts, W., & Claessens, F. (2002). Characterization of the two coactivator-interacting surfaces of the androgen receptor and their relative role in transcriptional control. *Journal of Biological Chemistry*, *277*, 49230–49237.

Claessens (2007). Diverse roles of androgen receptor (AR) domains in AR-mediated signaling. *Nuclear Receptor Signaling*, *4*.

Claessens, F., Alen, P., Devos, A., Peeters, B., Verhoeven, G., & Rombauts, W. (1996). The androgen-specific probasin response element 2 interacts differentially with androgen and glucocorticoid receptors. *Journal of Biological Chemistry*, *271*(32), 19013–19016.

Clegg, N. J., Wongvipat, J., Joseph, J. D., Tran, C., Ouk, S., Dilhas, A., Chen, Y., Grillot, K., Bischoff, E. D., Cai, L., Aparicio, A., Dorow, S., Arora, V., Shao, G., Qian, J., Zhao, H., Yang, G., Cao, C., Sensintaffar, J., Wasielewska, T., Herbert, M. R., Bonnefous, C., Darimont, B., Scher, H. I., Smith-Jones, P., Klang, M., Smith, N. D., De Stanchina, E., Wu, N., Ouerfelli, O.,

Rix, P. J., Heyman, R. A., Jung, M. E., Sawyers, C. L., & Hager, J. H. (2012). ARN-509: A novel antiandrogen for prostate cancer treatment. *Cancer Research*, *72*(6), 1494–1503.

Clinckemalie, L., Vanderschueren, D., Boonen, S., & Claessens, F. (2012). The hinge region in androgen receptor control. *Molecular and Cellular Endocrinology*, *358*(1), 1–8.

Comuzzi, B., Lambrinidis, L., Rogatsch, H., Godoy-Tundidor, S., Knezevic, N., Krhen, I., Marekovic, Z., Bartsch, G., Klocker, H., Hobisch, A., & Culig, Z. (2003). The transcriptional co-activator cAMP response element-binding protein-binding protein is expressed in prostate cancer and enhances androgen- and anti-androgen-induced androgen receptor function. *American Journal of Pathology*, *162*(1), 233–241.

Comuzzi, B., Nemes, C., Schmidt, S., Jasarevic, Z., Lodde, M., Pycha, A., Bartsch, G., Offner, F., Culig, Z., & Hobisch, A. (2004). The androgen receptor co-activator CBP is up-regulated following androgen withdrawal and is highly expressed in advanced prostate cancer. *Journal of Pathology*, *204*(2), 159–166.

Culig, Z., Comuzzi, B., Steiner, H., Bartsch, G., & Hobisch, A. (2004). Expression and function of androgen receptor coactivators in prostate cancer. *Journal of Steroid Biochemistry and Molecular Biology*, *92*(4), 265–271.

Darimont, B. D., Wagner, R. L., Apriletti, J. W., Stallcup, M. R., Kushner, P. J., Baxter, J. D., Fletterick, R. J., & Yamamoto, K. R. (1998). Structure and specificity of nuclear receptor-coactivator interactions. *Genes and Development*, *12*(21), 3343–3356.

Dasgupta, S., Putluri, N., Long, W., Zhang, B., Wang, J., Kaushik, A. K., Arnold, J. M., Bhowmik, S. K., Stashi, E., Brennan, C. A., Rajapakshe, K., Coarfa, C., Mitsiades, N., Ittmann, M. M., Chinnaiyan, A. M., Sreekumar, A., & O'Malley, B. W. (2015). Coactivator SRC-2'dependent metabolic reprogramming mediates prostate cancer survival and metastasis. *Journal of Clinical Investigation*, *125*(3), 1174–1188.

Davies, P., Watt, K., Kelly, S. M., Clark, C., Price, N. C., & McEwan, I. J. (2008). Consequences of poly-glutamine repeat length for the conformation and folding of the androgen receptor amino-terminal domain. *Journal of Molecular Endocrinology*, *41*(5-6), 301–314.

de Bono, J. S., Logothetis, C. J., Molina, A., Fizazi, K., North, S., Chu, L., Chi, K. N., Jones, R. J., Goodman, O. B., Saad, F., Staffurth, J. N., Mainwaring, P., Harland, S., Flaig, T. W., Hutson, T. E., Cheng, T., Patterson, H., Hainsworth, J. D., Ryan, C. J., Sternberg, C. N., Ellard, S. L., Fléchon, A., Saleh, M., Scholz, M., Efstathiou, E., Zivi, A., Bianchini, D., Loriot, Y., Chieffo, N., Kheoh, T., Haqq, C. M., & Scher, H. I. (2011). Abiraterone and Increased Survival in Metastatic Prostate Cancer. *New England Journal of Medicine*, *364*(21), 1995–2005.

De Marzo, A. M., Meeker, A. K., Zha, S., Luo, J., Nakayama, M., Platz, E. A., Isaacs, W. B., & Nelson, W. G. (2003). Human prostate cancer precursors and pathobiology. *Urology*, *62*(5 SUPPL. 1), 55–62.

De Mol, E., Fenwick, R. B., Phang, C. T., Buzón, V., Szulc, E., De La Fuente, A., Escobedo, A., García, J., Bertoncini, C. W., Estébanez-Perpiñá, E., McEwan, I. J., Riera, A., & Salvatella, X. (2016). EPI-001, A Compound Active against Castration-Resistant Prostate Cancer, Targets Transactivation Unit 5 of the Androgen Receptor. *ACS Chemical Biology*, *11*(9), 2499–2505.

Debes, J. D., & Tindall, D. J. (2002). The role of androgens and the androgen receptor in prostate cancer. *Cancer Letters*, *187*, 1–7.

Dehm, S. M., Regan, K. M., Schmidt, L. J., & Tindall, D. J. (2007). Selective role of an NH2-terminal WxxLF motif for aberrant androgen receptor activation in androgen depletion-independent prostate cancer cells. *Cancer Research*, *67*(20), 10067–10077.

Dehm, S. M., Schmidt, L. J., Heemers, H. V., Vessella, R. L., & Tindall, D. J. (2008). Splicing of a novel androgen receptor exon generates a constitutively active androgen receptor that mediates prostate cancer therapy resistance. *Cancer Research*, *68*(13), 5469–5477.

Dehm, S. M., & Tindall, D. J. (2007). Androgen receptor structural and functional elements: role and regulation in prostate cancer. *Molecular endocrinology (Baltimore, Md.)*, *21*(12), 2855–2863.

Dehm, S. M., & Tindall, D. J. (2011). Alternatively spliced androgen receptor variants. *Endocrine-Related Cancer*, *18*(5), 183–196.

Dubbink, H. J., Hersmus, R., Verma, C. S., Van Der Korput, H. A., Berrevoets, C. A., Van Tol, J., Ziel-Van Der Made, A. C., Brinkmann, A. O., Pike, A. C., & Trapman, J. (2004). Distinct recognition modes of FXXLF and LXXLL motifs by the androgen receptor. *Molecular Endocrinology*, *18*(9), 2132–2150.

Edwards, S. M., & Eeles, R. A. (2004). Unravelling the genetics of prostate cancer. *American Journal of Medical Genetics*, *129C*(1), 65–73.

Enthammer, M., Papadakis, E. S., Salome Gachet, M., Deutsch, M., Schwaiger, S., Koziel, K., Ashraf, M. I., Khalid, S., Wolber, G., Packham, G., Cutress, R. I., Stuppner, H., Troppmair, J., Salomé Gachet, M., Deutsch, M., Schwaiger, S., Koziel, K., Ashraf, M. I., Khalid, S., Wolber, G., Packham, G., Cutress, R. I., Stuppner, H., Troppmair, J., Gachet, M. S., Deutsch, M., Schwaiger, S., Koziel, K., Ashraf, M. I., Khalid, S., Wolber, G., Packham, G., Cutress, R. I., Stuppner, H., & Troppmair, J. (2013). Isolation of a novel thioflavin s-derived compound that inhibits BAG-1-mediated protein interactions and targets BRAF inhibitor-resistant cell lines. *Molecular Cancer Therapeutics*, *12*(11), 2400–2414.

Erbar, P. (2002). *Onkologie CompactLehrbuch - Pathophysiologie, Klinik und Therapie maligner Tumoren*. Stuttgart: Schattauer, 4. auflage ed.

Estébanez-Perpiñá, E., Arnold, L. a., Nguyen, P., Rodrigues, E. D., Mar, E., Bateman, R., Pallai, P., Shokat, K. M., Baxter, J. D., Guy, R. K., Webb, P., & Fletterick, R. J. (2007). A surface on the

androgen receptor that allosterically regulates coactivator binding. *Proceedings of the National Academy of Sciences of the United States of America*, *104*(41), 16074–16079.

Estébanez-Perpiñá, E., Moore, J. M., Mar, E., Delgado-Rodrigues, E., Nguyen, P., Baxter, J. D., Buehrer, B. M., Webb, P., Fletterick, R. J., & Guy, R. K. (2005). The molecular mechanisms of coactivator utilization in ligand-dependent transactivation by the androgen receptor. *Journal of Biological Chemistry*, *280*(9), 8060–8068.

Evans, R. M. (1988). The steroid and thyroid hormone receptor superfamily. *Science (New York, N.Y.)*, *240*(4854), 889–895.

Fizazi, K., Scher, H. I., Molina, A., Logothetis, C. J., Chi, K. N., Jones, R. J., Staffurth, J. N., North, S., Vogelzang, N. J., Saad, F., Mainwaring, P., Harland, S., Goodman, O. B., Sternberg, C. N., Li, J. H., Kheoh, T., Haqq, C. M., & de Bono, J. S. (2012). Abiraterone acetate for treatment of metastatic castration-resistant prostate cancer: Final overall survival analysis of the COU-AA-301 randomised, double-blind, placebo-controlled phase 3 study. *The Lancet Oncology*, *13*(10), 983–992.

Furr, B. J. (1988). ICI 176,334: a novel non-steroidal, peripherally-selective antiandrogen. *Progress in clinical and biological research*, *260*, 13–26.

Galletti, G., Leach, B. I., Lam, L., & Tagawa, S. T. (2017). Mechanisms of resistance to systemic therapy in metastatic castration-resistant prostate cancer. *Cancer Treatment Reviews*, *57*, 16–27.

Gamerdinger, M., Hajieva, P., Kaya, A. M., Wolfrum, U., Hartl, F. U., & Behl, C. (2009). Protein quality control during aging involves recruitment of the macroautophagy pathway by BAG3. *EMBO Journal*, *28*(7), 889–901.

Gao, Y., Chen, L., Du, Z. G., Gao, W. C., Wu, Z. M., Liu, X. J., Huang, H., Xu, D. F., & Li, Q. Q. (2019). Glutamate decarboxylase 65 signals through the androgen receptor to promote castration resistance in prostate cancer. *Cancer Research*, *79*(18), 4638–4649.

Gengler, L., & Finby, N. (1975). Rectal and sigmoid involvement secondary to carcinoma of the prostate. *The American Roentgen Ray Society*, *125*(4), 910–917.

Glass, C. K. (1994). Differential Recognition of Target Genes by Nuclear Receptor Monomers, Dimers, and Heterodimers*. *Endocrine Reviews*, *15*(3), 391–407.

Glass, C. K., & Rosenfeld, M. G. (2000). The coregulator exchange in transcriptional functions of nuclear receptors. *Genes and Development*, *14*(2), 121–141.

Gluzman, Y. (1981). SV40-transformed simian cells support the replication of early SV40 mutants. *Cell*, *23*(1), 175–182.

Goh, C. L., Schumacher, F. R., Easton, D., Muir, K., Henderson, B., Kote-Jarai, Z., & Eeles, R. A. (2012). Genetic variants associated with predisposition to prostate cancer and potential clinical implications. *Journal of Internal Medicine*, *271*(4), 353–365.

Goicochea, N. L., Garnovskaya, M., Blanton, M. G., Chan, G., Weisbart, R., & Lilly, M. B. (2017). Development of cell-penetrating bispecific antibodies targeting the N-terminal domain of androgen receptor for prostate cancer therapy. *Protein Engineering, Design and Selection*, *30*(12), 1–9.

Goodman, R. H., & Smolik, S. (2000). CBP/p300 in cell growth, transformation, and development. *Genes and Development*, *14*(13), 1553–1577.

Göppert, B., Sollich, T., Abaffy, P., Cecilia, A., Heckmann, J., Neeb, A., Bäcker, A., Baumbach, T., Gruhl, F. J., & Cato, A. C. (2016). Superporous Poly(ethylene glycol) Diacrylate Cryogel with a Defined Elastic Modulus for Prostate Cancer Cell Research. *Small (Weinheim an der Bergstrasse, Germany)*, *12*(29), 3985–3994.

Gough, D. R., & Cotter, T. G. (2011). Hydrogen peroxide: A Jekyll and Hyde signalling molecule. *Cell Death and Disease*, *2*(10), 1–8.

Greenlee, R. T., Hill-harmon, M. B., Murray, T., Cokkinides, V., Harris, A., Luke, E., & Brien, K. O. (2001). Cancer Statistics , 2001. *CA Cancer J Clin 2001;51:15-36.)*, *51*(1), 15–36.

Guo, Z., Yang, X., Sun, F., Jiang, R., Linn, D. E., Chen, H., Chen, H., Kong, X., Melamed, J., Tepper, C. G., Kung, H. J., Brodie, A. M., Edwards, J., & Qiu, Y. (2009). A novel androgen receptor splice variant is up-regulated during prostate cancer progression and promotes androgen depletion-resistant growth. *Cancer Research*, *69*(6), 2305–2313.

Haelens, A., Tanner, T., Denayer, S., Callewaert, L., & Claessens, F. (2007). The hinge region regulates DNA binding, nuclear translocation, and transactivation of the androgen receptor. *Cancer Research*, *67*(9), 4514–4523.

He, B., Kemppainen, J. A., & Wilson, E. M. (2000). FXXLF and WXXLF sequences mediate the NH2-terminal interaction with the ligand binding domain of the androgen receptor. *Journal of Biological Chemistry*, *275*(30), 22986–22994.

He, B., Minges, J. T., Lee, L. W., & Wilson, E. M. (2002). The FXXLF motif mediates androgen receptor-specific interactions with coregulators. *Journal of Biological Chemistry*, *277*(12), 10226–10235.

Heemers, H. V., Regan, K. M., Schmidt, L. J., Anderson, S. K., Ballman, K. V., & Tindall, D. J. (2009). Androgen Modulation of Coregulator Expression in Prostate Cancer Cells. *Molecular Endocrinology*, *23*(4), 572–583.

Heemers, H. V., & Tindall, D. J. (2005). Androgen Receptor Coregulatory Proteins as Potential Therapeutic Targets in the Treatment of Prostate Cancer. In *Current Cancer Therapy Reviews*, (pp. 175–186). Benhtam Science Publishers.

Heinlein, C. A., & Chang, C. (2002). The Roles of Androgen Receptors and Androgen-Binding Proteins in Nongenomic Androgen Actions. *Molecular Endocrinology*, *16*(10), 2181–2187.

Hörnberg, E., Ylitalo, E. B., Crnalic, S., Antti, H., Stattin, P., Widmark, A., Bergh, A., & Wikström, P. (2011). Expression of androgen receptor splice variants in prostate cancer bone metastases is associated with castration-resistance and short survival. *PLoS ONE*, *6*(4), e19059.

Horoszewicz, J. S., Leong, S. S., Kawinski, E., Karr, J. P., Rosenthal, H., Chu, T. M., Mirand, E. a., & Murphy, G. P. (1983). LNCaP Model of Human Prostatic Carcinoma LNCaP Model of Human Prostatic Carcinoma1. *Cancer Research*, *43*(April), 1809–1818.

Hsu, C. L., Chen, Y. L., Yeh, S., Ting, H. J., Hu, Y. C., Lin, H., Wang, X., & Chang, C. (2003). The use of phage display technique for the isolation of androgen receptor interacting peptides with (F/W)XXL(F/W) and FXXLY new signature motifs. *Journal of Biological Chemistry*, *278*(26), 23691–23698.

Hu, R., Dunn, T. A., Wei, S., Isharwal, S., Veltri, R. W., Humphreys, E., Han, M., Partin, A. W., Vessella, R. L., Isaacs, W. B., Bova, G. S., & Luo, J. (2009). Ligand-independent androgen receptor variants derived from splicing of cryptic exons signify hormone-refractory prostate cancer. *Cancer Research*, *69*(1), 16–22.

Huang, Y., Jiang, X., Liang, X., & Jiang, G. (2018). Molecular and cellular mechanisms of castration resistant prostate cancer. *Oncology Letters*, *15*(5), 6063–6076.

Huggins, C., & Hodges, C. V. (1941). Studies on prostatic cancer i. the effect of castration, of estrogen and of androgen injection on serum phosphatases in metastatic carcinoma of the prostate. *Cancer Research*, *1*(4), 293–297.

Hur, E., Pfaff, S. J., Sturgis Payne, E., Grøn, H., Buehrer, B. M., & Fletterick, R. J. (2004). Recognition and accommodation at the androgen receptor coactivator binding interface. *PLoS Biology*, *2*(9).

Jehle, K., Cato, L., Neeb, A., Muhle-Goll, C., Jung, N., Smith, E. W., Buzon, V., Carbó, L. R., Estébanez-Perpiñá, E., Schmitz, K., Fruk, L., Luy, B., Chen, Y., Cox, M. B., Bräse, S., Brown, M., & Cato, A. C. B. (2014). Coregulator control of androgen receptor action by a novel nuclear receptor-binding motif. *The Journal of biological chemistry*, *289*(13), 8839–51.

Jin, F., Claessenss, F., & Fondell, J. D. (2012). Regulation of androgen receptor-dependent transcription by coactivator MED1 is mediated through a newly discovered noncanonical binding motif. *Journal of Biological Chemistry*, *287*(2), 858–870.

Jin, Q., Yu, L. R., Wang, L., Zhang, Z., Kasper, L. H., Lee, J. E., Wang, C., Brindle, P. K., Dent, S. Y., & Ge, K. (2011). Distinct roles of GCN5/PCAF-mediated H3K9ac and CBP/p300-mediated H3K18/27ac in nuclear receptor transactivation. *EMBO Journal*, *30*(2), 249–262.

Kaku, N., Matsuda, K.-i., Tsujimura, A., & Kawata, M. (2008). Characterization of nuclear import of the domain-specific androgen receptor in association with the importin alpha/beta and Ran-guanosine 5'-triphosphate systems. *Endocrinology*, *149*(8), 3960–3969.

Katzenellenbogen, J. A., & Katzenellenbogen, B. S. (1996). Nuclear hormone receptors: Ligand-activated regulators of transcription and diverse cell responses. *Chemistry and Biology*, *3*(7), 529–536.

Krajewska, M., Turner, B. C., Shabaik, A., Krajewski, S., & Reed, J. C. (2006). Expression of BAG-1 Protein Correlates With Aggressive Behavior of Prostate Cancers. *The Prostate*, *66*, 801–810.

Krebsinformationsdienst des Deutschen Krebsforschungszentrums (DKFZ) (2017). Prostatakrebs: Anatomie, Entstehung und Häufigkeit.

Kumar, B., Koul, S., Khandrika, L., Meacham, R. B., & Koul, H. K. (2008). Oxidative stress is inherent in prostate cancer cells and is required for aggressive phenotype. *Cancer Research*, *68*(6), 1777–1785.

Kunkel, T. A. (1985). Rapid and efficient site-specific mutagenesis without phenotypic selection. *Proceedings of the National Academy of Sciences of the United States of America*, *82*(2), 488–492.

Labrie, F., Dupont, A., Belanger, A., Cusan, L., Lacourciere, Y., Monfette, G., Laberge, J. G., Emond, J. P., Fazekas, A. T., Raynaud, J. P., & Husson, J. M. (1982). New hormonal therapy in prostatic carcinoma: combined treatment with an LHRH agonist and an antiandrogen. *Clinical and investigative medicine. Medecine clinique et experimentale*, *5*(4), 267–275.

Lallous, N., Volik, S. V., Awrey, S., Leblanc, E., Tse, R., Murillo, J., Singh, K., Azad, A. A., Wyatt, A. W., LeBihan, S., Chi, K. N., Gleave, M. E., Rennie, P. S., Collins, C. C., & Cherkasov, A. (2016). Functional analysis of androgen receptor mutations that confer anti-androgen resistance identified in circulating cell-free DNA from prostate cancer patients. *Genome Biology*, *17*(1), 10.

Langley, E., Kemppainen, J. A., & Wilson, E. M. (1998). Intermolecular NH2-/carboxyl-terminal interactions in androgen receptor dimerization revealed by mutations that cause androgen insensitivity. *Journal of Biological Chemistry*, *273*(1), 92–101.

Lavery, D. N., & McEwan, I. J. (2008). Structural Characterization of the Native NH2-Terminal Transactivation Domain of the Human Androgen Receptor: A Collapsed Disordered Conforma-

tion Underlies Structural Plasticity and Protein-Induced Folding. *Biochemistry*, *47*(11), 3360–3369.

Lee, J., Demissie, K., Lu, S. E., & Rhoads, G. G. (2007). Cancer incidence among Korean-American immigrants in the United States and native Koreans in South Korea. *Cancer Control*, *14*(1), 78–85.

Li, X., Shao, H., R. Taylor, I., & E. Gestwicki, J. (2016). Targeting Allosteric Control Mechanisms in Heat Shock Protein 70 (Hsp70). *Current Topics in Medicinal Chemistry*, *16*(25), 2729–2740.

Link, K. A., Balasubramaniam, S., Sharma, A., Comstock, C. E., Godoy-Tundidor, S., Powers, N., Cao, K. H., Haelens, A., Claessens, F., Revelo, M. P., & Knudsen, K. E. (2008). Targeting the BAF57 SWI/SNF subunit in prostate cancer: A novel platform to control androgen receptor activity. *Cancer Research*, *68*(12), 4551–4558.

Liu, Q., Su, S., Blackwelder, A. J., Minges, J. T., & Wilson, E. M. (2011). Gain in transcriptional activity by primate-specific coevolution of melanoma antigen-A11 and its interaction site in androgen receptor. *Journal of Biological Chemistry*, *286*, 29951–29963.

Liu, S., Kumari, S., Hu, Q., Senapati, D., Venkadakrishnan, V. B., Wang, D., DePriest, A. D., Schlanger, S. E., Ben-Salem, S., Valenzuela, M. M., Willard, B., Mudambi, S., Swetzig, W. M., Das, G. M., Shourideh, M., Koochekpour, S., Falzarano, S. M., Magi-Galluzzi, C., Yadav, N., Chen, X., Lao, C., Wang, J., Billaud, J. N., & Heemers, H. V. (2017). Erratum: Correction: A comprehensive analysis of coregulator recruitment, androgen receptor function and gene expression in prostate cancer (eLife (2017) 6 PII: e33738). *eLife*, *6*.

Lu, C., & Luo, J. (2013). Decoding the androgen receptor splice variants. *Translational Andrology and Urology*, *2*(3), 178–186.

Lubahn, D. B., Joseph, D. R., Sullvan, P. M., Willard, H. F., French, F. S., Wilson, E. M., Willard, H. F., Genetics, M., & I, I. S. A. (2014). Cloning of Human Androgen Rector Complentry. *Science*, *240*, 327–330.

Lüders, J., Demand, J., & Höhfeld, J. (2000). The ubiquitin-related BAG-1 provides a link between the molecular chaperones Hsc70/Hsp70 and the proteasome. *Journal of Biological Chemistry*, *275*(7), 4613–4617.

Maki, H. E., Saramaki, O. R., Shatkina, L., Martikainen, P. M., Tammela, T. L., van Weerden, W. M., Vessella, R. L., Cato, A. C., & Visakorpi, T. (2007). Overexpression and gene amplification of BAG-1L in hormone-refractory prostate cancer. *Journal of Pathology*, *212*, 395–401.

Mangelsdorf, D. J., Thummel, C., Beato, M., Herrlich, P., Schütz, G., Umesono, K., Blumberg, B., Kastner, P., Mark, M., Chambon, P., & Evans, R. M. (1995). The nuclear receptor superfamily: The second decade. *Cell*, *83*(6), 835–839.

Mcewan, I. J., & Gustafsson, J. Å. (1997). Interaction of the human androgen receptor transactivation function with the general transcription factor TFIIF. *Proceedings of the National Academy of Sciences of the United States of America*, *94*(16), 8485–8490.

McKenna, N. J., Lanz, R. B., & O'Malley, B. W. (1999). Nuclear receptor coregulators: Cellular and molecular biology. *Endocrine Reviews*, *20*(3), 321–344.

McKenna, N. J., & O'Malley, B. W. (2002). Minireview: Nuclear receptor coactivators - An update. *Endocrinology*, *143*(7), 2461–2465.

McNeal, J. E., & Bostwick, D. G. (1986). Intraductal dysplasia: A premalignant lesion of the prostate. *Human Pathology*, *17*(1), 64–71.

Migeon, B. R., Brown, T. R., Axelman, J., & Migeon, C. J. (1981). Studies of the locus for androgen receptor: Localization on the human X chromosome and evidence for homology with the Tfm locus in the mouse. *Proceedings of the National Academy of Sciences of the United States of America*, *78*(10 I), 6339–6343.

Migliari, R., Muscas, G., Murru, M., Verdacchi, T., De Benedetto, G., & De Angelis, M. (1999). Antiandrogens: a summary review of pharmacodynamic properties and tolerability in prostate cancer therapy. *Archivio italiano di urologia, andrologia : organo ufficiale [di] Societa italiana di ecografia urologica e nefrologica*, *71*(5), 293–302.

Minges, J. T., Su, S., Grossman, G., Blackwelder, A. J., Pop, E. A., Mohler, J. L., & Wilson, E. M. (2013). Melanoma antigen-A11 (MAGE-A11) enhances transcriptional activity by linking androgen receptor dimers. *Journal of Biological Chemistry*, *288*, 1939–1952.

Moilanen, A. M., Riikonen, R., Oksala, R., Ravanti, L., Aho, E., Wohlfahrt, G., Nykänen, P. S., Törmäkangas, O. P., Palvimo, J. J., & Kallio, P. J. (2015). Discovery of ODM-201, a new-generation androgen receptor inhibitor targeting resistance mechanisms to androgen signaling-directed prostate cancer therapies. *Scientific Reports*, *5*(March), 1–11.

Montironi, R., Mazzucchelli, R., Lopez-Beltran, A., Cheng, L., & Scarpelli, M. (2007). Mechanisms of Disease: High-grade prostatic intraepithelial neoplasia and other proposed preneoplastic lesions in the prostate. *Nature Clinical Practice Urology*, *4*(6), 321–332.

Moras, D., & Gronemeyer, H. (1998). The nuclear receptor ligand-binding domain: Structure and function. *Current Opinion in Cell Biology*, *10*(3), 384–391.

Myung, J. K., Banuelos, C. A., Fernandez, J. G., Mawji, N. R., Wang, J., Tien, A. H., Yang, Y. C., Tavakoli, I., Haile, S., Watt, K., McEwan, I. J., Plymate, S., Andersen, R. J., & Sadar, M. D. (2013). An androgen receptor N-terminal domain antagonist for treating prostate cancer. *Journal of Clinical Investigation*, *123*(7), 2948–2960.

Nazareth, L. V., & Weigel, N. L. (1996). Activation of the human androgen receptor through a protein kinase A signaling pathway. *Journal of Biological Chemistry*, *271*(33), 19900–19907.

Neri, R. O., Monahan, M. D., Meyer, J. G., Afonso, B. A., & Tabachnick, I. A. (1967). Biological studies on an anti-androgen. *European Journal of Pharmacology*, *1*, 438–444.

Papadakis, E. S., Barker, C. R., Syed, H., Reeves, T., Schwaiger, S., Stuppner, H., Troppmair, J., Blaydes, J. P., & Cutress, R. I. (2016). The Bag-1 inhibitor, Thio-2, reverses an atypical 3D morphology driven by Bag-1L overexpression in a MCF-10A model of ductal carcinoma in situ. *Oncogenesis*, *5*(4), e215–8.

Partin, A. W., Epstein, J. I., Cho, K. R., Gittelsohn, A. M., & Walsh, P. C. (1989). Morphometric measurement of tumor volume and per cent of gland involvement as predictors of pathological stage in clinical stage B prostate cancer. *The Journal of urology*, *141*(2), 341–345.

Patlevič, P., Vašková, J., Švorc, P., Vaško, L., & Švorc, P. (2016). Reactive oxygen species and antioxidant defense in human gastrointestinal diseases. *Integrative Medicine Research*, *5*(4), 250–258.

Perera, L., Li, Y., Coons, L. A., Houtman, R., van Beuningen, R., Goodwin, B., Auerbach, S. S., & Teng, C. T. (2017). Binding of bisphenol A, bisphenol AF, and bisphenol S on the androgen receptor: Coregulator recruitment and stimulation of potential interaction sites. *Toxicology in Vitro*, *44*, 287–302.

Peterziel, H., Mink, S., Schonert, A., Becker, M., Klocker, H., & Cato, A. C. (1999). Rapid signalling by androgen receptor in prostate cancer cells. *Oncogene*, *18*(46), 6322–6329.

Petrylak, D. P., Tangen, C. M., Hussain, M. H., Lara, P. N., Jones, J. A., Taplin, M. E., Burch, P. A., Berry, D., Moinpour, C., Kohli, M., Benson, M. C., Small, E. J., Raghavan, D., & Crawford, E. D. (2004). Docetaxel and estramustine compared with mitoxantrone and prednisone for advanced refractory prostate cancer. *New England Journal of Medicine*, *351*(15), 1513–1520.

Pflug, B. R., Reiter, R. E., & Nelson, J. B. (1999). Caveolin expression is decreased following androgen deprivation in human prostate cancer cell lines. *Prostate*, *40*(4), 269–273.

Ponnusamy, S., He, Y., Hwang, D. J., Thiyagarajan, T., Houtman, R., Bocharova, V., Sumpter, B. G., Fernandez, E., Johnson, D., Du, Z., Pfeffer, L. M., Getzenberg, R. H., McEwan, I. J., Miller, D. D., & Narayanan, R. (2019). Orally bioavailable androgen receptor degrader, potential next-generation therapeutic for enzalutamide-resistant prostate cancer. *Clinical Cancer Research*, *25*(22), 6764–6780.

Qu, Y., Dai, B., Ye, D., Kong, Y., Chang, K., Jia, Z., Yang, X., Zhang, H., Zhu, Y., & Shi, G. (2015). Constitutively Active AR-V7 Plays an Essential Role in the Development and Progression of Castration-Resistant Prostate Cancer. *Scientific Reports*, *5*, 1–6.

Raynaud, J. P., Bonne, C., Bouton, M. M., Lagace, L., & Labrie, F. (1979). Action of a non-steroid anti-androgen, RU 23908, in peripheral and central tissues. *Journal of Steroid Biochemistry*, *11*(1 PART 1), 93–99.

Rennie, P. S., Bruchovsky, N., Leco, K. J., Sheppard, P. C., McQueen, S. A., Cheng, H., Snoek, R., Hamel, A., Bock, M. E., MacDonald, B. S., Nickel, B. E., Chang, C., Liao, S., Cattini, P. A., & Matusik, R. J. (1993). Characterization of two cis-acting DNA elements involved in the androgen regulation of the probasin gene. *Molecular Endocrinology*, *7*(1), 23–36.

Rice, M. A., Malhotra, S. V., & Stoyanova, T. (2019). Second-generation antiandrogens: From discovery to standard of care in castration resistant prostate cancer. *Frontiers in Neurology*, *10*(AUG), 1–12.

Robert-Koch-Institut (2016). Krebs in Deutschland für 2015 / 2016 Krebs in Deutschland. Tech. rep., Zentrum für Krebsregisterdaten.

Roche, P. J., Hoare, S. A., & Parker, M. G. (1992). A consensus dna-binding site for the androgen receptor. *Molecular Endocrinology*, *6*(12), 2229–2235.

Rowlands, M. G., Barrie, S. E., Chan, F., Houghton, J., Jarman, M., McCague, R., & Potter, G. A. (1995). Esters of 3-Pyridylacetic Acid That Combine Potent Inhibition of 17α-Hydroxylase/C17,20-Lyase (Cytochrome P45017α) with Resistance to Esterase Hydrolysis. *Journal of Medicinal Chemistry*, *38*(21), 4191–4197.

Rundlett, S. E., & Miesfeld, R. L. (1995). Quantitative differences in androgen and glucocorticoid receptor DNA binding properties contribute to receptor-selective transcriptional regulation. *Molecular and Cellular Endocrinology*, *109*(1), 1–10.

Sadar, M. D., Williams, D. E., Mawji, N. R., Patrick, B. O., Wikanta, T., Chasanah, E., Irianto, H. E., Van Soest, R., & Andersen, R. J. (2008). Sintokamides A to E, chlorinated peptides from the sponge Dysidea sp. that inhibit transactivation of the N-terminus of the androgen receptor in prostate cancer cells. *Organic Letters*, *10*(21), 4947–4950.

Sauer, H., Wartenberg, M., & Hescheler, J. (2001). Reactive oxygen species as intracellular messengers during cell growth and differentiation. *Cellular Physiology and Biochemistry*, *11*(4), 173–186.

Sawyers, C. L., & Rauscher, F. J. I. (2014). *Molecular Oncology*. Cambridge University Press.

Schally, A., Arimura, A., Baba, Y., Nair, R., Matsuo, H., Redding, T., & Debeljuk, L. (1971). Isolation and properties of the FSH and LH-releasing hormone. *Biochemical and Biophysical Research Communication*, *43*(2), 393–399.

Schottenfeld, D., & Fraumeni Jr., J. F. (1997). *Cancer Epidemiology and Prevention*. Oxford University Press, 3 ed.

Schweizer, M. T., Haugk, K., McKiernan, J. S., Gulati, R., Cheng, H. H., Maes, J. L., Dumpit, R. F., Nelson, P. S., Montgomery, B., McCune, J. S., Plymate, S. R., & Yu, E. Y. (2018). A phase I study of niclosamide in combination with enzalutamide in men with castration-resistant prostate cancer. *PLoS ONE*, *13*(6), 1–12.

Shang, Y., Myers, M., & Brown, M. (2002). Formation of the androgen receptor transcription complex. *Molecular Cell*, *9*(3), 601–610.

Sharma, P. C., Sinhmar, A., Sharma, A., Rajak, H., & Pathak, D. P. (2012). Medicinal significance of benzothiazole scaffold: An insight view. *Journal of Enzyme Inhibition and Medicinal Chemistry*, *28*(2), 240–266.

Shatkina, L., Mink, S., Rogatsch, H., Klocker, H., Langer, G., Nestl, A., & Cato, A. C. B. (2003). The cochaperone Bag-1L enhances androgen receptor action via interaction with the NH2-terminal region of the receptor. *Molecular and cellular biology*, *23*(20), 7189–97.

Shiota, M., Yokomizo, A., Tada, Y., Inokuchi, J., Tatsugami, K., Kuroiwa, K., Uchiumi, T., Fujimoto, N., Seki, N., & Naito, S. (2010). Peroxisome proliferator-activated receptor γ coactivator-1α interacts with the androgen receptor (AR) and promotes prostate cancer cell growth by activating the AR. *Molecular Endocrinology*, *24*(1), 114–127.

Siegel, R. L., Miller, K. D., & Jemal, A. (2019). Cancer statistics, 2019. *CA: a cancer journal for clinicians*, *69*(1), 7–34.

Singh, S. M., Labrie, S. G., & Fernand (2000). Androgen Receptor Antagonists (Antiandrogens) Structure-Activity Relationships.

Sondermann, H., Scheufler, C., Schneider, C., Hohfeld, J., Hartl, F. U., & Moarefi, I. (2001). Structure of a Bag/Hsc70 complex: convergent functional evolution of Hsp70 nucleotide exchange factors. *Science (New York, N.Y.)*, *291*(5508), 1553–1557.

Sullivan, L. B., & Chandel, N. S. (2014). Mitochondrial reactive oxygen species and cancer. *Cancer and Metabolism*, *2*(1), 1–12.

Sun, S., Sprenger, C. C. T., Vessella, R. L., Haugk, K., Soriano, K., Mostaghel, E. A., Page, S. T., Coleman, I. M., Nguyen, H. M., Sun, H., Nelson, P. S., & Plymate, S. R. (2010). Castration resistance in human prostate cancer is conferred by a frequently occurring androgen receptor splice variant. *The Journal of Clinical Investigation*, *120*(8).

Suzman, D. L., & Antonarakis, E. S. (2014). Castration-resistant prostate cancer: Latest evidence and therapeutic implications. *Therapeutic Advances in Medical Oncology*, *6*(4), 167–179.

Takayama, S., Bimston, D. N., Matsuzawa, S.-I., Freeman, B. C., Aime-Sempe, C., Xie, Z., Morimoto, R. I., & Reed, J. C. (1997). BAG-1 modulates the chaperone activity of Hsp70 / Hsc70. *The EMBO Journal*, *16*(16), 4887–4896.

Takayama, S., Krajewski, S., Krajewska, M., Kitada, S., Zapata, J. M., Kochel, K., Knee, D., Scudiero, D., Tudor, G., Miller, G. J., Miyashita, T., Yamada, M., & Reed, J. C. (1998). Expression and location of Hsp70/Hsc-binding anti-apoptotic protein BAG-1 and its variants in normal tissues and tumor cell lines. *Cancer research*, *58*(619), 3116–3131.

Takayama, S., & Reed, J. C. (2001). Molecular chaperone targeting and regulation by BAG family proteins. *Nature cell biology*, *3*(10), E237–41.

Takayama, S., Sato, T., Krajewski, S., Kochel, K., Irie, S., Milian, J. A., & Reed, J. C. (1995). Cloning and functional analysis of BAG-1: A novel Bcl-2-binding protein with anti-cell death activity. *Cell*, *80*(2), 279–284.

Tan, M. E., Li, J., Xu, H. E., Melcher, K., & Yong, E.-L. (2014). Androgen receptor: structure, role in prostate cancer and drug discovery. *Acta pharmacologica Sinica*, *36*(1), 1–21.

Tan, M. E., Li, J., Xu, H. E., Melcher, K., & Yong, E. L. (2015). Androgen receptor: Structure, role in prostate cancer and drug discovery. *Acta Pharmacologica Sinica*, *36*(1), 3–23.

Tannock, I. F., De Wit, R., Berry, W. R., Horti, J., Pluzanska, A., Chi, K. N., Oudard, S., Théodore, C., James, N. D., Turesson, I., Rosenthal, M. A., & Eisenberger, M. A. (2004). Docetaxel plus prednisone or mitoxantrone plus prednisone for advanced prostate cancer. *New England Journal of Medicine*, *351*(15), 1502–1512.

Taplin, M. E., Rajeshkumar, B., Halabi, S., Werner, C. P., Woda, B. A., Picus, J., Stadler, W., Hayes, D. F., Kantoff, P. W., Vogelzang, N. J., & Small, E. J. (2003). Androgen receptor mutations in androgen-independent prostate cancer: Cancer and leukemia group B study 9663. *Journal of Clinical Oncology*, *21*(14), 2673–2678.

Touriol, C., Bornes, S., Bonnal, S., Audigier, S., Prats, H., Prats, A. C., & Vagner, S. (2003). Generation of protein isoform diversity by alternative initiation of translation at non-AUG codons. *Biology of the Cell*, *95*(3-4), 169–178.

Townsend, P. a., Cutress, R. I., Sharp, A., Brimmell, M., & Packham, G. (2003). BAG-1 Prevents Stress-induced Long-term Growth Inhibition in Breast Cancer Cells via a Chaperone-dependent Pathway. *Cancer Research*, *63*, 4150–4157.

Tran, C., Ouk, S., Clegg, N. J., Chen, Y., Watson, P. a., Wongvipat, J., Smith-jones, P. M., Yoo, D., Kwon, A., Welsbie, D., Chen, C., Higano, C. S., Beer, T. M., Hung, D. T., Scher, H. I., Jung, M., & Sawyers, C. L. (2010). Development of a Second-Generation Antiandrogen for Treatment of Advanced Prostate Cancer. *Science*, *324*(5928), 787–790.

Umesono, K., & Evans, R. M. (1989). Determinants of target gene specificity for steroid/thyroid hormone receptors. *Cell*, *57*(7), 1139–1146.

Uyar, B., Weatheritt, R. J., Dinkel, H., Davey, N. E., & Gibson, T. J. (2014). Proteome-wide analysis of human disease mutations in short linear motifs: Neglected players in cancer? *Molecular BioSystems*, *10*(10), 2626–2642.

van der Steen, T., Tindall, D. J., & Huang, H. (2013). Posttranslational modification of the androgen receptor in prostate cancer. *International Journal of Molecular Sciences*, *14*(7), 14833–14859.

Van Roey, K., Uyar, B., Weatheritt, R. J., Dinkel, H., Seiler, M., Budd, A., Gibson, T. J., & Davey, N. E. (2014). Short linear motifs: Ubiquitous and functionally diverse protein interaction modules directing cell regulation. *Chemical Reviews*, *114*(13), 6733–6778.

Verrijdt, G., Haelens, A., Schoenmakers, E., Rombauts, W., & Claessens, F. (2002). Comparative analysis of the influence of the high-mobility group box 1 protein on DNA binding and transcriptional activation by the androgen, glucocorticoid, progesterone and mineralocorticoid receptors. *Biochemical Journal*, *361*(1), 97–103.

Visakorpi, T., Hyytinen, E., Koivisto, P., Tanner, M., Keinänen, R., Palmberg, C., Palotie, A., Tammela, T., Isola, J., & Kallioniemi, O. P. (1995a). In vivo amplification of the androgen receptor gene and progression of human prostate cancer. *Nat Genet*, *9*(4), 401–406.

Visakorpi, T., Hyytinen, E., Koivisto, P., Tanner, M., Keinänen, R., Palmberg, C., Palotie, A., Tammela, T., Isola, J., & Kallioniemi, O. P. (1995b). In vivo amplification of the androgen receptor gene and progression of human prostate cancer. *Nat Genet*, *9*(4), 401–406.

Wang, L., Hsu, C. L., & Chang, C. (2005). Androgen receptor corepressors: An overview. *Prostate*, *63*(2), 117–130.

Wang, L., Hsu, C.-L., Ni, J., Wang, P.-H., Yeh, S., Keng, P., & Chang, C. (2004). Human Checkpoint Protein hRad9 Functions as a Negative Coregulator To Repress Androgen Receptor Transactivation in Prostate Cancer Cells. *Molecular and Cellular Biology*, *24*(5), 2202–2213.

Watson, P. A., Arora, V. K., & Sawyers, C. L. (2015). Emerging Mechanisms of Resistance to Androgen Receptor Inhibitors in Prostate Cancer. *Nat Rev Cancer*, *15*(12), 701–711.

Watson, P. A., Chen, Y. F., Balbas, M. D., Wongvipat, J., Socci, N. D., Viale, A., Kim, K., & Sawyers, C. L. (2010). Constitutively active androgen receptor splice variants expressed in castration-resistant prostate cancer require full-length androgen receptor. *Proceedings of the National Academy of Sciences of the United States of America*, *107*(39), 16759–16765.

Werner, R., Holterhus, P. M., Binder, G., Schwarz, H. P., Morlot, M., Struve, D., Marschke, C., & Hiort, O. (2006). The A645D mutation in the hinge region of the human androgen receptor (AR) gene modulates AR activity, depending on the context of the polymorphic glutamine and glycine repeats. *Journal of Clinical Endocrinology and Metabolism*, *91*(9), 3515–3520.

Wiederschain, D., Wee, S., Chen, L., Loo, A., Yang, G., Huang, A., Chen, Y., Caponigro, G., Yao, Y. M., Lengauer, C., Sellers, W. R., & Benson, J. D. (2009). Single-vector inducible lentiviral RNAi system for oncology target validation. *Cell Cycle*, *8*(3), 498–504.

Williamson, M. P. (1994). The structure and function of proline-rich regions in proteins. *Biochemical Journal*, *297*(2), 249–260.

Wirth, M., Weißbach, L., Ackermann, R., Alberti, W., Albrecht, C., Wolff, J., & Wörmann, B. (2009). Interdisziplinäre Leitlinie der Qualität S3 zur Früherkennung , Diagnose und Therapie der verschiedenen Stadien des Prostatakarzinoms. *Therapie*, *043*, 1–620.

Wright, P. E., & Dyson, H. J. (2015). Intrinsically Disordered Proteins in Cellular Signaling and Regulation. *Nat Rev Mol Cell Biol*, *16*(1), 18–29.

Xu, J., Wu, R.-C., & O'Malleya, B. W. (2009). Normal and Cancer-Related Functions of the p160 Steroid Receptor Coactivator (SRC) Family. *Nat Rev Cancer*, *9*(9), 615–630.

Yang, F., Li, X., Sharma, M., Zarnegar, M., Lim, B., & Sun, Z. (2001). Androgen Receptor Specifically Interacts with a Novel p21-activated Kinase, PAK6. *Journal of Biological Chemistry*, *276*(18), 15345–15353.

Yang, X., Chernenko, G., Hao, Y., Ding, Z., Pater, M. M., Pater, a., & Tang, S. C. (1998). Human BAG-1/RAP46 protein is generated as four isoforms by alternative translation initiation and overexpressed in cancer cells. *Oncogene*, *17*(8), 981–989.

Zeiner, M., Niyaz, Y., & Gehring, U. (1999). The hsp70-associating protein Hap46 binds to DNA and stimulates transcription. *Proceedings of the National Academy of Sciences of the United States of America*, *96*(18), 10194–10199.

Zhou, Z. X., Lane, M. V., Kemppainen, J. A., French, F. S., & Wilson, E. M. (1995). Specificity of ligand-dependent androgen receptor stabilization: Receptor domain interactions influence ligand dissociation and receptor stability. *Molecular Endocrinology*, *9*(2), 208–218.

Zhou, Z.-x., Sar, M., Simental, J. a., Lane, M. V., & Wilsons, E. M. (1994). A Ligand-dependent Bipartite Nuclear Targeting Signal in the Human Androgen Receptor. *The Journal of biological chemistry*, *269*(18), 13115–13123.

Acknowledgements

First of all, I would like to express my gratitude to my supervisor, apl. Prof. Dr. Andrew Cato, for giving me the opportunity to work in his lab and for his support during my PhD. I would like to thank you for your criticisms, your optimism and for always lending an ear whenever it is needed.

Furthermore, I would like to thank Prof. Dr. Jörg Kämper for taking over the second assessment of this work.

I would also like to express my gratitude to Laura Cato, Irene Lee, Jaice Rottenberg, Claudia Muhle-Goll, Nicole Jung and Simone Gräßle for their support in this work.

A special thanks goes to Jutta for her help in the lab and the nice conversations in the lab and at lunch break and for being the good soul she always is. Furthermore, I would like to thank Rebecca for her support in lab and the nice time we had in the lab. I would also like to thank Valeria for her advices and the nice atmosphere in the lab. I also want to thank all past members of lab 109/114 for the nice atmosphere and for all the help I received.

A very special 'Thank you' is for Marga, for always providing us with coffee and for all her knowledge she is willing to share.

A great thank you is for Karo for her friendship, her support and her honest kind. Furthermore, I would like to thank Wilko, Leo, Qing, Helen and Lisa for making this Institute a small family to me.

My biggest thanks goes to my parents who made all of this possible through their caring support. Thank you for always being there for me.

And last but definitely not least, I want to thank Andreas for always supporting, advicing and motivating me. Thank you for cheering me up and calming me down whenever needed.